



Prepared for:

DG Rijkswaterstaat

Rijks-Instituut voor Kust en Zee/RIKZ

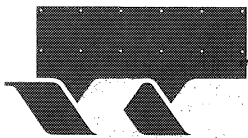
Database for sand concentrations
and sand transport; ST Database 2000

Data report

November 1999

Database for sand concentrations
and sand transport; ST Database 2000

L.C. van Rijn



wl | delft hydraulics



CLIENT: DG Rijkswaterstaat; Rijks-Instituut voor Kust en Zee/RIKZ

TITLE: Database for sand concentrations and sand transport; ST-Database 2000

ABSTRACT:

This report describes the redesign and improvement of an existing database for sand concentrations and sand transport. The redesigned database (based on EXCEL software) for sand concentrations and sand transport consists of two subdatabases:
 - Database TAP for Time Averaged Parameters and
 - Database TAPTS for Time Averaged Parameters and Time Series.

The Database TAP is available as a finalized product and contains 1004 datasets with velocity profiles, sand concentration profiles and current-related sand transport for steady flow, oscillatory flow as well as combined steady-oscillatory flow both in laboratory and field conditions. The parameters stored in the database generally consist of measured parameters and additional parameters, the latter being defined as parameters computed from the measured parameters (for example: depth-averaged fluid velocity, depth-integrated sand transport).

The file of the Database TAP consists of two EXCEL worksheets. The first worksheet, 'Data', containing all data from the original database. In the second worksheet, 'Graph', plots of velocity and concentration profiles of individual data sets are shown. Each data set is stored in one data row. A row consists of 238 fields containing the data of the set. These data rows are identified by a unique identification number (NR). This NR-number can be used for fast searching in the database files.

The present report of Database only includes the Database TAP (see Appendix A for available datasets). The database TAPTS will contain both time-averaged parameters and time series of instantaneous parameters. This will be produced at a later stage.

Datasets related to graded sediments have sofar not been included in the database. In 1999 experiments have been carried out in the wave tunnel of Delft Hydraulics and in a flume of the laboratory of Fluid Mechanics of the Technical University of Delft. The basic data of both experiments are described in Appendix B and in Appendix C. The data will be stored in the Database TAPTS at a later stage. Furthermore, it is recommended to compile the data of all relevant wave tunnel experiments and field experiments at Egmond to be stored in the present database.

The Database TAP has been used and will be used within various national (NCK; National Centre for Coastal Research) and international research programmes (Mas 2; Mas3-SEDMOC) with the aim to improve the methods for prediction of sand transport. The database is available (free of charge) for research institutes (NCK) in The Netherlands and SEDMOC-partners in the European Union. The database is commercially available for research institutes outside the EU.

REFERENCES: Contract RIKZ -725 RIKZ/OS 996415

SEDMOC MAS3-CT97-0115

VER.	ORIGINATOR	DATE	REMARKS	REVIEW	APPROVED BY
	L.C. van Rijn	9 Nov. 1999		A. Roelfzema M.J.F. Stive	T. Schilperoort

PROJECT IDENTIFICATION: Z2733.10/Z2099.10/Z2099.30

KEYWORDS: Database sand transport

CONTENTS:	TEXT PAGES	15	TABLES	3	FIGURES	5	APPENDICES	3
------------------	-------------------	----	---------------	---	----------------	---	-------------------	---

STATUS: PRELIMINARY DRAFT FINAL

Contents

1	Introduction.....	1-1
1.1	Background.....	1-1
1.2	Objectives	1-1
1.3	Acknowledgements.....	1-1
2	Database system	2-1
2.1	General description of datasets.....	2-1
2.2	System organisation.....	2-2
2.2.1	Time-averaged parameters TAP.....	2-2
2.2.2	Plots of time-averaged parameters	2-3
2.2.3	Time series parameters	2-4
2.3	Exporting information from the Database TAP	2-4
2.4	Parameter fields	2-4
3	Parameters of Database.....	3-1
3.1	Introduction.....	3-1
3.2	Database TAP	3-1
3.2.1	Definition of parameters.....	3-1
3.2.2	Extrapolation of velocity profiles.....	3-3
3.2.3	Extrapolation of concentration profiles	3-4
3.2.4	Computation of depth-averaged fluid velocity.....	3-6
3.2.5	Computation of depth-integrated suspended sediment load.....	3-6
3.2.6	Computation of depth-integrated suspended transport.....	3-7
3.3	Dataset TAPTS	3-7
3.3.1	Definition of parameters.....	3-7
4	Conclusions and recommendations.....	4-1
5	References.....	5-2

Appendices

- A Database TAP**

- B Data report Gradation effects on sand transport under oscillatory sheet-flow conditions**

- C Data report Sediment concentrations due to currents and irregular waves; measurement report**

Summary

Sediment transport and morphology is an important aspect of many hydraulic studies related to human interference in rivers, estuaries and coasts. Since our theoretical knowledge of the complicated dynamic processes of sediment transport and morphology is rather limited, we have to rely largely on empirical information. All over the world this information has been collected both in flumes and in nature.

Rapid analysis of the empirical data and comparison of the data with theoretical models requires the application of a consistent and easy-accessible database system. Such a database system for sand concentrations and sand transport has been implemented by Delft Hydraulics (1991). Within the European SEDMOC project (1998-2001) this database is being modified by the Hydraulics Engineering Section of the Technical University of Delft in cooperation with Delft Hydraulics. Excel software is now used as data managing system. The database (EXCEL software) consists of two subdatabases:

- Database TAP for Time Averaged Parameters and
- Database TAPTS for Time Averaged Parameters and Time Series.

The Database TAP is available as a finalized product and contains 1004 datasets with velocity profiles, sand concentration profiles and current-related sand transport for steady flow, oscillatory flow as well as combined steady-oscillatory flow both in laboratory and field conditions. The parameters stored in the database generally consist of measured parameters and additional parameters, the latter being defined as parameters computed from the measured parameters (for example: depth-averaged fluid velocity, depth-integrated sand transport). The file of the Database TAP consists of two EXCEL worksheets. The first worksheet, 'Data', containing all data from the original database. In the second worksheet, 'Graph', plots of velocity and concentration profiles of individual data sets are shown.

Each data set is stored in one data row. A row consists of 238 fields containing the data of the set. These data rows are identified by a unique identification number (NR). This NR-number can be used for fast searching in the database files.

The objectives of the present work can be summarized as:

- to update the software of the existing database TAP (from Dbase III to Excel),
- to include time series of velocities and sand concentrations (Database TAPTS),
- to include wave-related sand transport components (Database TAPTS),
- to identify and store relevant data sets of laboratory and field measurements.

The present report of Database only includes the Database TAP (Appendix A).

The database TAPTS will contain both time-averaged parameters and time series of instantaneous parameters. This will be produced at a later stage.

Datasets related to graded sediments have so far not been included in the database. In 1999 experiments have been carried out in the wave tunnel of Delft Hydraulics and in a flume of the laboratory of Fluid Mechanics of the Technical University of Delft. The basic data of both experiments are described in Appendix B and in Appendix C. The data will be stored in the Database TAPTS at a later stage. Furthermore, it is recommended to compile the data of all relevant wave tunnel experiments and field experiments at Egmond to be stored in the present database.

The Database TAP has been used and will be used within various national (NCK; National Centre for Coastal Research) and international research programmes (Mas2; Mas3-SEDMOC) with the aim to improve the methods for prediction of sand transport.

The database is available (free of charge) for research institutes (NCK) in The Netherlands and SEDMOC-partners in the European Union. The database is commercially available for research institutes outside the EU.

I Introduction

I.1 Background

Sediment transport and morphology is an important aspect of many hydraulic studies related to human interference in rivers, estuaries and coasts. Since our theoretical knowledge of the complicated dynamic processes of sediment transport and morphology is rather limited, we have to rely largely on empirical information. All over the world this information has been collected both in flumes and in nature.

Rapid analysis of the empirical data and comparison of the data with theoretical models requires the application of a consistent and easy-accessible database system. Such a database system (based on DBASE III software) has been developed by the working group 'Sand Transport in Coastal Conditions' (as a part of the Applied Research Programme, TOW, of the Dutch Ministry of Transport and Public Works) supervised by Delft Hydraulics (Delft Hydraulics, 1991)

The database system contains sand concentration profiles (of particles larger than 50 μm) and fluid velocity profiles (if available) and the relevant hydraulic and sediment parameters for current and/or wave conditions in flume and field conditions.

In the framework of the MAST III project SEDMOC (SEDiment transport MODelling in marine Coastal environments) this database is being revised and converted to a better accessible EXCEL database. Measurements carried out within the framework of the SEDMOC project (1998-2001) as well as other relevant datasets will be stored in an updated and extended version of this database.

This work is being done by the Hydraulics Engineering Section (P. Sistermans and M. van Goor) of the Technical University of Delft in cooperation with Delft Hydraulics and RIKZ of Rijkswaterstaat.

I.2 Objectives

The objectives of the present work are:

- to update/redesign the software of the existing database (from DBASE III to EXCEL),
- to include time series of velocities and sand concentrations,
- to include wave-related sand transport components,
- to identify and store relevant data sets of laboratory and field measurements.

I.3 Acknowledgements

This work is jointly funded by the MAST-3 SEDMOC project (Sediment Transport Modelling in Marine Coastal Environments) in the framework of the EU-sponsored Marine Science and Technology Programme (MAST-3) under contract MAS3-CT97-0115, the Dutch Ministry of Transport and Public Works (Rijkswaterstaat) under contract no. RKZ-725 (Part IV) and the Scientific Research Programme of Delft Hydraulics.

2 Database system

2.1 General description of datasets

A dataset is defined as a set of parameters representing one case of measured sand transport rate. The measured time interval involved may vary between say 15 minutes ('burst') for field conditions with waves and tidal flow to several days for a flume experiment with constant hydrodynamic conditions.

Each dataset is identified by a unique identification number (ID).

The database consists of two data subsets as a result of modification of the database since 1991. The available subsets are given in the following table. The present report of the Database only includes the Database TAP (see also Appendix A).

Sub-databases	Range of ID numbers	Measured parameters	Computed parameters
Database TAP (Time Averaged Parameters)	1-1004	Time-averaged velocities Time-averaged concentrations Time-averaged bed load transport	Depth-averaged velocity Depth-integrated suspended load (3 methods) Depth-integrated current-related suspended transport (3 methods)
Database TAPTS (Time Averaged Parameters and Time series)	1-.....	Time-averaged velocities Time-averaged concentrations Time-averaged bed load transport Time series of velocity and concentration	Depth-averaged velocity Depth-integrated suspended load Depth-integrated current-related suspended transport Depth-integrated wave-related suspended transport Net bed load transport Net total transport

Remarks:

- *computed parameters are partly based on extrapolation techniques;*
- *current-related transport is defined as the transport of sand by the mean steady flow with or without waves superimposed on the flow;*
- *wave-related transport is defined as the transport of sand by the oscillating flow components*

Datasets related to graded sediments have so far not been included in the database. In 1999 experiments have been carried out in the wave tunnel of Delft Hydraulics and in a flume of the laboratory of Fluids Mechanics of the Technical University of Delft. The basic data of both experiments are described in Appendix B and in Appendix C. The data will be stored in the Database TAPTS at a later stage. Furthermore, it is recommended to compile the data

of all relevant wave tunnel experiments and field experiments at Egmond to be stored in the database TAPTS.

2.2 System organisation

2.2.1 Time-averaged parameters TAP

The data is stored (actually 'zipped') on one floppy disk, using Microsoft Excel as the database manager. It is accessible using the same program or any other program that can read these Excel files. The file consists of two worksheets. The first worksheet, 'Data', containing all data from the original database. In the second worksheet, 'Graph', plots of velocity and concentration profiles of individual data sets are shown.

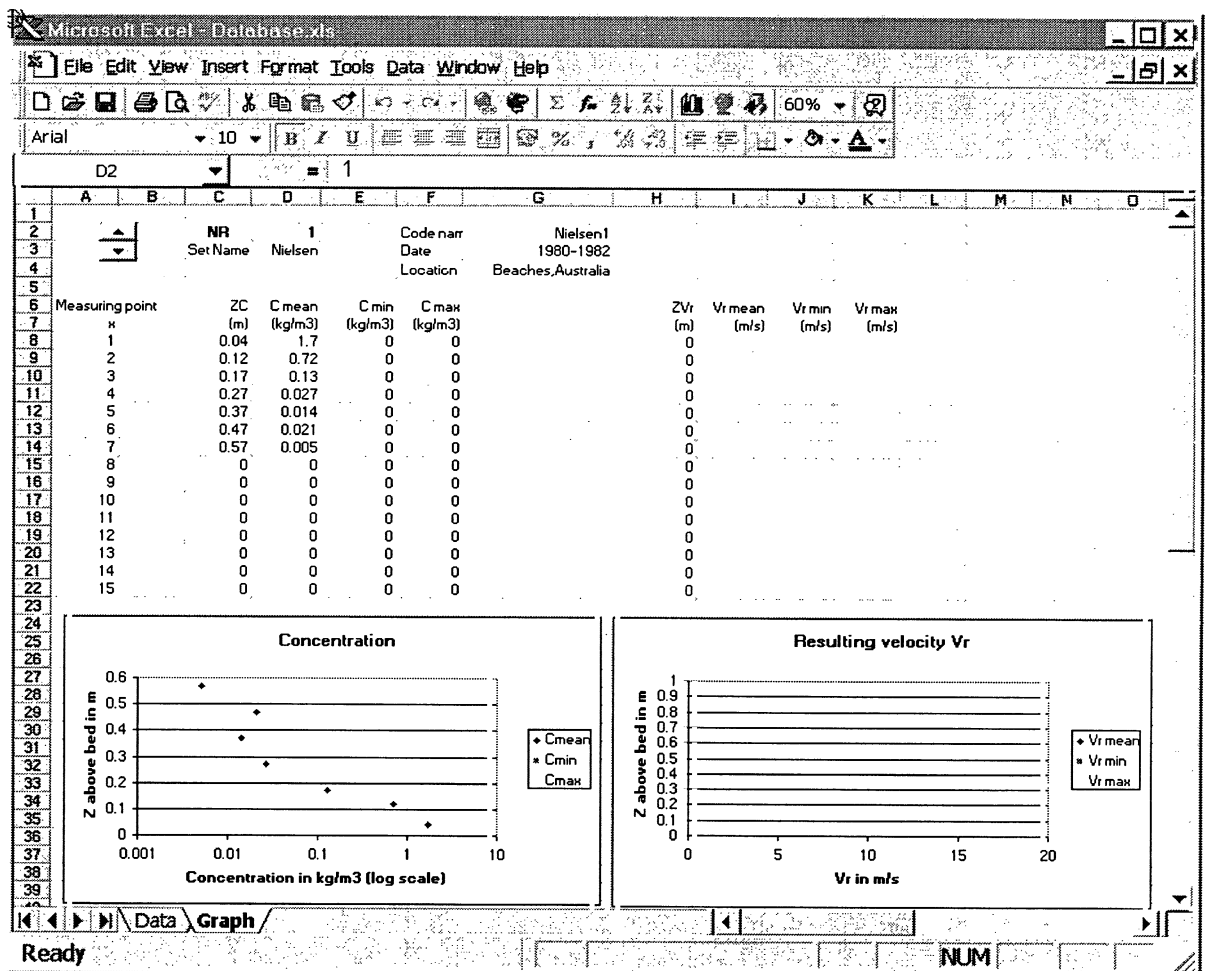
Each data set is stored in one data row (see below). A row consists of 238 fields containing the data of the set. These data rows are identified by a unique identification number (NR). This NR-number is the first field on the data worksheet, and can be used for fast searching in the database files. Some NR-numbers are not available because the corresponding data-sets appeared to be unreliable and have therefore been removed (NR 156 to NR 159 and NR 162 to NR 165).

	A	C	D	E	F
	NR	CODE	MODEL	TEST	LOCATION
1					
2	1	Nielsen1		run1	Beaches,Australia
3	2	Nielsen2		run2	Beaches,Australia
4	3	Nielsen3		run3	Beaches,Australia
5	4	Nielsen4		run4	Beaches,Australia
6	5	Nielsen5		run8	Beaches,Australia
7	6	Nielsen6		run9	Beaches,Australia
8	7	Nielsen7		run10	Beaches,Australia
9	8	Nielsen8		run11	Beaches,Australia
10	9	Nielsen9		run12	Beaches,Australia
11	10	Nielsen10		run13	Beaches,Australia
12	11	Nielsen11		run14	Beaches,Australia
13	12	Nielsen12		run15	Beaches,Australia
14	13	Nielsen13		run16	Beaches,Australia
15	14	Nielsen14		run17	Beaches,Australia
16	15	Nielsen15		run20	Beaches,Australia
17	16	Nielsen16		run21	Beaches,Australia
18	17	Nielsen17		run22	Beaches,Australia
19	18	Nielsen18		run23	Beaches,Australia
20	19	Nielsen19		run24	Beaches,Australia
21	20	Nielsen20		run25	Beaches,Australia
22	21	Nielsen21		run26	Beaches,Australia

To make better use of the data it is possible to filter or search data by specific fields. By clicking on the field filter option in row 1, one can select the data of interest. The selected data sets appear with a blue coloured row number. By clicking on the row number (which is not identical to the identification NR-number !) the user selects all the field information of the selected data rows. By holding the mouse indicator over the field tab one can obtain information concerning the field (like unit or dimension).

2.2.2 Plots of time-averaged parameters

To make rapid analyses it is possible to plot the main measured values of a data-set (like velocity profile and concentration profile) by selecting the data set NR number in the Graph worksheet (see below).



The NR scroll option makes it possible to click trough the data sets.

2.2.3 Time series parameters

Time series parameters such as instantaneous velocities, sand concentrations and sand transport rates are not yet included in the Database. This will be done as a future extension of the database (TAPTS).

2.3 Exporting information from the Database TAP

The easiest way to export data is to copy the selected data rows into a blank Excel worksheet and export the data from there. To copy the data in a blank Excel worksheet one can select the row numbers of interest and press CTRL + C. In the blank Excel sheet the data is pasted by pressing CTRL + V. From this Excel sheet it is possible to export the data to an external database. This can be done by selecting 'Save as' in the 'File' menu and choosing the format (in the 'Save as type' window) in which the exported data should be saved (e.g. text, dbase, etc). Some database systems also have the option to 'Import' Excel files (e.g. Access).

2.4 Parameter fields

Database TAP

The data of the 1004 sets are stored in rows. Each row represents one data set which consist of 238 fields. This dataset only contains time-averaged parameters. These fields are :

Field name	Description	Unit
NR	identity number(NR)	-
STT	set name	-
CODE	code name	-
MODEL	model name	-
TEST	test name	-
LOCATION	location	-
Field name	Description	Unit
DATE	date	-
TIME	time	-
H	water depth	m
WS	water surface slope	-
HSG	sign wave height	m
HM	mean wave height	m
HRMS	rms wave height	m
TZ	zero-cross period	s
TP	peak period	s
UM	mean velocity parallel to shore	m/s
VM	mean velocity perpendicular to shore	m/s
VMR	mean result velocity	m/s
VPROF	mean velocity profile	m/s
URMS	rms velocity at bed	m/s
UMAX	maximum velocity at bed	m/s
U15	velocity exceed by 15%	m/s
PHI	angle flow-waves	degr.
BT	breaker type	-
D10	bed material size	µm
D50	bed material size	µm

D90	bed material size	μm
DS	mean suspended material size	μm
DSMIN	min suspended material size	μm
DSMAX	max suspended material size	μm
WSB	fall velocity bed material	m/s
WSS	mean fall velocity suspended material	m/s
WSSMIN	min fall velocity suspended material	m/s
WSSMAX	max fall velocity suspended material	m/s
TE	water temperature	$^{\circ}\text{C}$
LB	bed load	kg/m^2
LS1	suspended load, method 1	kg/m^2
LS2	suspended load, method 2	kg/m^2
LS3	suspended load, method 3	kg/m^2
SB	bed load transport	kg/sm
SS1	suspended transport, method 1	kg/sm
SS2	suspended transport, method 2	kg/sm
SS3	suspended transport, method 3	kg/sm
BFH	mean bedform height	m
BFHMIN	min bedform height	m
BFHMAX	max bedform height	m
BFL	mean bedform length	m
BFLMIN	min bedform length	m
BFLMAX	max bedform length	m
BFT	bedform type	-
BS	local bed slope normal to shore	-
DMB	dist. between meas. loc. and breakerline	m
URMS_ON	rms velocity at bed in onshore direction	m/s
URMS_OFF	rms velocity at bed in offshore direction	m/s
CBED1	bed concentration, method 1	kg/m^3
CBED2	bed concentration, method 2	kg/m^3
CBED3	bed concentration, method 3	kg/m^3
x	measuring points 1 to 15	-
ZC_x	Z at concentration point x	m
C_x	C mean at concentration point x	kg/m^3
CML_x	C min at concentration point x	kg/m^3
CMA_x	C max at concentration point x	kg/m^3
ZV_x	Z at velocity point x	m
V_x	V mean at velocity point x	m/s
VML_x	V min at velocity point x	m/s
VMA_x	V max at velocity point x	m/s
ZD_x	Z at point x	m
D_x	D_{50} at point x	μm

3 Parameters of Database

3.1 Introduction

The parameters stored in the database generally consist of measured parameters and additional parameters, the latter being defined as parameters computed from the measured parameters. Because of modifications of the database since 1991, the database consists of two subsets, as explained in Section 2.1. These subsets are: Database TAP and Database TAPTS

3.2 Database TAP

3.2.1 Definition of parameters

The database system contains the data records of the hydraulic and sediment variables, the velocity profiles, the sediment concentration profiles and the d_{50} -profiles of the suspended sediment.

The following parameters are defined:

H	waterdepth (m)
WS	water surface slope (-)
Hsig	significant wave height (m)
Hm	mean wave height (m)
Hrms	root-mean-square wave height (m)
Tz	zero-crossing wave period (s)
Tp	wave period related to peak of spectrum (s)
Um	depth-averaged (mean) velocity parallel to shore (m/s)
Vm	depth-averaged (mean) velocity normal to shore (m/s)
Vmr	resulting velocity of mean velocities parallel and normal to shore (m/s)
Vprof	depth- averaged velocity computed from measured velocity profile (m/s)
Urms	root-mean-square value of orbital velocities at bed (m/s)
U15	peak value of orbital velocity at bed exceeded by 15% (m/s)
Umax	peak value of orbital velocity at bed (m/s)
PHI	angle between current and wave direction (0 to 180 degrees)
BT	breaker type
DMB	distance between measuring location and breakerline (m)
Urms,on	root-mean-square value of orbital velocities at bed in onshore direction (m/s)

Urms,off	root-mean-square value of orbital velocities at bed in offshore direction (m/s)
Te	water temperature (C)
BS	local bottom slope
D10	particle size of bed material (um)
D50	particle size of bed material (um)
D90	particle size of bed material (um)
Ds -mean	mean particle size of suspended sediment (um)
Ds-min	minimum particle size of suspended sediment (um)
Ds -max	maximum particle size of suspended sediment (um)
WSB	mean fall velocity of bed material (m/s)
WSS-mean	mean fall velocity of suspended sediment (m/s)
WSS-min	minimum fall velocity of suspended sediment (m/s)
WSS-max	maximum fall velocity of suspended sediment (m/s)
Cbed,1	bed concentration extrapolated to z=0 according to method 1 (kg/m ³)
Cbed,2	bed concentration extrapolated to z=0.001 m according to method 2 (kg/m ³)
Cbed,3	bed concentration extrapolated to z=0 m according to method 3 (kg/m ³)
Lb	bed load (kg/m ²)
Ls1	computed depth-integrated suspended load according method 1 (kg/m ²)
Ls2	computed depth-integrated suspended load according method 2 (kg/m ²)
Ls3	computed depth-integrated suspended load according method 3 (kg/m ²)
Sb	bed load transport (kg/m/s)
Ss1	computed depth-integrated current-related suspended transport, method 1 (kg/m/s)
Ss2	computed depth-integrated current-related suspended transport, method 2 (kg/m/s)
Ss3	computed depth-integrated current-related suspended transport, method 3 (kg/m/s)
BFH-mean	mean bed form height (m)
BFH-min	minimum bed form height (m)
BFH-max	maximum bed form height (m)
BFL-mean	mean bed form length (m)
BFL-min	minimum bed form length (m)
BFL-max	maximum bed form length (m)
BFT	bed form type
Z	height above mean bed level (m)
C-mean	mean sediment concentration at height Z (kg/m ³)
C-min	minimum sediment concentration at height Z (kg/m ³)

C-max	maximum sediment concentration at height Z (kg/m ³)
Vr-mean	mean resulting velocity at height Z (m/s)
Vr-min	minimum resulting velocity at height Z (m/s)
Vr-max	maximum resulting velocity at height Z (m/s)
Breaker type:	non breaking, spilling, plunging, occasional spilling, occasional plunging
Bed form type:	flat bed, ripples, dunes, mega-ripples, mega-dunes, transitional bed, anti-dunes, ripples on dunes

Additional software has been used to compute the depth-averaged fluid velocity, the depth-integrated suspended sediment load and transport, using the measured parameters. These latter variables are also stored in the database.

The computation program executes the following steps:

- extrapolation of velocity and concentration profiles,
- numerical computation of depth-averaged fluid velocity (V_{prof}), depth-integrated suspended sediment load (L_s), suspended sediment transport (S_s), and bed concentrations (C_{bed}).

The computational methods are described hereafter.

3.2.2 Extrapolation of velocity profiles

To compute the depth-integrated suspended sediment load transport, the velocity and concentration profiles must be fully defined from the bed to the water surface. Since there are always small zones ('unmeasured' zones) near the bed and the water surface where velocity and concentration measurements cannot be performed, extrapolation methods are necessary to complete the data.

The velocities between the bed and the first measuring point (Z_1) are represented by the following function (see Fig. 3):

$$V = V_1 \left(\frac{Z}{Z_1} \right)^{0.25} \quad \text{for } 0 < Z < Z_1 \quad (3.1)$$

in which:

V_1 = fluid velocity in first measuring point above the bed

Z_1 = height above bed of first measuring point

The velocities between the last measuring point (Z_L) and the water surface are assumed to be equal to the velocity (V_L) in the last measuring point (see Fig. 3). Thus:

$$V = V_L \quad \text{for } Z_L < Z < h \quad (3.2)$$

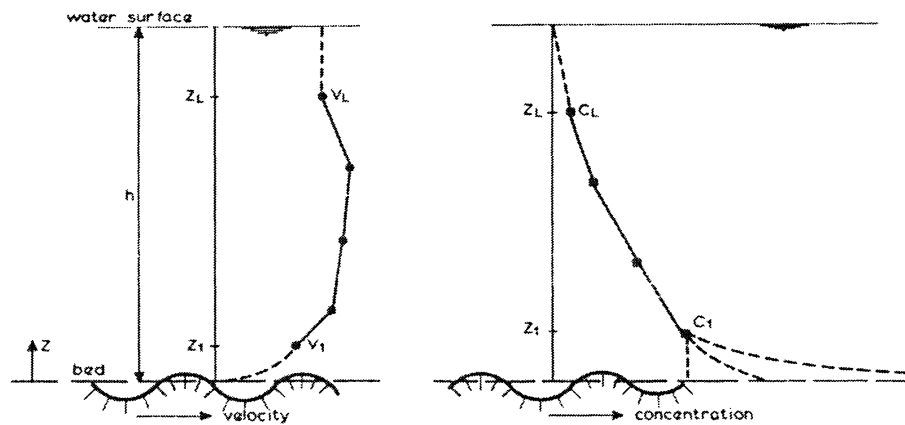


Figure 3 *Extrapolation of velocity and concentration profiles*

3.2.3 Extrapolation of concentration profiles

The sediment concentrations between the last measuring point and the water surface are represented by a linear function giving a zero concentration at the surface, as follows (see Fig. 3)

$$C = \left(\frac{h - Z}{h - Z_L} \right) C_L \quad \text{for } Z_L < Z < h \quad (3.3)$$

in which:

C_L = concentration in last measuring point

Z_L = height above bed of last measuring point.

Since the exact distribution of the sediment concentrations in the near-bed zone is not known and considering the relative importance of the concentrations in this zone, three different extrapolation methods (methods 1, 2 and 3) are applied to represent the concentration profile between the bed and the first measuring point.

Method 1 is supposed to give an under limit, while method 2 is supposed to give an upper limit.

Method 1

The sediment concentrations between the bed ($z = 0$ m) and the first measuring point ($Z = Z_1$) are assumed to be equal to the concentration (C_1) in the first measuring point (see Fig. 3). Thus:

$$C = C_1 \quad \text{for } 0 < Z < Z_1 \quad (3.4)$$

Method 2

The sediment concentrations between the bed ($z = 0.001$ m) and the first measuring point are computed by (See Fig. 4):

$$C = AY^B \quad \text{for } 0.001 < Z < Z_1 \quad (3.5)$$

in which:

$Y = (h-Z)/Z =$ dimensionless vertical co-ordinate

$Z =$ vertical co-ordinate above bed

$h =$ water depth

$A, B =$ coefficients

The A and B coefficients are determined by a regression method applying the measured concentrations of the first three measuring points above the bed, as follows:

- select $B = 0.1$

- compute $A = \frac{\sum_{k=1}^3 (Y_k^B C_k)}{\sum_{k=1}^3 (Y_k^B Y_k^B)}$

- compute $T = \sum_{k=1}^3 (A Y_k^B - C_k)$

- select $B = 0.2$ (B is varied over the range 0.1 to 5), repeat procedure

Finally, the A and B coefficients corresponding to a minimum T -value are selected as the 'best' coefficients. Applying Eq. 3.5, the sediment concentrations are computed in 50 (equidistant) points between the bed (defined at $Z = 0.001$ m) and the first measuring point ($Z = Z_1$). The maximum concentration is assumed to be 1590 kg/m^3 .

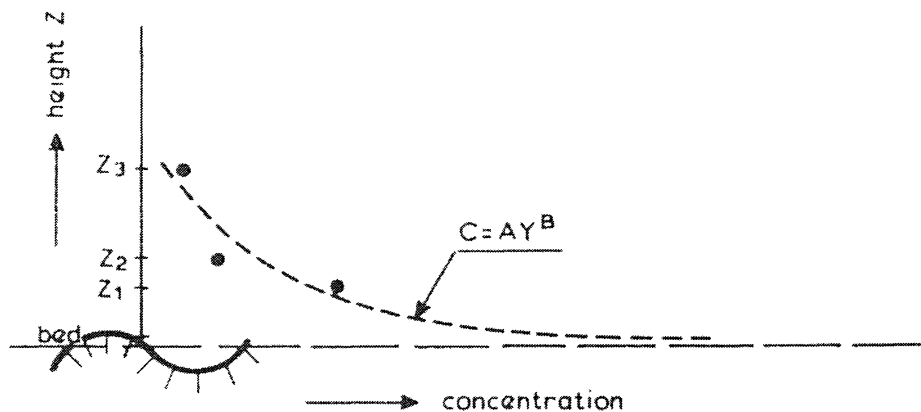


Figure 4 Regression of concentration profile (method 2)

Method 3

The sediment concentrations between the bed and the first measuring point are represented by (Fig. 5):

$$C = e^{AZ+B} \quad \text{for } 0 < Z < Z_1 \quad (3.6)$$

in which:

$Z =$ height above bed

$A, B =$ coefficients

The depth-integrated suspended sediment load (Ls) is computed as:

3.2.5 Computation of depth-integrated suspended sediment load

in which:
 h = water depth
 V_i = fluid velocity at height Z_i above the bed
 N = total number of points (including extrapolated values)

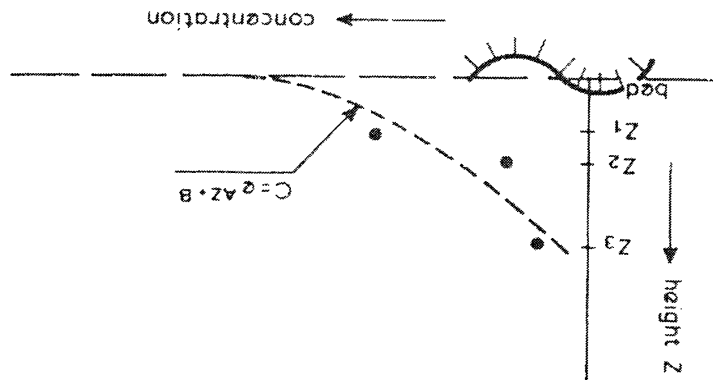
$$V_{\text{prof}} = \frac{1}{N} \sum_{i=1}^N \frac{h}{2} (V_i + V_{i-1})(Z_i - Z_{i-1}) \quad (3.9)$$

The depth-averaged fluid velocity is computed as:

3.2.4 Computation of depth-averaged fluid velocity

Applying Eq. 3.6, the sediment concentration are computed in 50 (equidistant) points between the bed (defined at $Z = 0$ m) and the first measuring point ($Z = Z_1$). The maximum concentration is assumed to be 1590 kg/m^3 .

Figure 5 Regression of concentration profile (method 3)



$$B = \frac{\sum_{k=1}^3 (Z_k Z_k) \sum_{k=1}^3 (\ln C_k) - \sum_{k=1}^3 (Z_k) \sum_{k=1}^3 (Z_k \ln C_k)}{3 \sum_{k=1}^3 (Z_k Z_k) - (\sum_{k=1}^3 Z_k)^2} \quad (3.8)$$

$$A = \frac{\sum_{k=1}^3 (Z_k \ln C_k) - \sum_{k=1}^3 (Z_k) \sum_{k=1}^3 (\ln C_k)}{3 \sum_{k=1}^3 (Z_k Z_k) - (\sum_{k=1}^3 Z_k)^2} \quad (3.7)$$

The A and B coefficients are determined by a linear regression method applying the measured concentrations of the first three measuring points above the bed, as follows:

$$L_s = \sum_{i=1}^N \frac{1}{2} (C_i + C_{i-1})(Z_i - Z_{i-1}) \quad (3.10)$$

in which:

C_i = sediment concentration at height Z_i above bed

N = total number of points (including extrapolated values)

Since three different methods are applied to represent the sediment concentrations in the unmeasured zone near the bed, three different values of the suspended sediment load are obtained and implemented in the database (L_{s1} , L_{s2} and L_{s3}).

3.2.6 Computation of depth-integrated suspended transport

Numerical computation of the depth-integrated suspended sediment transport (S_s) requires the specification of velocities and concentrations at equal elevations above the bed (at equal Z -values). When the Z -values of the velocities and concentrations are not corresponding, linear interpolation is applied to obtain the required data.

The depth-integrated suspended sediment transport (S_s) is computed as:

$$S_s = \sum_{i=1}^N \frac{1}{2} (V_i C_i + V_{i-1} C_{i-1})(Z_i - Z_{i-1}) \quad (3.11)$$

in which:

V_i = fluid velocity at height Z_i above the bed

C_i = sediment concentration at height Z_i above the bed

N = total number of points (including extrapolated and interpolated values).

Since three different methods are applied to represent the sediment concentrations in the unmeasured zone near the bed, three different values of the suspended sediment transport are obtained and implemented in the database (S_{s1} , S_{s2} , S_{s3}).

3.3 Dataset TAPTS

3.3.1 Definition of parameters

Additional parameters have been defined, which will be described at a later stage.

It is recommended to compile the data of all relevant wave tunnel experiments and field experiments at Egmond to be stored in the database TAPTS.

A list of possible datasets is given in Chapter 5.

4 Conclusions and recommendations

An existing database for sand concentrations and sand transport has been redesigned and improved based EXCEL software. The database consists of two subdatabases:

- Database TAP for Time Averaged Parameters and
- Database TAPTS for Time Averaged Parameters and Time Series.

The Database TAP contains 1004 datasets with velocity profiles, sand concentration profiles and current-related sand transport for steady flow, oscillatory flow as well as combined steady-oscillatory flow both in laboratory and field conditions. The parameters stored in the database generally consist of measured parameters and additional parameters, the latter being defined as parameters computed from the measured parameters (for example: depth-averaged fluid velocity, depth-integrated sand transport).

The file of the Database TAP consists of two EXCEL worksheets. The first worksheet, 'Data', containing all data from the original database. In the second worksheet, 'Graph', plots of velocity and concentration profiles of individual data sets are shown.

Each data set is stored in one data row. A row consists of 238 fields containing the data of the set. These data rows are identified by a unique identification number (NR). This NR-number is the first field on the data worksheet, and can be used for fast searching in the database files.

The Database TAP has been used and will be used within various national (NCK; National Centre for Coastal Research) and international research programmes (Mas 2; Mas3-SEDMOC) with the aim to improve the methods for prediction of sand transport.

Time series parameters such as instantaneous velocities, sand concentrations and sand transport rates are not yet included in the Database. This will be done as a future extension of the database (TAPTS).

Datasets related to graded sediments have so far not been included in the database. In 1999 experiments have been carried out in the wave tunnel of Delft Hydraulics and in a flume of the laboratory of Fluids Mechanics of the Technical University of Delft. The basic data of both experiments are described in Appendix B and in Appendix C. The data will be stored in the Database TAPTS at a later stage. Furthermore, it is recommended to compile the data of all relevant wave tunnel experiments and field experiments at Egmond to be stored in the present database.

The database is available (free of charge) for research institutes (NCK; National Centre Coastal Research) in The Netherlands and for SEDMOC-partners in the European Union. The database is commercially available for research institutes outside the EU.

5 References

General

Delft Hydraulics, 1991. Database manual, Sand concentration profiles and sand transport for currents and/or waves. Report H1148-04/05 Delft, The Netherlands

Database TAP

References of implemented data sets are specified in Appendix A.

Database TAPTS

Dohmen-Janssen, M., 1999. Grain size influence on sediment transport in oscillatory sheet flow. Doc. Thesis, Dep. of Civil Engineering, Univ. of Twente, The Netherlands

Grasmeijer, B., 2000. Sand transport measurements Egmond. Doc. Thesis to be published, Dep. of Phys. Geography. Univ. of Utrecht

Hassan, W. et al., 1999. Gradation effects on sand transport under oscillatory sheet flow conditions. Report Z2099.10, Delft Hydraulics, Delft, The Netherlands

Jacobs, C. and Dekker, S., 2000. Sediment concentrations and transport due to currents and irregular waves (to be published); Dep. of Coastal Engineering, Technical University of Delft, The Netherlands

A Database TAP

DATABASE TAP

The following data sets are stored in the database:

Set:	NR numbers:	Environment:
Nielsen	1-65	Current and Waves (field)
Bosman	66-133	Currents and Waves (flume)
Vellinga	134-150	Waves (large scale flume)
Steetzel	151-161	Waves (flume)
Anderson	166-188	Current (field)
Scott	189-211	Current (flume)
Barton-Lin	212-237	Current (flume)
Vessem	238-307	Current and Waves (flume)
Steetzel	308-412	Wave tunnel
Velden	413-566	Wave tunnel
Roelvink	567-592	Waves (large scale flume)
Steetzel	593-600	Waves (large scale flume)
Van Rijn	601-613	Waves (large scale flume)
Nieuwjaar / Van der Kaay	614-641	Current and Waves (flume)
Nap/ Van Kampen	642-671	Current and Waves (flume)
Voogt	672-731	Tidal current (field)
Culbertson	732-753	Current (field)
Dette	754-764	Waves (large scale flume)
Laursen	765-776	Current (flume)
Ribberink	777-824	Waves (tunnel)
Havinga	828-852	Current and Waves (basin)
Kroon	853-914	Current and Waves (field)
Ribberink	915-937	Wave tunnel
Grasmeijer/ Sies	938-1004	Current and Waves (flume)

Set: NIELSEN (NR 1-65)

Description

Field measurements were carried out near the sand coasts of Australia to study vertical concentration profiles.

Run	Location
1-2	Southern end of Palm Beach, Sydney, October 26, 1980
3-24	Gable Beach, Broome, November 1980
25-35	Southern end of Meroo Beach, Ulladulla, February, 1981
36-43	Northern end of Seven Mile Beach, Kiama, March, 1981
44-47	Pearl Beach, Sydney, March, 1981
48-60	Eastern Beach at Lakes Entrance, Victoria, May, 1981
61-66	Northern end of Seven Mile Beach, Kiama, March, 1982
67-69	Warriewood Beach, Sydney, April, 1982
70-71	Fens Embayment, Hawk's Nest, Newcastle, July, 1982

Measuring instruments

Velocities were measured by use of two bi-directional impellor flow meters, one shore normal and one shore parallel. Sediment concentrations were measured by use of a suction sampler, which is driven by the pressure difference between the intake nozzles (inner diameters of 3 and 6 mm) and the sample jars (2.2 litres). The intake nozzles were attached to a glass-fiber mast, which was pressed into the bed. The intake nozzles were oriented perpendicularly to the dominating flow component. In case of a rippled bed, the intake nozzles are always placed above the crests. The jars were filled up in about 3.5 minutes (intake velocity = 1.5 m/s). Wave heights were measured by use of a pressure transducer.

References

Nielsen, P., 1984

Field Measurements of Time-averaged Suspended Sediment Concentrations under Waves. Coastal Engineering, 8, p. 51-72.

Set: BOSMAN (NR 66-133)

Description

Flume measurements were carried out at the Delft Hydraulics Laboratory to study the vertical concentration distribution. The flume had a length of about 50 m, a width of 1.2 m and a depth of 1.2 m. The bed consisted of fine sand ($D_{50}=100\ \mu\text{m}$). Various water depths and bed slopes (1:25, 1:80) were used. The bottom slopes reported in this data set are the initial slopes. In some tests a current (opposing or following) was superimposed on the waves by re-circulating the water by use of a pump.

Wave conditions

Irregular waves were generated using 4 different wave spectra (S1, S2, S3, S4).

Measuring instruments

Velocities were measured by using an acoustical-Doppler probe. Sand concentrations were determined by taking water-sediment samples by use of a pump sampler. All samples in each vertical were collected simultaneously. The intake nozzles had an inner diameter of 3 mm and were placed normal to the velocity direction. The intake velocity was 1.65 m/s. The measuring period varied from 7 to 15 minutes (time averaging). During the measuring period all intake nozzles were moved forwards and backwards over a distance of 0.28 m to average over the ripples (bed form averaging). Bed forms were ripples with heights in the range of 0.01 to 0.02 m.

References

Bosman, J. , 1982

Concentration Distribution under Waves and Current (in Dutch)

Report M1875, Delft Hydraulics Laboratory, Delft, The Netherlands.

Set: VELLINGA (NR 134-150)

Description

Measurements were carried out in the Deltaflume of the Delft Hydraulics Laboratory. The flume had a length of 233 m, a width of 5 m and a depth of 7m. The objective of the large-scale experiments was to study the dune erosion process. In all, 5 tests were carried out using different hydraulic conditions and initial bed level profiles. The bed consisted of medium fine sand ($D_{50}=225 \mu\text{m}$). The silt content was about 2%. The bed was laid in layers of 0.4 m. The porosity factor was about 0.4. The concentration profiles reported in this data set are those measured outside the dune erosion zone.

Wave conditions

Irregular waves were generated with a Pierson-Moskowitz energy spectrum.

Measuring methods

Orbital velocities were measured by use of an acoustical-Doppler probe. The time-averaging period was 3 minutes. Wave heights were measured by use of a water surface follower (accuracy = 0.02m) and an acoustical probe (accuracy-0.1 m). The mean water depths were measured at still water. Sand concentrations were determined by taking water-sediment samples (pump sampler). Six samples were collected simultaneously in each vertical. The time-averaging period was 2.5 minutes. The intake velocity was 4 m/s.

References

Vellinga, P., 1984

Large-scale Dune Erosion Tests in the Deltaflume (in Dutch)

Report M1263-III A/B, Delft Hydraulics Laboratory, Delft, The Netherlands.

Set: STEETZEL (NR 151-161)

Description

Flume experiments were carried out at the Delft Hydraulics Laboratory to study the dune erosion process. The flume had a length of 50 m, a width of 1.2 m and a depth of 1.2 m. The bed consisted of fine sand ($D_{50}=100 \mu\text{m}$). The concentration profiles reported in this set are those measured outside the dune erosion zone.

Wave conditions

Irregular waves were generated with a Pierson-Moskowitz energy spectrum.

Measuring instruments

Orbital velocities were measured by use of an acoustical-Doppler probe (measuring period of 5 to 10 minutes). Sand concentrations were measured by use of a pump sampler. Seven samples were collected simultaneously in each vertical. The time-averaging period was 10 minutes. Bedform averaging was used over a distance of 0.3 m.

Reference

Steetzel, H.J., 1985

Model Tests of Scour near the Toe of Dune Revetments (in Dutch).

Report M 2051-II, Delft Hydraulics Laboratory, Delft, The Netherlands

Set: ANDERSON (NR 166-188)

Description

Field measurements were carried out in the Enoree river (USA) to study the vertical concentration distribution. At the point of sample collection the river was about 50 feet wide with almost vertical banks. The sand bed consisted of non-uniform material with a mean size of about 700 μm . This data set comprises concentration profiles for the size fraction 175-250, 250-350, 350-500 and 500-700 μm . This is indicated by the letter A, B, C or D in the code of the measuring data (for example: Anderson IIA). The total concentration can be obtained by summation over the size-fractions.

Measuring instruments

The sampling instruments for the concentrations consisted of a number of tube-type samplers attached at regular intervals to the support which in turn was suspended on a sounding cable from a gaging car. The samples were collected in pint milk bottles. The suspended sand samples were splitted in a number of size fractions.

References

Anderson, A.A., 1942
Distribution of Suspended Sediment in a Natural Stream,
Transactions American Geophysical Union, USA

Set: SCOTT (NR 189-211)

Description

Field measurements were carried out in the Mississippi River at St. Louis, Missouri in 1961-1963 to determine the sediment discharges. Four sets of hydraulic and sediment data were obtained at ranges of mean velocity from 1 to 1.8 m/s, of mean depth from 6.6 to 11.1 m, of width from 470 to 500 m, of mean water surface slopes from 0.000054 to 0.000109. The medium size of the bed material was about 400 μm for three sets of measurements and about 180 μm for the other set. A dune bed form was present during all data collection periods.

Measuring methods

Velocities were measured by use of propeller-type instruments. Sediment concentrations were measured by use of the U.S.P -46 point- integrating sampler. The lowest sampling point was 1.5 feet above the bed. The BM-54 sampler was used to collect bed-material samples.

References

Scott, G.H. and Stephens, H.D., 1966
Special Sediment Investigation, Mississippi River at St. Louis,
Missouri, 1961-1963
Geol. Survey Water-supply Paper 1819-J, Washington, USA

Set: BARTON-LIN (NR 212-237)

Description

Flume measurements were carried out in the Colorado College, Fort Collins, USA. The experiments were performed in a tilting flume with a length of 21 m, a width of 1.2 m and a depth of 0.6 m. The sand bed consisted of 180 μ m material.

Measuring methods

Velocities were measured by use of pitot tubes. Suspended sand concentrations were measured by use of a pump sampler connected to a brass intake nozzle. All measurements were made in the centre line of the flume. The velocities and sand concentrations are given with respect to the mean elevation at the bed. The average water depth was determined by smoothing out the bed after the water has been shut off.

Reference

Barton, J.R., and Lin, P.N., 1955

A Study of the Sediment Transport in Alluvial Channels

Civ. Eng. Dep., Report No. 55JRBZ, Colorado College, Fort Collins, USA

Set: VESSEM (NR 238-307)

Description

Field measurements were carried out near the Galgeplaat, a tidal flat in the Eastern Scheldt estuary in the Netherlands. The measurements were performed during current and wave conditions from a fixed sampling station, which allowed an accurate positioning of the instruments in vertical direction. The local sand bed consisted of relatively fine material with a median size of about 150 μm . The local water depth varied in the range of 0.5 to 4 m. The velocities were not larger than about 1 m/s. The maximum significant wave height was about 0.7 m.

Measuring methods

Velocities were measured by use of an acoustical-Doppler probe at 0.3 m above the sand bed. Sand concentrations were determined by using a pump sampler. The intake nozzles of the sampler had an inner diameter of 3 mm. Seven to eight samples were collected simultaneously in each vertical. A volumetric method was used to determine the sand content. The measuring period was in the range of 5 to 10 minutes. The reported resulting depth-averaged velocity (V_{mr}) is an estimate based on extrapolation of the velocity measured at 0.3 m above the bed. The reported bed form height is an estimate based on the analysis of velocity profiles resulting in an effective roughness and based on visual inspection of the relict bed forms during the ebb period when the flat was dry.

Reference

Rijkswaterstaat, Deltadienst, Den Haag
Project Geomor

Set: STEETZEL (NR 308-412)

Description

The measurements were carried out in the (small) water tunnel of the Delft Hydraulics Laboratory applying a sinusoidal oscillating motion. The tunnel dimensions are: width-0.3 m, height-0.6 m. The sand bed (D10-155 μm , D50-220 μm , D90-310 μm) had a thickness of about 0.2 m and a length of about 4 m. The water depth above the sand bed was about 0.4 m. The test procedure was, as follows:(1) levelling of sand bed (flat bed), (2) vertical positioning of intake nozzles of concentration sampler, (3) generating of equilibrium bed forms and concentration profiles (1 hour), (4) measuring of concentration profiles, (5) levelling of sand bed (flat bed) and (6) measuring of vertical position of intake nozzles of concentration sampler. During the actual sampling period a series of about 5 sand concentration profiles was measured. Only, the profiles with smallest and largest concentrations are stored in this database. This is indicated by the letter A (largest concentrations) or the letter B (smallest concentrations) in the code of the measuring data (for example, STEETZEL 3A and STEETZEL 3B).

Measuring instruments

A Laser-Doppler velocity meter was used to measure the velocities in one reference point outside the bed boundary layer. A Siphon sampling system was used to take water-sediment samples and hence to determine the sediment concentrations. The Siphon sampling system consisted of a series of 10 intake nozzles connected to plastic hoses. The intake nozzles had an inner diameter of 0.003 m and were situated perpendicular (transverse) to the direction of the water motion. The intake velocity was about 4 m/s. All samples of each concentration profile were collected simultaneously. The sampling period was about 6 to 7 minutes (time-averaging). During the sampling period all intake nozzles were moved forwards and backwards over a horizontal length of about 0.3 m to average over the bed forms (bed-form averaging).

Reference

Steetzel, H.J., 1984

Sediment Suspension in an oscillating Water Motion close to the Sand Bed (in Dutch)
Coastal Engineering Dep, Delft Univ. of Technology, Delft, The Netherlands

Set: VELDEN (NR 413-566)

Description

The measurements were carried out in the (small) water tunnel of the Delft Hydraulics Laboratory applying a sinusoidal oscillating motion. The tunnel dimensions are: width-0.3 m, height-0.6 m. The sand bed had a thickness of about 0.2 m and a length of about 4 m. The water depth above the sand bed was about 0.4 m. Three types of sand material were used: D50-100, 200 and 360 μm . The test procedure was, as follows:(1) levelling of sand bed (flatbed), (2) vertical positioning of intake nozzles of concentration sampler, (3)generating of equilibrium bed forms and concentration profiles (1 hour), (4)measuring of concentration profiles, (5) levelling of sand bed (flat bed) and(6) measuring of vertical position of intake nozzles of concentration sampler. During the actual sampling period a series of about 5 sand concentration profiles was measured. Only, the profiles with smallest and largest concentrations are stored in this database. This is indicated by the letter A (largest concentrations) or the letter B (smallest concentrations) in the code of the measuring data (for example, VELDEN 110 A and VELDEN 110 B).

Measuring instruments

A Laser-Doppler velocity meter was used to measure the velocities in one reference point outside the bed boundary layer. A Siphon sampling system was used to take water-sediment samples and hence to determine the sediment concentrations. The Siphon sampling system consisted of a series of 10 intake nozzles connected to plastic hoses. The intake nozzles had an inner diameter of 0.003 m and were situated perpendicular (transverse) to the direction of the water motion. The intake velocity was about 4 m/s, All samples of each concentration profile were collected simultaneously. The sampling period was about 6 to 7 minutes (time-averaging). During the sampling period all intake nozzles were moved forwards and backwards over a horizontal length of about 0.3 m to average over the bed forms (bed-form averaging).

Reference

Velden, E van der 1986

Sediment Suspension in an oscillating Water Motion close to the Sand Bed (in Dutch)
Coastal Engineering Dep, Delft Univ. of Technology, Delft, The Netherlands

Set: ROELVINK (NR 567-592)

Description

Fluid velocities and sand concentrations were measured in breaking and non-breaking waves over a sand bed of about 210 μm in the DELTA-flume (length=233 m, width=5m, depth=7m) of DELFT HYDRAULICS.

Basically, cross-shore sediment transport was investigated. The initial bed profile consisted of a beach with a slope of 1:50, followed by a small section with a slope of 1:10 and a long flat section. In all, nine tests were carried out with different hydraulic conditions. Irregular waves were generated (Pierson-Moskowitz spectrum). The measurements reported here were carried out after the establishment of an equilibrium bed profile.

Measurements

Instantaneous fluid velocities were measured by use of an electro-magnetic current meter. Time-averaged sand concentrations were determined by collecting water-sediment samples with a pump sampling instrument. This latter instrument consisted of 10 intake nozzles (inner diameter =0.003 m) connected to a vertical rod which was attached to a carriage above the flume. The intake nozzles were situated perpendicular to the orbital plane. The 10 samples were collected simultaneously. The sampling period was about 15 minutes. The intake velocity was about 1 m/s. The fluid velocities were measured instantaneously at various elevations above the bed. The following characteristic values are stored in this database: the time-averaged fluid velocities (V_r) in the lower part of the water column representing the return flow of the breaking waves and the rms-value (U_{rms}) of the peak-velocities at 0.05 m above the bed (lowest measuring point). The significant values were computed as $U_{sig} = 1.41 U_{rms}$. Additionally, the significant values of the peak-velocities in landward and in seaward direction at 0.05 m above the bed are reported below:

NR	U_{sig} (m/s), landwards	U_{sig} (m/s), seawards
567	0.74	0.60
568	0.64	0.56
569	0.63	0.55
570	0.66	0.56
571	0.65	0.57
572	0.51	0.45
573	0.51	0.45
574	0.72	0.54
575	0.76	0.56
576	0.64	0.59
577	0.62	0.56
578	0.70	0.57
579	0.76	0.59
580	0.62	0.50
581	0.61	0.47
582	0.56	0.50
583	0.67	0.57
584	0.69	0.58
585	0.60	0.52
586	0.69	0.55
587	0.90	0.79

588	0.89	0.66
589	0.61	0.53
590	0.65	0.55
591	1.24	0.95
592	0.91	0.66

Bed-form data determined by analysing recordings of an echo-sounder and by visual observation after emptying the flume for some tests. In case of non-breaking waves the bed was covered with 3D-ripples (height approx. 0.02 m and length approx. 1 m).

References

Roelvink, J.A., 1987

Large scale investigation of cross-shore sediment transport
Report H596, Delft Hydraulics, Delft, The Netherlands

Set: STEETZEL (NR 593-600)

Description

Fluid velocities and sand concentrations were measured in breaking waves (inside breaker zone) over a sand bed of about 210 μm in the DELTA-flume (length=233m, width=5 m, depth=7 m) of DELFT HYDRAULYCS. Basically, dune erosion was investigated. The initial bed profile consisted of a protected dune with a slope of 1:2 and a foreshore with decreasing slopes of 1:10, 1:35 and 1:90. In all, three tests (T1, T2, T3) were carried out with different hydraulic conditions. Irregular waves were generated (Pierson-Moskowitz spectrum). The measurements reported here were carried out after the establishment of an equilibrium bed profile.

Measurements

Instantaneous fluid velocities were measured by use of an electro-magnetic current meter. Time-averaged sand concentrations were determined by collecting water-sediment samples with a pump sampling instrument. This latter instrument consisted of 10 intake nozzles (inner diameter = 0.003 m) connected to a vertical rod which was attached to a carriage above the flume. The intake nozzles were situated perpendicular to the orbital plane. The 10 samples were collected simultaneously. The sampling period was about 15 minutes. The intake velocity was about 1 m/s. The fluid velocities were measured instantaneously at various elevations above the bed. The following characteristic values are stored in this database: the time-averaged velocities (V_r) in the lower part of the water column representing the return flow of the breaking waves. Additionally, the significant values of the peak-velocities in landward and in seaward direction at 0.05 m above the bed are reported below:

NR	U_{sig} (m/s), landwards	U_{sig} (m/s), seawards
593	1.65	1.20
594	1.80	1.30
595	1.80	1.40
596	1.40	1.00
597	1.60	1.10
598	1.80	1.30
599	1.40	1.00
600	1.40	0.90

The values of the particle sizes and fall velocities stored in the database are averages of all samples collected in the breaker zone. Data of the bed forms were not collected. Probably, the bed was smooth in the breaker zone.

References

Steetzel, H.J., 1987
Systematic Investigation of Dune Revetments; Large-scale model tests
Report H298-I, Delft Hydraulics, Delft, The Netherlands

Set: VAN RIJN (NR 601-613)

Description

Fluid velocities and sand concentrations were measured in breaking and non-breaking waves over a sand bed of about 200 μm in the DELTA-flume (length=233m, width=5m, depth=7m) of DELFT HYDRAULICS.

The measurements were performed at various locations, outside the breaker zone, where the local bed slope was almost zero. Irregular waves were generated (Pierson-Moskowitz spectrum).

Measurements

Instantaneous velocities were measured at 0.2 m above the bed using an electromagnetic current meter. The rms-value of the peak-velocities is reported in this database. Time-averaged sand concentrations were determined by collecting water-sediment samples with pump samplers. This latter instrument consisted of 10 intake nozzles (inner diameter = 0.003 m) connected to a vertical rod which was attached to a carriage above the flume. The intake nozzles were situated perpendicular to the orbital plane. The 10 samples were collected simultaneously. The intake velocity was about 1 m/s. The sampling period was about 15 minutes. Only time-averaged sand concentrations were measured. Bed-form data were determined by analysing recordings of an echo-sounder and by visual observation after emptying the flume. Very small ripples with a height of a few millimetres were present in case of relatively large waves. Large-scale three-dimensional bed forms with a height of 0.02 m and a length of about 1 m were present in case of relatively small waves. These large-scale bed forms were superimposed by small-scale two-dimensional ripples with a height of 0.005 m and a length of 0.1 m.

References

Van Rijn, L.C., 1988

Handbook of Sediment Transport in currents and waves

Delft Hydraulics, Delft, The Netherlands

Set: NIEUWJAAR (NR 614-641)

Description

Time-averaged fluid velocities and sand concentrations were measured in irregular non-breaking waves combined with opposing and following currents over a sand bed of about 200 μm . The measurements were performed in a flume (length =35m, width=0.8m, depth=1.0m) of the Delft University of Technology. The water depth was about 0.5 m in all tests. The depth-averaged velocities were in the range of 0.1 to 0.4 m/s. The significant wave heights were in the range of 0.075 to 1.75 m.

Measurements

Instantaneous fluid velocities were measured by use of an electromagnetic current meter. Time-averaged values were obtained by applying an electronic time integrator. The averaging period was 256 seconds. The fluid velocities were measured in 10 points above the bed by raising the velocity probe after each measurement. The velocity probe was attached to a carriage on top of the flume. Time-averaged sand concentrations were determined by collecting water-sediment samples with a pump-sampling instrument. This instrument consisted of 10 intake nozzles (inner diameter 0.003 m) connected to a vertical rod which was attached to the carriage on top of the flume. The intake nozzles were situated perpendicular to the orbital plane. The 10 samples were collected simultaneously at 10 points above the bed. The sampling period was about 15 minutes. The intake velocity was about 1.4 m/s. During measurement of the fluid velocities and sand concentrations, the carriage on top of the flume was moving forward and backward over a distance of about 0.6 m to average over the bed forms.

References

- Nieuwjaar, M. and Kaay, Th. van der, 1987
Sediment Concentrations and Sediment Transport in case of Irregular Non-Breaking Waves with a Current.
Delft University, Civil Engineering, Delft, The Netherlands

Set: NAP/ VAN KAMPEN (NR 642-671)

Description

Time-averaged fluid velocities and sand concentrations were measured in irregular non-breaking waves combined with opposing and following currents over a sand bed of about 100 μm . The measurements were performed in a flume (length =35m, width=0.8m, depth=1.0m) of the Delft University of Technology. The water depth was about 0.5 m in all tests. The depth-averaged velocities were in the range of 0.1 to 0.4 m/s. The significant wave heights were in the range of 0.075 to 0.18 m.

Measurements

Instantaneous fluid velocities were measured by use of an electromagnetic current meter. Time-averaged values were obtained by applying an electronic time integrator. The averaging period was 256 seconds. The fluid velocities were measured in 10 points above the bed by raising the velocity probe after each measurement. The velocity probe was attached to a carriage on top of the flume. Time-averaged sand concentrations were determined by collecting water-sediment samples with a pump-sampling instrument. This instrument consisted of 10 intake nozzles (inner diameter =0.003 m) connected to a vertical rod which was attached to the carriage on top of the flume. The intake nozzles were situated perpendicular to the orbital plane. The 10 samples were collected simultaneously at 10 points above the bed. The sampling period was about 15 minutes. The intake velocity was about 1.4 m/s. During measurement of the fluid velocities and sand concentrations, the carriage on top of the flume was moving forward and backward over a distance of about 0.6 m to average over the bed forms.

References

NAP, E.N. and Van KAMPEN, H.F.A., 1988
Sediment Concentrations and Sediment Transport in case of
Irregular Non-Breaking Waves with a Current.
Delft University, Coastal Engineering Department, Delft, The Netherlands

Set: VOOGT (NR 672-731)

Description

Fluid velocities sand concentrations were measured in a tidal channel(Krammer) of the Eastern Scheldt estuary in the south west part of The Netherlands. The measurements were carried out on top of a sand dam. The median particle size of the bed material was about 250 μm .

The measuring dates and locations are as follows:

Station	Date	Time (MET)
Mp1/Mp6	01-04-1987	8.15 - 11.09
Mp2	08-04-1987	6.34 - 10.24
Mp2	11-04-1987	11.15- 14.09
Mp3	11-04-1987	11.00- 13.56
Mp2	14-04-1987	13.30- 15.39

Measurements

The flow velocities and concentrations were measured using an acoustic sand transport meter (ASTM) at elevations of 0.2 m, 1.0 m, at mid depth and at 2 m below the water surface. Additionally, concentrations were measured at elevations of 0.05 m, 0.1 m and 0.2 m above the bed using a pump system. The flow velocities at these latter elevations were obtained from extrapolation applying the ASTM-measurements between 0.2 m and the water surface. Bed form data were analysed to determine the bed roughness. The effective bed roughness was found to be 0.4 m at velocities of 1.5 m/s, about 0.5 m at velocities of 1.8 m/s and about 0.2 m at velocities of 2.2 m/s.

References

Voogt, L. , Van Rijn, L.C. and Van de Berg, J.H. 1991
Bed Roughness and Transport of Fine Sands at High Velocities.
Journal of Hydraulic Engineering, ASCE, HY6.

Set: CULBERTSON (NR 732-753)

Description

Field measurements were carried out at high discharges in the Rio Grande Conveyance Channel, New Mexico in the period from 1965 to 1969. The channel bed consisted of fine sands with median diameters ranging from 150 to 350 μm and the bed forms varied from dunes to flat bed. The channel banks were composed of a sandy clay and were fairly well stabilised by salt cedar and range grass.

Measurements

Vertical velocity profiles were obtained with standard Price current meters. Five current meters were mounted on a sounding rod. The measuring period was one minute. The average of five individual measurements are given. Sand concentration profiles (material larger than 62 μm) were obtained at five points over the water depth. The samples were taken with a U.S. DH-48 sampler modified for point sampling. The sampling period was about 6 seconds for high velocity flows. One to three samples were taken in each point and the results were averaged. The mean suspended sediment size (particle larger than 62 μm) reported herein is the median particle diameter of depth-integrated samples. Water surface slopes were determined from staff-gage readings near the banks. Generally, these values were consistent for any given day. Profiles of the streambed were obtained with an ultra sonic sounder mounted in a boat.

Reference

Culbertson, J.K., Scott, C.H. and Bennet, J.P., 1972

Summary of Alluvial Channel Data from Rio Grande Conveyance Channel, New Mexico 1965-1969

Geological Survey Professional Paper 562-J, Washington, USA

Set: DETTE (NR 754-764)

Description

Sand concentration measurements were carried out in the large wave flume of Hannover (length=324m, depth=7m, width=5m). Three test series were carried out, being:

NR	Test Serie
754-757	Coastal dune without foreshore, regular waves
758-761	Coastal dune without foreshore, irregular waves
762-764	Coastal dune with foreshore, regular waves

The dune had an initial slope of 1 to 4. The foreshore had an initial slope of 1 to 20. The sand concentrations were determined at various locations in the breaker zone after the establishment of an equilibrium bed profile. The profiles are given by Dette and Uliczka (see reference).

Wave conditions

Regular and irregular waves (Jonswap spectrum) were generated.

Measuring instruments

Sand-water samples were collected in ten points above the bed simultaneously by use of a pumping system. The intake nozzles had an inner diameter of 3 mm. The intake velocity at the nozzle was about 1 m/s. The nozzles were attached to a vertical pipe. The intake direction was perpendicular to the orbital plane.

References

Dette, H. and Uliczka, K., 1986.

Sediment Concentration at Prototype Equilibrium Profile.

Technical Report No. 4 - SFB 205/TP A6, University of Hannover, 1986

Dette, H. and Uliczka, K., 1986.

Velocity and sediment concentration Fields across Surf Zones.

Twentieth Coastal Eng. Conf., Taiwan

Set: LAURSEN (NR 765-776)

Description

Sand concentration and flow velocity measurements were carried out in a flume of the IOWA Institute of Hydraulic Research, USA. The flume was a re-circulating, tilting flume with a length of about 30m, a width of 0.9 m and a depth of 0.45 m. Two size classes of bed material were used: 40 μm - sand and 100 μm - sand. The water depths were in the range of 0.07 to 0.3 m, the depth-averaged velocities were in the range of 0.4 to 0.7 m/s. For the coarser sand, only centreline distributions of velocity and concentrations were determined. For the finer sand, complete traverses were made across the flow section. Measurements of the dune sizes could be obtained in the case of the coarser sand.

Measuring instruments

Values of velocity and concentration at a point were obtained by two pitot tubes mounted on each side of a water intake nozzle. A variable speed pump was used to establish the desired rate of flow into the sampler-intake nozzle. The amount of sediment in the samples was determined by weighing.

Reference

Laursen, E.M., 1957

An Investigation of the Total Sediment Load

IOWA Institute of Hydraulic Research, State University of Iowa, Iowa City,
United States of America.

Set: RIBBERINK (NR 777-824)

Description

Sand concentration measurements were carried out in the large oscillating wave tunnel of Delft Hydraulics (length=14.0m, width=0.3m, depth=1.1m). Regular and irregular waves were generated.

Eight experiments (T1 to T5) were carried out in the low velocity regime and twenty experiments (T10-T29) were carried out in the high velocity regime.

The experimental procedure in each experiment was, as follows:

- * flatten sand bed
- * measure bed level
- * start oscillating water motion, measure velocity
- * establish equilibrium conditions (full grown ripples)
- * measure time-averaged concentrations
- * measure ripple dimensions

Measuring instruments

The instantaneous horizontal flow velocity was measured by a Laser Doppler system outside the wave boundary layer. The time-averaged sand concentrations were determined from water-sediment samples taken by use of pumps (transverse suction). All concentrations were measured simultaneously.

For the experiments T1 to T8 the intake nozzles were attached to a carriage moving forwards and backwards during sampling (bed form averaging). For the experiments T10 to T29 the concentration profiles were measured at fixed positions above the bed (crest, trough, and side slopes (not reported herein)). The height of the lowest intake nozzle is given with respect to the average bed level (after flattening of the bed forms) for the experiments T1 to T18 and with respect to the local bed level for the experiments T19 to T29.

References

Ribberink, J.S. and Al-Salem, A.A., 1989

Bed forms, Near-bed sediment concentrations and Sediment Transport in simulated regular wave conditions. Report H840, part III, Delft Hydraulics, Delft, The Netherlands

Set: HAVINGA (NR 828-852)

Description

Time-averaged fluid velocities and sand concentrations were measured in irregular non-breaking waves combined with a current. The measurements were performed in a wave-current basin (20 x 26 m²). The current was confined in a channel (length=26m, width=4m, parallel to wave generator) by guiding plates normal to the wave generator. The bed of the channel consisted of fine sand ($d_{50} = 100 \mu\text{m}$, $d_{90} = 130 \mu\text{m}$). The water depth was approx. 0.4 m in all tests. The significant wave height was ranging from 0.07 to 0.14 m, peak period of 2.3 s. The depth-averaged velocities were ranging from 0.1 to 0.3 m/s. The angle between the current and wave direction was 60°, 90° and 120° respectively. The test numbers refer to the hydraulic conditions. For example T14.30 means a significant wave height of approx. 14 cm, a current velocity of approx. 30 cm/s and a wave-current angle of approx. 90°.

Measurements

Instantaneous fluid velocities were measured by use of an electromagnetic current meter. Time-averaged values were obtained by applying an electronic time integrator. The averaging period was 256 seconds. The fluid velocities were measured in 10 points above the bed raising the velocity probe after each measurement. The velocity probe was attached to a carriage above the channel. Time-averaged sand concentrations were obtained by collecting water-sediment samples with a pump-sampling instrument. This instrument consisted of 10 intake nozzles (inner diameter = 0.003 m) connected to a vertical rod which was attached to the carriage. The intake nozzles were situated perpendicular to the orbital plane. The 10 samples were collected simultaneously at 10 points above the bed. The sampling period was about 15 minutes.

The intake velocity was about 1.4 m/s. During measurement of the fluid velocities and sand concentrations, the carriage was moving forward and backward over a distance of about 0.6 m to average over the bed forms. Bed form dimensions were measured by means of a bed profile follower. The dimensions of the bed forms in the wave and in the current direction are reported in the following table:

NR	Bed form height (m)		Bed form length (m)	
	in wave direction	in current direction	in wave direction	in current direction
828	0.0081	0.0079	0.054	0.147
829	0.0066	0.0070	0.056	0.090
830	0.0078	0.0095	0.104	0.085
831	0.0068	0.0078	0.051	0.140
832	0.0075	0.0073	0.057	0.111
833	0.0081	0.0081	0.064	0.086
834	0.0073	0.0073	0.060	0.135
835	0.0083	0.0097	0.067	0.126
836	0.0078	0.0098	0.061	0.120
837	0.0038	0.0085	0.040	0.106
838	0.0122	0.0134	0.107	0.097
839	0.0114	0.0100	0.093	0.088
840	0.0076	0.0076	0.057	0.112
841	0.0123	0.0129	0.106	0.095
842	0.0097	0.0124	0.086	0.091
843	0.0078	0.0060	0.066	0.118

844	0.0097	0.0104	0.079	0.092
845	0.0134	0.0139	0.120	0.101
846	0.0066	0.0085	0.061	0.068
847	0.0066	0.0069	0.051	0.084
848	0.0074	0.0087	0.065	0.093
849	0.0126	0.0137	0.097	0.113
850	0.0072	0.0079	0.060	0.099
851	0.0077	0.0089	0.067	0.082
852	0.010	0.0091	0.092	0.099

References:

Havinga, F.J., 1992

Sediment Concentrations and Sediment Transport in case of Irregular Non-Breaking Waves with a Current.

Dep. of Coastal Eng., Delft University of Technology, Delft, The Netherlands.

Set: KROON (NR 853-914)

Description

Fluid velocities and sediment concentrations were measured in the (coastal)swash zone and surf zone near Egmond aan Zee, The Netherlands. The measurements were performed from a small ($2 \times 2 \text{ m}^2$) movable platform. The morphology of the nearshore zone is characterised by two breaker bars and a swash bar on the beach. The foreshore is rather steep ranging from 2° to 7° . The mean grain size is between 250 and 350 μm . The mean annual significant height of the incoming waves is 1.3 m (south western to north western directions). The mean semi-diurnal range of the tide is 1.65 m. The tidal velocity curve is asymmetrical with a 4 hour flood period and an 8 hour ebb period.

Measurements

Instantaneous fluid velocities were measured by electromagnetic current meters. Instantaneous water level elevations were measured by a capacity wire. The data were stored on a data logging system. Time-averaged sediment concentrations were obtained from water-sediment samples taken by a pump system. Simultaneous measurements in 7 to 10 points were performed. The sampling period was about 10 to 15 minutes. Each data set is given in two data sheets (1A, 1B, 2A, 2B etc). Both sheets are different with respect to the velocity profile. Sheet A refers to the cross-shore velocities; sheet B refers to the longshore velocities. The other data on both sheets are identical. The peak orbital velocities (significant values) near the bed in the onshore and offshore directions are given in the following table.

NR	$\bar{U}_{\text{on,sig}}(\text{m/s})$	$\bar{U}_{\text{off,sig}}(\text{m/s})$
853,854	1.36	0.818
855,856	0.868	0.585
857,858	0.982	0.679
859,860	0.902	0.647
861,862	0.982	0.639
863,864	1.2	0.794
865,866	1.37	0.909
867,868	1.47	0.983
869,870	1.6	1.09
871,872	1.86	1.08
873,874	1.81	1.11
875,876	0.8706	0.6248
877,878	0.714	0.5708
879,880	0.7766	0.5989
881,882	0.886	0.78
883,884	0.927	0.7717
885,886	0.9507	0.6846
887,888	1.2225	0.8376
889,890	0.5624	0.4642
891,892	0.5033	0.4529
893,894	0.4818	0.4417
895,896	0.5542	0.4593
897,898	1.649	1.4378
899,900	1.3543	1.1932
901,902	1.4984	1.2749

903,904	1.6224	1.5137
905,906	1.4353	1.0919
907,908	1.0449	0.839
909,910	0.9879	0.7786
911,912	0.9521	0.7538
913,914	0.9313	0.7582

References

Kroon, A, 1991

Suspended-Sediment Concentrations in a Barred Nearshore Zone
Coastal Sediments, Seattle, USA.

Kroon, A., and Van Rijn, L.C., 1992

Suspended Sediment Fluxes in the Nearshore Zone at Egmond.
Dep. of Phys. Geography, Univ. of Utrecht, The Netherlands.

Set: RIBBERINK (NR 915-937)

Description

Sand concentration measurements were carried out in the large oscillating wave tunnel of Delft Hydraulics (length=14.0m, width=0.3m, depth=1.1m). Regular and irregular waves were generated. The experiments were carried out in the high and low velocity regime. The experimental procedure in each experiment was, as follows:

- * flatten sand bed
- * measure bed level
- * start oscillating water motion, measure velocity
- * establish equilibrium conditions (full grown ripples)
- * measure time-averaged concentrations with respect to flattened bed
- * measure ripple dimensions

Measuring instruments

The instantaneous horizontal flow velocity was measured by a Laser Doppler system outside the wave boundary layer. During tests T1 to T12 and B13 to B20, the time-averaged sand concentrations were obtained from water-sediment samples taken by use of a pump system (transverse suction). All concentrations were measured simultaneously. The concentration profiles were measured at fixed locations during approx. 15 minutes. The height of the lowest intake nozzle is given with respect to the average bed level (after flattening of the bed forms). During the test C9 to C10, the time-averaged concentrations were measured by means of an optical probe. Each concentration was measured separately starting at the lowest point and working upwards. The measurements were repeated several times to eliminate random errors related to the measuring location. Net transport rates (in wave propagation, positive sign) were also measured from bed level changes before and after each test. These transport rates are stored as bed-load transport data. The peak orbital velocity near the bed during passage of the wave crest (\hat{U}_c) and the wave trough (\hat{U}_t) are reported in the following tables. The significant values are reported for irregular waves.

Irregular asymmetric waves (Jonswap spectrum)

NR	Test	$\hat{U}_{c, sig}$ (m/s)	$\hat{U}_{t, sig}$ (m/s)
915	1	1.20	0.73
916	2	0.80	0.52
917	3	1.08	0.70
918	4	1.17	0.73
919	5	0.79	0.49
920	6	1.11	0.70

Regular asymmetric waves

NR	Test	\hat{U}_c (m/s)	\hat{U}_t (m/s)
921	7	0.95	0.5
922	8	1.31	0.7
923	9	1.72	0.86
924	10	0.96	0.53
925	11	1.25	0.69
926	12	1.75	0.99

Regular asymmetric waves

NR	Test	\bar{U}_c (m/s)	\bar{U}_t (m/s)
927	B13	1.20	0.90
928	B14	1.19	0.92
929	B15	0.98	0.54
930	B16	1.03	0.63

Irregular asymmetric waves (Jonswap spectrum)

NR	Test	$\bar{U}_{c,sig}$ (m/s)	$\bar{U}_{t,sig}$ (m/s)
931	B17	0.44	0.28
932	B18	0.64	0.37
933	B19	0.66	0.39
934	B20	0.60	0.38

Regular asymmetric waves

NR	Test	\bar{U}_c (m/s)	\bar{U}_t (m/s)
935	C8	1.10	0.60
936	C9	1.10	0.60

Regular symmetric waves

NR	Test	\bar{U}_c (m/s)	\bar{U}_t (m/s)
937	C10	1.7	1.7

References

Ribberink, J.S. and Al-Salem, A., 1991

Sediment Transport, Sediment Concentrations and Bed Forms in Simulated Asymmetric Wave Conditions.

Report H840.20 Part IV, Delft Hydraulics, The Netherlands.

Ribberink, J.S., and Al-Salem, A., 1992

Sediment Transport, Sediment Concentrations and Bed Forms in Simulated Asymmetric Wave Conditions.

Report H840.20 Part V, Delft Hydraulics, Delft, The Netherlands.

Ribberink, J.S., and Al-Salem, A., 1992

Time-Dependent Sediment Transport Phenomena in Oscillatory Boundary Layer Flow under Sheet Flow Conditions.

Report H840.20 Part VI, Delft Hydraulics, Delft, The Netherlands.

Set: GRASMEIJER/ SIES (NR 938-1004)

Description

All experiments were conducted in the 'Grote Spuurwerk'-flume, a flume of the Laboratory of Fluid Mechanics of the Faculty of Civil Engineering of the Delft University of Technology. The total length of the flume is 45 m, the width 0.8 m and the flume has a depth of 1.0 m. This makes it possible to perform experiments with a 30 m bed length. The irregular waves are generated by the irregular movements of the wave paddle. The desired wave spectrum is created by a computer file. The spectrum is single topped, with a peak frequency of 0.4 Hz and a JONSWAP-shape. In this experiment only current in wave direction is investigated.

For test series A at the front of the sand bed a fixed-bed slope of 1:20 was situated to create a water depth of approximately $h=0.30$ m at the test section. The sand bed has a slope of 1:100 to provide enough length in which the wave height and percentage breaking waves remained constant.

In series B the sediment transport processes over a sand bar are studied. The sand bar is a representation of the sand bar at Egmond, the Netherlands. The seaward upsloping part of the sand bar has a slope of 1:20. The water depth on top of the bar is 0.30 m. The downsloping part of the sand bar has a slope of 1:25, and the landward upsloping part in the profile has a slope of 1:63.

Measurements

A time- and bed averaging method was used to reduce variations in the concentration measurements. The bed-averaging was performed as in former studies: the measuring instruments were mounted on a moving carriage. In series A the carriage moved over 0.70 m and vice versa, with a speed of 0.02 m/s. In series B the carriage moved over only 15 cm, because of the presence of the steep bar slopes. To determine the mean bed level in the measuring section, a Profile Follower (PROFO) was used. This instrument was mounted on the moving carriage. To get an estimation of the desired current velocity U_m , the discharge Q was measured using a Rehbock weir. Near the wave board the water level was determined using a point gauge.

In each experiment (series A and B), the wave spectrum was determined at two locations in the flume. In series A one wave height meter was placed on the carriage and the second was placed 0.70 m behind the carriage, to check the first. In series B one wave height meter was placed on the carriage and one on top of the sand bar.

The sediment concentration measurements were carried out using an array of 10 brass intake tubes of 3mm internal diameter. This concentration sampling instrument was attached to the moving carriage; the openings of the intake tubes were placed perpendicular to the current direction. Each tube was connected to a pump, bringing the sediment and water mixture with a 1.5 m/s intake velocity in a 10 litre bucket. The intake tubes were used to determine the concentration distribution over the water depth. In all experiments instantaneous sediment concentrations were measured by means of the ASTM.

The fluid velocities were measured using an Electro Magnetic Velocity meter (EMS). The EMS was also attached to the moving carriage. The fluid velocities were measured at the

same height position above mean bed level as the intake tubes of the concentration sampler. In each experiment ripple registrations were made using the PROFO and a pen recorder. These registrations were done before and after each test.

Two bed material samples were taken during all tests. These two samples were analysed in the Visual Accumulation Tube of Delft Hydraulics. Also the suspended sediment samples of each experiment, were analysed in the Visual Accumulation Tube. Based on these results the particle diameters D_{10} , D_{50} and D_{90} , and the fall velocity parameters w_{10} , w_{50} and w_{90} can be determined.

The experiments in series A are identified by a test number:

T xx yy zz

in which:

xx	significant wave height H_s	(cm)
yy	depth-averaged fluid velocity U_m	(cm/s)
zz	order number	

In series B measurements have been made in 10 cross-sections. In series B1 a relatively small wave height was present. The wave height on top of the bar was 0.177 m. The incoming wave height was 0.160 m.

In series B2 the wave height was slightly larger. On top of the sand bar a wave height of 0.201 m was measured. The incoming wave height was 0.189 m.

References

Grasmeijer B., Sies R., 1995

Sediment concentrations and sediment transport in irregular breaking waves.

Experimental results series A and B. Delft University of Technology, The Netherlands.

B Data report

Gradation effects on sand transport under oscillatory sheet-flow conditions

by

W.N. Hassan, D.F. Kroekenstoel, J.S. Ribberink, L.C. van Rijn

University of Twente

WL Delft Hydraulics

Contents

List of Tables

List of Figures

1.	INTRODUCTION	2
1.1	Sand transport problem	2
1.2	Previous work (literature)	2
1.3	Objectives of present experiments	3
1.4	Framework and execution of the study	3
1.5	Summary	4
2	EXPERIMENTAL SET-UP	5
2.1	Measurement programme	5
2.2	Bed material (sand)	8
2.3	Wave tunnel and instruments	9
2.3.1	Large Oscillating Water Tunnel	9
2.3.2	Measuring instruments	12
2.4	Analysis methods	21
2.4.1	Computation of net sand transport rates (mass conservation technique)	21
2.4.2	Computation of net sand transport rates per fraction	21
2.4.3	Computation of orbital velocities outside wave boundary layer	22
2.4.4	Computation of sand concentration in sheet-flow layer (CCM results)	23
2.4.5	Computation of particle size composition from settling tube tests (VAT)	24
2.5	Steering signals, data acquisition and storage	25

3	EXPERIMENTAL RESULTS	27
3.1	Orbital velocities outside wave boundary layer	27
3.2	Net sand transport rates	30
	3.2.1 Introduction	30
	3.2.2 Net sand transport rates for both fractions	30
	3.2.3 Net sand transport rates per fraction	35
3.3	Composition of sand	36
	3.3.1 Composition of bed material before and after tests	36
	3.3.2 Composition of bed load transport (PBLT)	38
	3.3.3 Composition of sand from sand traps	40
	3.3.4 Composition of suspended sand (TSS)	42
3.4	Sand concentrations in sheet-flow layer, CCM results	43
3.5	Bed load and suspended concentrations	49
	3.5.1 Bed load concentrations	49
	3.5.2 Suspended sediment concentrations (TSS)	50
3.6	Bed level variations based on video recording	52
4	EVALUATION OF EXPERIMENTAL RESULTS	53
4.1	Summary of present results (graded sand)	53
4.2	Summary of previous experimental results (uniform and graded sand)	56

List of Tables

Chapter 2

Table 2.1:	Test programme series P
Table 2.2:	Overview of instruments used for each test
Table 2.3:	Measuring instruments/methods for series P
Table 2.4:	Test results of PBLT during previous tests in wave tunnel
Table 2.5:	Measured signals, channel codes and calibration factors

Chapter 3

Table 3.1:	Flow velocities for all tests of condition P6A (measured by LDA)
Table 3.2:	Flow velocities for all tests of condition P7A (measured by LDA)
Table 3.3:	Flow velocities for all tests of condition P9A (measured by LDA)
Table 3.4:	Flow velocities for different conditions, sand type B (measured by LDA)
Table 3.5:	Total net sand transport rates (series P)
Table 3.6:	Net sand transport rates per fraction (series P)
Table 3.7:	Composition bed load transport (PBLT)
Table 3.8:	Composition of sand from sand traps
Table 3.9:	Bed load concentrations (PBLT)
Table 3.10:	Bed level variations during the wave cycle, for different flow conditions

Chapter 4

Table 4.1:	Summary of present experiments
Table 4.2:	Standard deviation and relative error of present experiments
Table 4.3:	Summary of previous experiments with 2 nd order Stokes waves
Table 4.4:	Sand characteristics for series K
Table 4.5:	Sand characteristics for series P

Appendix A

Table A.1:	Net sand transport rates, tests of condition P6A
Table A.2:	Net sand transport rates, tests of condition P7A
Table A.3:	Net sand transport rates, tests of condition P9A
Table A.4:	Net sand transport rates for coarse sand, different flow conditions
Table A.5:	Intervals used for determining net sand transport rates, condition P6A
Table A.6:	Intervals used for determining net sand transport rates, condition P7A
Table A.7:	Intervals used for determining net sand transport rates, condition P9A
Table A.8:	Intervals used for determining net sand transport rates for tests with coarse sand, different flow conditions

Appendix B

Table B.1:	Sand bed composition before and after each test, different layers along the tunnel, condition P6A
Table B.2:	Sand bed composition before and after each test, different layers along the tunnel, condition P7A
Table B.3:	Sand bed composition before and after each test, different layers along the tunnel, condition P9A
Table B.4:	Composition of sand collected inside the two sand traps, condition P6A
Table B.5:	Composition of sand collected inside the two sand traps, condition P7A
Table B.6:	Composition of sand collected inside the two sand traps, condition P9A

Appendix C

Table C.1:	Bed load concentrations and composition measured by PBLT, condition P6A
Table C.2:	Bed load concentrations and composition measured by PBLT, condition P7A
Table C.3:	Bed load concentrations and composition measured by PBLT, condition P9A
Table C.4:	Total sand transport rates and transport rates per fraction, condition P6A
Table C.5:	Total sand transport rates and transport rates per fraction, condition P7A
Table C.6:	Total sand transport rates and transport rates per fraction, condition P9A
Table C.7:	Calculation of net sand transport rates per fraction, condition P6A
Table C.8:	Calculation of net sand transport rates per fraction, condition P7A
Table C.9:	Calculation of net sand transport rates per fraction, condition P9A

Appendix D

Table D.1:	Concentration and composition of suspended load, measured by TSS, condition P6A
Table D.2:	Concentration and composition of suspended load, measured by TSS, condition P7A
Table D.3:	Concentration and composition of suspended load, measured by TSS, condition P9A

Appendix E

Table E.1:	CCM elevations, time intervals for data processing and time- and ensemble-averaged values, all tests of condition P6A
Table E.2:	CCM elevations, time intervals for data processing and time- and ensemble-averaged values, all tests of condition P7A
Table E.3:	CCM elevations, time intervals for data processing and time- and ensemble-averaged values, all tests of condition P9A

List of Figures

Chapter 2

- Figure 2.1: Grain-size distribution of the base materials and the mixture
Figure 2.2: General outline of wave tunnel
Figure 2.3: Laser-beam configuration in the tunnel
Figure 2.4: Configuration of Bed Level Sounding System (BLSS), measurement carriage
Figure 2.5: Configuration of Bed Level Sounding System (BLSS), general layout
Figure 2.6: General outline of Transverse Suction System (TSS)
Figure 2.7: CCM configuration in the tunnel and CCM probe outline
Figure 2.8: Configuration of measured velocity components by LDA in the tunnel

Chapter 3

- Figure 3.1: Ensemble-averaged flow velocities outside the wave boundary layers, measured by LDA for different flow conditions
Figure 3.2: Net sand transport rates for different flow conditions (sand type A)
Figure 3.3: Net sand transport rates for different flow conditions (sand type B)
Figure 3.4: Net sand transport rates per fraction for different flow conditions
Figure 3.5: Distribution of the percentage of coarse fraction with depth for different flow conditions
Figure 3.6: Bed load composition, measured by PBLT, for different flow conditions
Figure 3.7: Composition sand from sand traps for different flow conditions
Figure 3.8: Vertical distribution of d_{50} of suspended sediment (TSS), 3 flow conditions
Figure 3.9: Time-averaged concentration profile inside the sheet-flow layer, measured by CCM, on log-linear scale, for different flow conditions
Figure 3.10: Ensemble-averaged concentrations inside the sheet-flow layer, measured by CCM at different elevations above the bed, together with the free-stream velocity, condition P6A
Figure 3.11: Ensemble-averaged concentrations inside the sheet-flow layer, measured by CCM at different elevations above the bed, together with the free-stream velocity, condition P7A
Figure 3.12: Ensemble-averaged concentrations inside the sheet-flow layer, measured by CCM at different elevations above the bed, together with the free-stream velocity, condition P9A
Figure 3.13: Bed load concentrations, measured by PBLT, for different flow conditions
Figure 3.14: Time-averaged suspended concentrations (TSS), 3 flow conditions, on a log-linear scale
Figure 3.15: Definition sketch of overall bed lowering and bed level variation during wave cycle

Appendix A

- Figure A.1: Net sand transport rates along the tunnel, tests of condition P6A
Figure A.2: Net sand transport rates along the tunnel, tests of condition P7A
Figure A.3: Net sand transport rates along the tunnel, tests of condition P9A
Figure A.4: Net sand transport rates along the tunnel, coarse sand, test P6B1
Figure A.5: Net sand transport rates along the tunnel, coarse sand, test P6B2
Figure A.6: Net sand transport rates along the tunnel, coarse sand, test P7B1
Figure A.7: Net sand transport rates along the tunnel, coarse sand, test P9B1
Figure A.8: Net sand transport rates along the tunnel, coarse sand, sine wave + net current, test PSB1
Figure A.9: Bed levels, measured before and after, and net change of bed level, test P6A1
Figure A.10: Bed levels, measured before and after, and net change of bed level, test P6A2
Figure A.11: Bed levels, measured before and after, and net change of bed level, test P6A3
Figure A.12: Bed levels, measured before and after, and net change of bed level, test P6A4
Figure A.13: Bed levels, measured before and after, and net change of bed level, test P7A2
Figure A.14: Bed levels, measured before and after, and net change of bed level, test P7A3
Figure A.15: Bed levels, measured before and after, and net change of bed level, test P7A4
Figure A.16: Bed levels, measured before and after, and net change of bed level, test P7A5
Figure A.17: Bed levels, measured before and after, and net change of bed level, test P9A1
Figure A.18: Bed levels, measured before and after, and net change of bed level, test P9A2
Figure A.19: Bed levels, measured before and after, and net change of bed level, test P9A3
Figure A.20: Bed levels, measured before and after, and net change of bed level, test P9A4
Figure A.21: Bed levels, measured before and after, and net change of bed level, test P6B1

- Figure A.22: Bed levels, measured before and after, and net change of bed level, test P6B2
 Figure A.23: Bed levels, measured before and after, and net change of bed level, test P7B1
 Figure A.24: Bed levels, measured before and after, and net change of bed level, test P9B1

Appendix B

- Figure B.1: Distribution of the percentage of coarse fraction with depth, tests of condition P6A
 Figure B.2: Distribution of the percentage of coarse fraction with depth, average of condition P6A
 Figure B.3: Distribution of the percentage of coarse fraction with depth, tests of condition P7A
 Figure B.4: Distribution of the percentage of coarse fraction with depth, average of condition P7A
 Figure B.5: Distribution of the percentage of coarse fraction with depth, tests of condition P9A
 Figure B.6: Distribution of the percentage of coarse fraction with depth, average of condition P9A
 Figure B.7: Bed composition, measured after, test P6A1
 Figure B.8: Bed composition, measured after, test P6A2
 Figure B.9: Bed composition, measured after, test P6A3
 Figure B.10: Bed composition, measured after, test P6A4
 Figure B.11: Bed composition, measured after, average of condition P6A
 Figure B.12: Bed composition, measured after, average of top 9 mm, average of condition P6A
 Figure B.13: Bed composition, measured after, test P7A1
 Figure B.14: Bed composition, measured after, test P7A2
 Figure B.15: Bed composition, measured after, test P7A3
 Figure B.16: Bed composition, measured after, test P7A4
 Figure B.17: Bed composition, measured after, test P7A5
 Figure B.18: Bed composition, measured after, average of condition P7A
 Figure B.19: Bed composition, measured after, average of top 9 mm, average of condition P7A
 Figure B.20: Bed composition, measured after, test P9A1
 Figure B.21: Bed composition, measured after, test P9A2
 Figure B.22: Bed composition, measured after, test P9A3
 Figure B.23: Bed composition, measured after, test P9A4
 Figure B.24: Bed composition, measured after, average of condition P9A
 Figure B.25: Bed composition, measured after, average of top 9 mm, average of condition P9A
 Figure B.26: Bed composition, measured after, average composition of top 50 mm of sand bed, tests P6A3, P7A4 and P9A3
 Figure B.27: Grain-size distribution sand from sand traps, tests of condition P6A
 Figure B.28: Grain-size distribution sand from sand traps, tests of condition P7A
 Figure B.29: Grain-size distribution sand from sand traps, tests of condition P9A
 Figure B.30: Grain-size distribution forward sand trap, for different flow conditions
 Figure B.31: Grain-size distribution backward sand trap, for different flow conditions

Appendix C

- Figure C.1: Grain-size distribution bed load transport (PBLT), tests of condition P6A
 Figure C.2: Grain-size distribution bed load transport (PBLT), tests of condition P7A
 Figure C.3: Grain-size distribution bed load transport (PBLT), tests of condition P9A
 Figure C.4: Grain-size distribution bed load transport onshore (PBLT), for different flow conditions
 Figure C.5: Grain-size distribution bed load transport offshore (PBLT), for different flow conditions

Appendix D

- Figure D.1: Time-averaged suspended concentrations (TSS), tests of condition P6A, on a log-linear scale
- Figure D.2: Time-averaged suspended concentrations (TSS), condition P6A, on a log-linear scale
- Figure D.3: Time-averaged suspended concentrations (TSS), tests of condition P7A, on a log-linear scale
- Figure D.4: Time-averaged suspended concentrations (TSS), condition P7A, on a log-linear scale
- Figure D.5: Time-averaged suspended concentrations (TSS), tests of condition P9A, on a log-linear scale
- Figure D.6: Time-averaged suspended concentrations (TSS), condition P9A, on a log-linear scale
- Figure D.7: Time-averaged suspended concentrations (TSS), 3 flow conditions, on a log-log scale
- Figure D.8: Vertical distribution of the d_{50} of suspended sediment (TSS), tests of condition P6A
- Figure D.9: Vertical distribution of the d_{50} of suspended sediment (TSS), tests of condition P7A
- Figure D.10: Vertical distribution of the d_{50} of suspended sediment (TSS), tests of condition P9A
- Figure D.11: Time-averaged concentration profile P6A (CCM, PBLT, TSS)
- Figure D.12: Time-averaged concentration profile P7A (CCM, PBLT, TSS)
- Figure D.13: Time-averaged concentration profile P9A (CCM, PBLT, TSS)

Appendix E

- Figure E.1: Time-averaged concentration profile inside the sheet-flow layer, measured by CCM, on log-linear scale, condition P6A
- Figure E.2: Time-averaged concentration profile inside the sheet-flow layer, measured by CCM, on log-linear scale, condition P7A
- Figure E.3: Time-averaged concentration profile inside the sheet-flow layer, measured by CCM, on log-linear scale, condition P9A

1. INTRODUCTION

1.1 Sand transport problem

Sediment transport is a process that is caused by the interaction of waves, currents and a bed consisting of gravel, sand or finer material. In the coastal zone waves play an important role. In shallow water they create an oscillating water motion close to the bed which can be strong enough to move the grains.

Under storm conditions high waves occur, the oscillating velocities close to the bottom are high, creating high shear stresses, and if the shear stress becomes high enough a so-called sheet-flow regime develops: the existing bed forms (ripples) are wiped out because of the strong water motion. Just above the bed a thin layer with extremely large sediment concentrations develops. The combination of large sediment concentrations and velocities can cause high sediment transport rates. This is of interest for e.g. the forecasting of accretion or erosion at the shoreline caused by storms.

Furthermore field observations show that there is a variation in bed material composition along the coastal profile: the material found close to the shore might have other grain characteristics than the material from more offshore locations. These variations, called sorting, are at least partly due to selective transport processes.

At present there is little known about the net cross-shore sediment transport quantities and these selective transport processes during storm conditions.

Measurements in the field in and above the wave boundary layer are very difficult. Sand transport can hardly be measured directly. Therefore most of the measurements are carried out in laboratory experiments using facilities like wave flumes or water tunnels. These measurements can be performed in either small-scale or full-scale experiments. The advantage of large facilities is that natural material can be used and scaling of the sediment is not necessary.

In a large oscillating water tunnel the transport processes close to the bottom can be simulated at full scale. At Delft Hydraulics such a large-scale facility is available: the Large Oscillating Water Tunnel (LOWT). This tunnel has been designed for full-scale simulation of the near bed horizontal oscillating water motion, which can be combined with a steady current.

The present experiments are carried out with a mixture of two sands in order to get more insight in the selective transport processes.

1.2 Previous work (literature)

In the past many experiments have been carried out in the Large Oscillating Water Tunnel of WL | DELFT HYDRAULICS. Experiments with oscillatory flow only and experiments with oscillatory flow and a net current have been done.

The following experimental series were carried out under sheet-flow conditions with asymmetric oscillatory flow only:

- Series B (*Al-Salem, 1993*)
Net sediment transport rate measurements in sheet-flow conditions under regular and irregular asymmetric waves ($d_{50}=0.21$ mm).
- Series C (*Al-Salem, 1993*)
Time dependent velocity and concentration measurements under regular sinusoidal and asymmetric (2^{nd} order Stokes) waves ($d_{50}=0.21$ mm).
- Series D (*Ribberink and Chen, 1993*)
Measurements in sheet-flow conditions of net sediment transport rates and time-averaged concentration profiles under regular 2^{nd} order Stokes waves ($d_{50}=0.13$ mm).
- Series K (*Cloin, 1998*)
Time-averaged velocity and concentration measurements under regular sinusoidal waves with a current and regular asymmetric waves (2^{nd} order Stokes). Goal: to gain more insight and quantitative data of selective transport processes under sheet-flow conditions (50% fine sand, $d_{50}=0.13$ mm and 50% coarse sand, $d_{50}=0.32$ mm).

1.3 Objectives of present experiments

The main objectives of the present experiments are:

- To gain more insight and data about the selective transport processes under sheet-flow conditions for regular asymmetric waves (2^{nd} order Stokes) without a current.
- To obtain quantitative information about net sediment transport rates, net transport rates per fraction, suspended sediment concentrations and composition, bed load concentrations and composition and the change of composition of the sand bed in order to verify and develop new and existing models for graded sediment transport.

1.4 Framework and execution of the study

The experimental investigation (series P) is a part of the research programme “SEDMOC” (Sediment Transport Modelling in Marine Coastal Environments) funded by the European Union. The experiments were performed in the large oscillating water tunnel of WL | DELFT HYDRAULICS (project number Z2099.10), under the supervision of Prof. Dr. Ir. Leo Van Rijn (DELFT HYDRAULICS) and Dr. Ir. J.S.Ribberink (University of Twente, UT).

The data analysis and reporting was done in the framework of the Ph.D.-project of Wael Hassan of University of Twente (UT) and the M.Sc.-project of David Kroekenstoel of University of Twente (UT).

The experiments were carried out in the weeks 11 to 15 (March – April) and weeks 20 to 22 (May) of 1999. The tunnel was operated by Johan Koopmans, David Kroekenstoel and Wael Hassan. Leo Van Rijn did the project management.

1.5 Summary

Chapter 2 includes the experimental set-up of the study. Brief descriptions of the experimental facility, the imposed and measured parameters, the bed material, the measurement programme, the analysis methods and the data acquisition and storage is given.

In Chapter 3, the experimental results of series P are presented and briefly discussed. It includes the main results of the net transport rates (total and per fraction), time-averaged concentration profiles, time-dependent sediment concentrations inside the sheet-flow layer and the measured flow velocities outside the wave boundary layer.

Chapter 4 presents a summary of the present results and the previous experimental results, which have been carried out with uniform and graded sand in the wave tunnel.

2 EXPERIMENTAL SET-UP

2.1 Measurement programme

Wave conditions

One of the main goals of the present experiments is to gain more insight in the selective transport processes under sheet-flow conditions for regular asymmetric waves without a current.

In the past some experimental series were carried out with regular asymmetric waves without a current (2nd order Stokes waves) and uniform sand with one fraction (series B and C). For reasons of comparison it is therefore logical to choose the same flow conditions as in those previous experiments to study the influence of the use of two fractions (graded sand).

The experimental program consisted of three asymmetric wave conditions consisting of 2nd order Stokes waves (no superimposed current) and a wave period of 6.5 seconds.

The 2nd order Stokes waves were chosen, as follows:

$U_{rms}=0.6$ m/s (condition P6), $U_{rms}=0.7$ m/s (condition P7) and $U_{rms}=0.9$ m/s (condition P9).

The 2nd order stokes wave can be described with: $u(t) = u_1 \cos(\omega t) + u_2 \cos(2\omega t)$.

Where: u_1 and u_2 are the first and second-order components of the horizontal velocity
 ω is the angular frequency of the wave (which is equal to $2\pi/T$).

The wave period T was the same for all three conditions ($T = 6.5$ s). The root mean square is equal to: $\sqrt{1/2(u_1^2 + u_2^2)}$. The degree of asymmetry R , defined as $(u_1 + u_2)/2 u_1$ was kept at around 0.66.

Only for test PSB1 another wave condition was used: a sine wave ($U_{max}=1.5$ m/s) superimposed on a net current (+0.25 m/s). The test program is given in Table 2.1. The different instruments used for each individual test are mentioned in Table 2.2 and Table 2.3. These instruments will be described in detail in section 2.3.2.

Table 2.1 Test program series P

Test name	Wave condition	Sand type
P6A1 to P6A6	2 nd order Stokes waves $U_{rms}=0.6$ m/s, $T=6.5$ s	A
P7A1 to P7A7	2 nd order Stokes waves $U_{rms}=0.7$ m/s, $T=6.5$ s	A
P9A1 to P9A6	2 nd order Stokes waves $U_{rms}=0.9$ m/s, $T=6.5$ s	A
P6B1 and P6B2	2 nd order Stokes waves $U_{rms}=0.6$ m/s, $T=6.5$ s	B
P7B1	2 nd order Stokes waves $U_{rms}=0.7$ m/s, $T=6.5$ s	B
P9B1	2 nd order Stokes waves $U_{rms}=0.9$ m/s, $T=6.5$ s	B
PSB1	Sine wave + net current, $T=7.2$ s	B

Regular asymmetric (2nd order Stokes) wave motions were generated in the wave tunnel. Orbital velocities were measured by means of a Laser Doppler Flow Meter at about 0.2 m above the bed. Most tests were repeated three or four times to show the variations related to small differences in bed arrangement (refilling of sand in the tunnel).

The test procedure was as follows (in short):

- Preparation of sand bed (flattening the sand bed, filling the erosion holes at both ends of the tunnel and replacing the upper 5 cm of the sand bed by new sand mixture (70% fine sand and 30% coarse sand);
- Sounding of bed surface using bed profiling system;
- Collection of bed material samples (sample thickness of about 2 to 3 cm) at three positions along the tunnel (See Figure 2.2 and Table 2.3);
- Filling the tunnel with water;
- Positioning of instruments;
- Generation of oscillatory flow in the tunnel for 10 to 20 minutes;
- Recording the time series of the steering signal, the measured piston position, piston velocity, piston pressure, the two components of the velocity measured by LDA and the CCM on computer files;
- Bed load trap samples were obtained during most of the repeated tests. Suspended load samples were obtained only during two tests (bed load trap was replaced by suspended sampler during these tests to reduce instrument-related disturbance). See Table 2.3 for locations.
- Collection of the suspended and bed load samples started 2 minutes after the generation of wave motion (to avoid the initial effects) for about 5 to 10 minutes;
- Draining of tunnel after ending of wave motion;
- Sounding of bed surface using bed profiling system;
- Collection of bed material samples (sample thickness of 1 to 5 cm; samples were split in sub samples of 3 to 10 mm) at three positions along the tunnel $x = -2.5$ m, $x = +1$ m and $x = +3.5$ m with respect to middle section ($x = 0$ m). In some tests more samples were collected (more positions and more sub samples);
- Removal of sand from both sand traps; determination of wet sand mass by weighing under water;
- Determination of bed load concentrations and/or suspended load concentrations from the sand masses and the water volumes collected;
- Analysis of sand samples in settling tube to determine grain-size distribution (d_{10} , d_{50} , d_{90}) and percentages of fine and coarse fractions in samples;

- Determination of net sand transport rates from bed level soundings and sand collected in sand traps.

Table 2.2 Overview of instruments used for each test

Instrument	BLSS (bed level)	CCM (concentration)	LDA (velocity)	PBLT (concentration)	Sand traps (net transport)	TSS (concentration)	Suction Tube (bed sampling)
P6A1	X	X	X	X	X		X
P6A2	X	X	X	X	X		X
P6A3	X	X	X		X	X	X
P6A4	X	X	X		X	X	X
P6A5		X	X	X			
P6A6		X	X	X			
P7A1		X	X	X	X		X
P7A2	X	X	X	X	X		X
P7A3	X	X	X	X	X		X
P7A4	X	X	X		X	X	X
P7A5	X	X	X		X	X	X
P7A6		X	X	X			
P7A7		X	X	X			
P9A1	X	X	X	X	X		X
P9A2	X	X	X	X	X		X
P9A3	X	X	X		X	X	X
P9A4	X	X	X		X	X	X
P9A5		X	X	X			
P9A6		X	X	X			
P6B1	X		X		X		
P6B2	X		X		X		
P7B1	X		X		X		
P9B1	X		X		X		
PSB1	X		X		X		

The abbreviations of the instruments mentioned in the above table will be explained in section 2.3.2. Locations are given in Figure 2.2 and Table 2.3.

2.2 Bed material (sand)

Two different sand types were used: sand type A and sand type B. Sand type A consisted of a mixture of 70% uniform fine sand ($d_{50}=0.21$ mm) and 30% uniform coarse sand ($d_{50}=0.97$ mm). Sand type B consisted of 100% uniform coarse sand ($d_{50}=0.97$ mm). Only a few tests were performed using sand type B, for reasons of comparison. The test programme is shown in detail in Table 2.1. Particle size distributions of the base materials and mixture A are shown in Figure 2.1. The characteristic particle diameters of mixture A are: $d_{10} = 0.16$ mm; $d_{50} = 0.24$ mm, $d_{90} = 0.99$ mm.

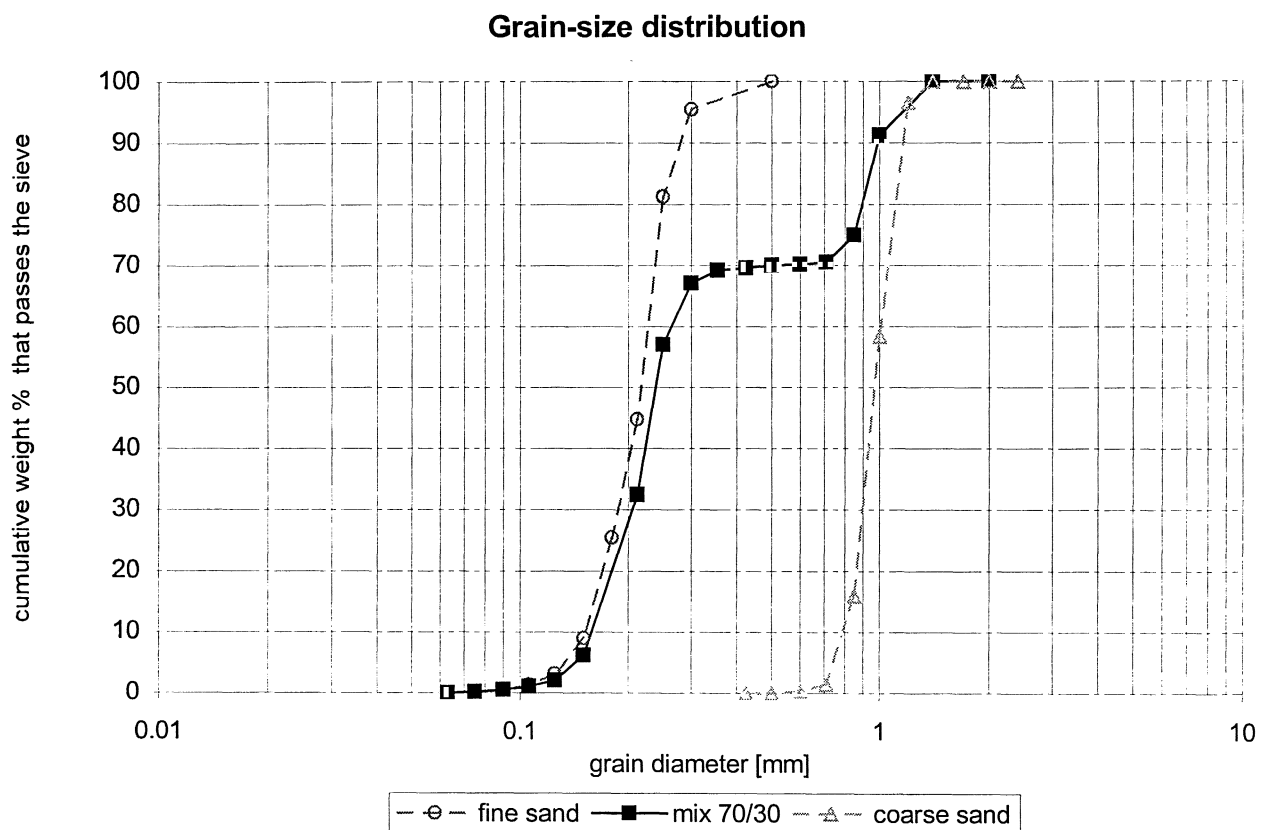


Figure 2.1 Grain-size distribution of the base materials and the mixture (sand type A)

The mixture was made by mixing the dry base materials in a mechanical mixer with a volume of about 100 litres.

Special tests were done to determine the porosity of the base materials and the mixture, as follows:

- a volume glass of 1 litre was filled with dry material;
- the sand was poured in a bucket;
- water was added until the water surface was flush with the sand surface;
- the volume of water added was determined by weighing.

The porosity values (estimated accuracy of about 10%) of the relatively loose materials were:

- 0.33 for fine sand ($d_{50} = 0.21$ mm);
- 0.36 for coarse sand ($d_{50} = 0.97$ mm);
- 0.30 for mixture A (70% fine/30% coarse).

After each test the upper layer of the sand bed (type A) was removed (about 5 cm) from the tunnel and replaced with new sand to eliminate the probable effect of selective transport processes.

2.3 Wave tunnel and instruments

2.3.1 Large Oscillating Water Tunnel

The experiments were carried out in the Large Oscillating Water Tunnel (LOWT) of WL | Delft Hydraulics. The general outline of the wave tunnel is shown in Figure 2.2.

The tunnel has the shape of a vertical U-tube, with a long horizontal rectangular test section. At each end there is a vertical cylindrical tube. One of them has an open connection to the air, in the other a piston is constructed. This piston is in direct contact with the water and is driven by a hydraulic servo-cylinder mounted on the top of the riser. An electric/hydraulic valve controls the piston motion based on the measured difference between the (measured) actual piston position and the desired piston position (feedback system).

In the horizontal test section an oscillating water motion is induced by the motion of the piston simulating the orbital wave motion close to the bed. It is possible to generate purely sinusoidal, regular a-symmetric and irregular oscillatory motions within the test section of the wave tunnel, although there are some constraints for piston velocity and piston acceleration.

The maximum piston amplitude is 0.75 m, which results in a maximum semi-excursion length of the water particles in the test section of 2.45 m. The range of the velocity amplitudes is 0.2-1.8 m/s and the range of oscillating periods is 4-15 seconds.

The test section has a length of 14 m, a height of 1.1 m, a width of 0.3 m and is provided with flow straighteners at each end. The sidewalls of the test section consist of thick glass windows in a steel frame (I-beams). Usually a 0.3 m thick layer of sand is brought into the test section, so 0.8 m height is left for the oscillating water flow. The roof of the test section is formed by 13 steel plates, which can be removed separately. By removal of some steel plates it is possible to install some instruments inside the test section, to put the sand in or to remove it.

At the bottom of both vertical tubes sand traps are constructed in order to collect the sand that leaves the test section during a test. This sand can be removed after a test.

In 1992 the wave tunnel was extended with a recirculating flow system in order to superimpose a net current on the oscillating motion. The recirculating flow system is provided with a third sand trap consisting of a 12 m long pipe with an diameter of 1.2 m. Downstream of the trap two pumps are installed for generating a net current. With exception of test PSB1, no net current was superimposed to the oscillating water motion, therefore the recirculating system and the third sand trap were not used.

Due to the large dimensions of the wave tunnel, the velocities close to the bed in the tunnel are comparable to the velocities occurring in nature. Therefore it is possible to perform full-scale experiments.

But still there are some differences between the orbital flow field in nature and the simulated flow field in the tunnel. In nature waves propagate in a certain direction and they change phase along the direction of wave propagation. Along the wave tunnel the same phase occurs at every location. Furthermore vertical orbital motions are not simulated in the tunnel, just as time-dependent horizontal pressure gradients along a horizontal line due to phase differences are not simulated.

The measurement section ($x = 0$) is in the middle of the tunnel (see Figure 2.2).

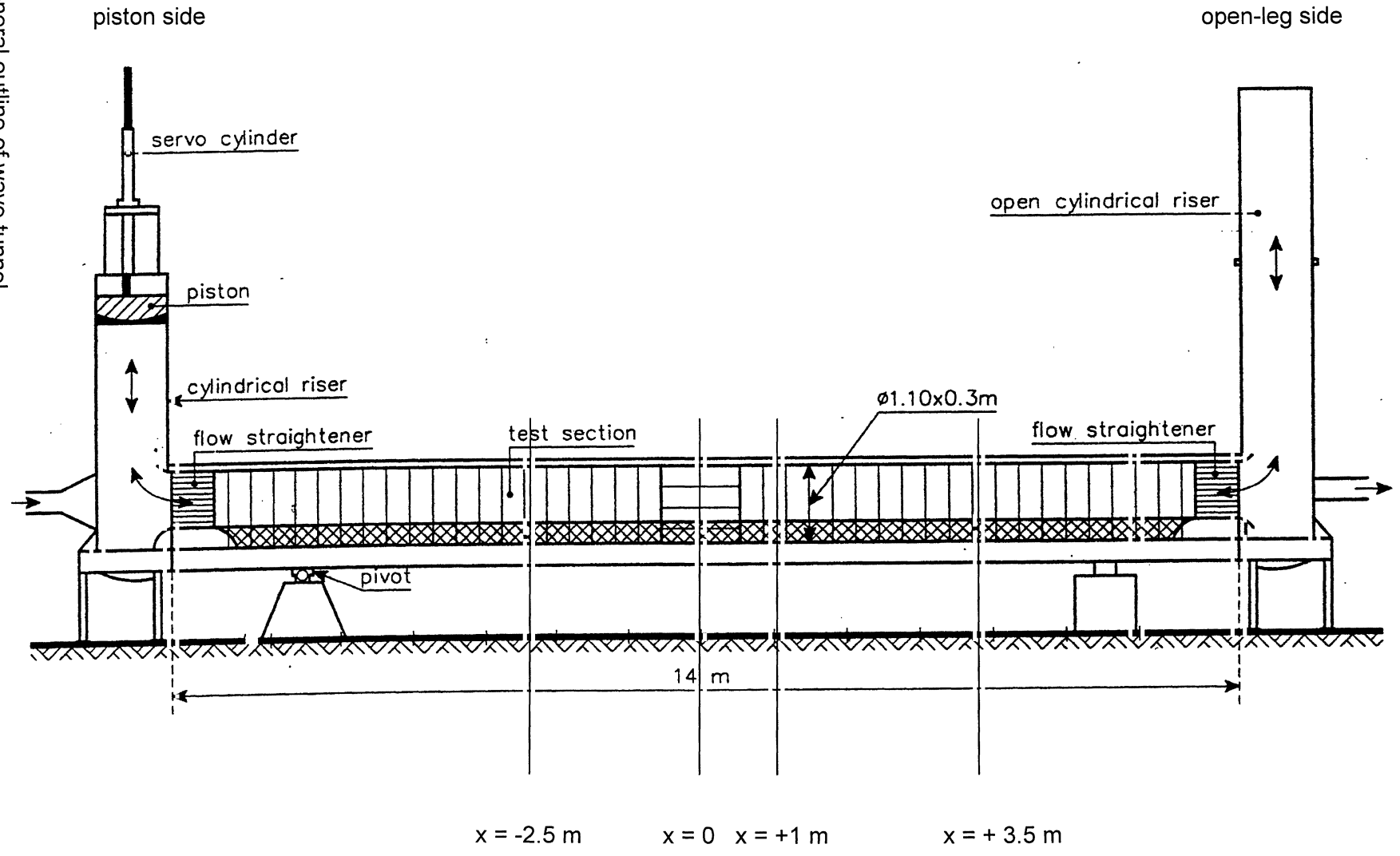


Figure 2.2 General outline of wave tunnel

2.3.2 Measuring instruments

Table 2.3 shows the different instruments and methods which have been used during the present experiments (series P) and their positions along the tunnel section (note: $x = 0.0$ means the middle of the tunnel section; see Figure 2.2).

Table 2.3 Measuring instruments/methods for series P

Instrument / method	Position along tunnel	Parameter
Bed Level Sounding System (BLSS), Sand in traps	Along tunnel length	net sand transport
Laser Doppler Velocity Meter (LDA)	$x = + 2.0$ m	Instantaneous orbital velocity at 0.2 m above bed
Conductivity Concentration Meter (CCM)	$x = + 2.0$ m	Instantaneous sand concentration in bed and inside sheet-flow layer
Transverse Suction System (TSS)	$x = + 0.35$ m	time-averaged suspended sand concentrations simultaneous at 10 elevations above sheet flow layer
Bed Load Trap sampler (PBLT)	$x = 0.0$ m (middle)	time-averaged bed load concentration in sheet-flow layer
Suction tube	$x = -2.5$ m, $+ 1.0$ m and $+ 3.5$ m	Sand bed samples (thickness of max. 5 cm)
Video camera	$x = + 2.5$ m	Bed level variations and sheet-flow layer thickness

Laser Doppler Velocity Meter (LDA)

A forward scatter Laser Doppler Anemometer (LDA), developed by WL | DELFT HYDRAULICS (see Klopman, 1994), was used for two dimensional flow-velocity measurement in a vertical plane along the centre of the tunnel test section. The LDA has a relatively small measuring volume, with a height and width of approximately 0.22 mm. The length of the measuring volume in direction perpendicular to the flow is approximately 6.47 mm. The standard range of bi-directional velocities which can be measured with this system is 0.001 – 2.0 m/s.

The LDA was positioned on a measurement carriage that stands over the tunnel, rather than on top of it, in order to eliminate the effect of tunnel vibrations. The LDA measures two velocity components, at about 45° to the x-axis, in order to increase the velocity range. The two velocity components are transferred to horizontal and vertical directions afterwards. Figure 2.3 shows the configuration of the LDA-beam in the test section of the tunnel.

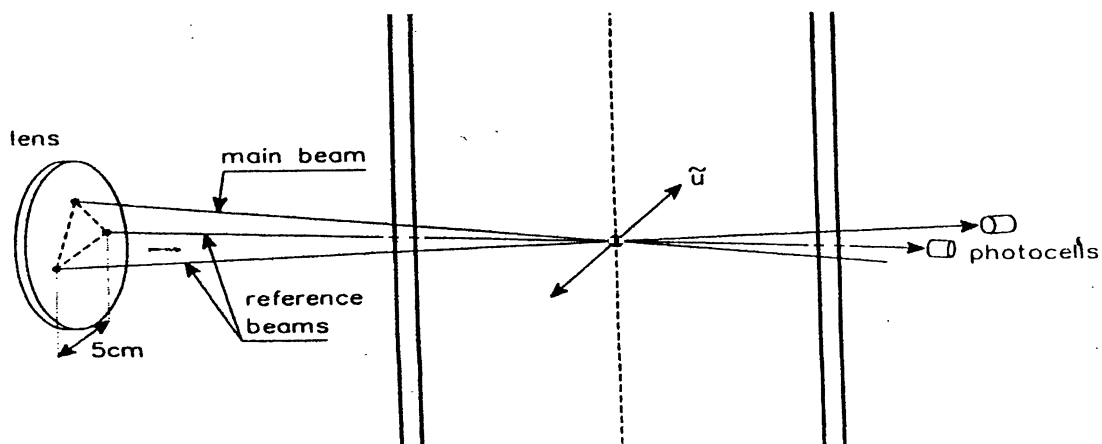


Figure 2.3 Laser-beam configuration in the tunnel (top view)

Bed level sounding system (BLSS)

The bed level sounding system was used to measure the bed level before and after a test. The system consists of three profilers on a carriage along the horizontal axis, a positioning counter (which determines the exact location of the three profilers along the horizontal axis) and measuring and processing software installed on a computer. Each profile measures the vertical position of the bed surface.

The carriage can be installed on rails inside the wave tunnel and can be moved along the whole test section. The three profiles on the carriage are installed normal to the direction of motion, so that the bed level can be measured at three locations along the width of the tunnel (at the centre, 0.10 m to the left and 0.10 m to the right, that is 0.05 m off the side walls).

The bed level in the tunnel is then determined by averaging the bed level measurements of the three locations across the width of the tunnel. In Figures 2.4 and 2.5 the configuration of the BLSS is shown.

The measuring technique of the profiler is based on conductivity. While moving along the tunnel, the conductivity in the sampling volume at the end of each profiler remains constant. That means that the probe tip is kept at a constant distance from the bed. A potential meter measures the vertical position of the probe, which is directly related to the bed level in the tunnel.

At every centimetre along the length of the tunnel the level of the three profilers is stored by a computer, giving a detailed description of height of the sand bed.

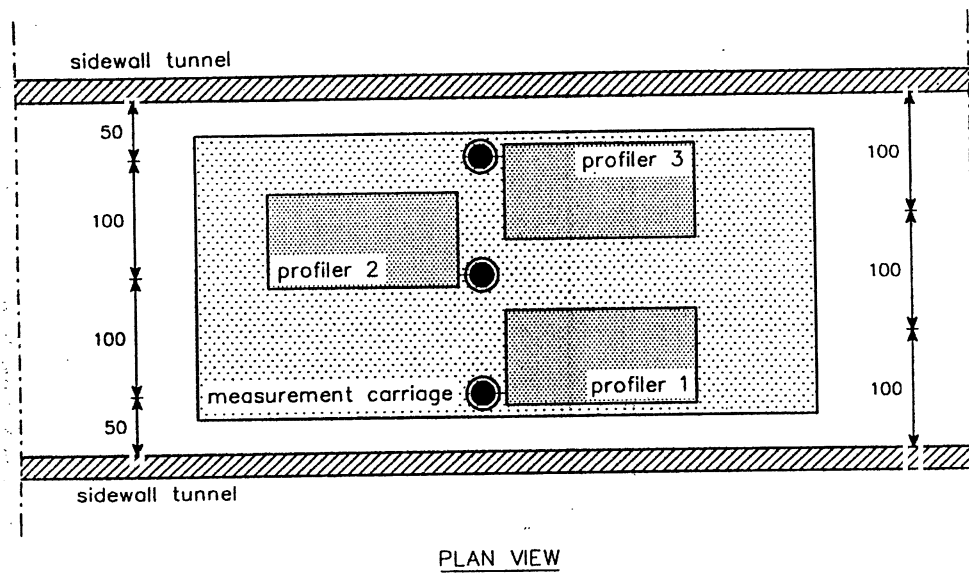


Figure 2.4 Configuration of Bed Level Sounding System (BLSS), measurement carriage (Top view)

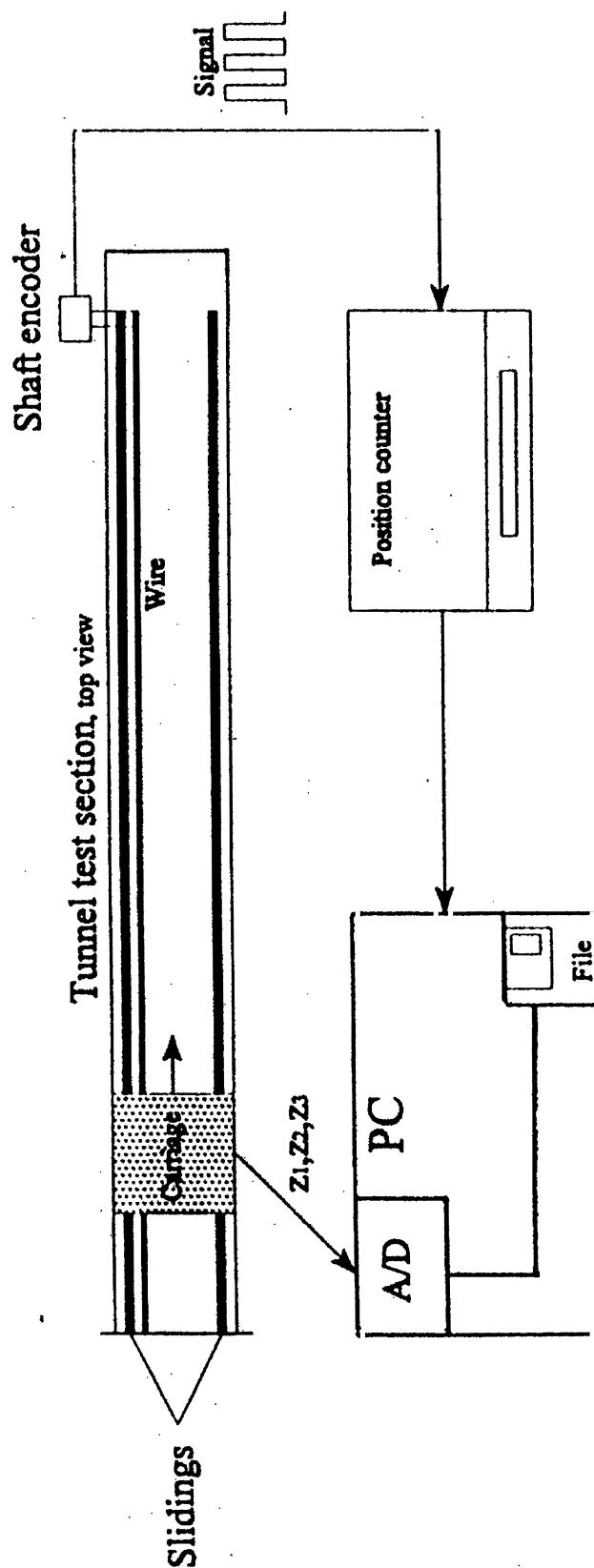


Figure 2.5 Configuration of Bed Level Sounding System (BLSS), general layout (top view)

Transverse Suction System (TSS)

The Transverse Suction System was used for measuring the time-averaged concentration profiles of the suspended sediment, by extracting water-sediment samples in a direction normal to the flow. The system consists of 10 separate intake nozzles with an inner diameter of 3 mm placed above each other at an increasing distance. Figure 2.6 gives the general outline of the TSS. The numbers in this figure present the distance (cm) between the nozzles.

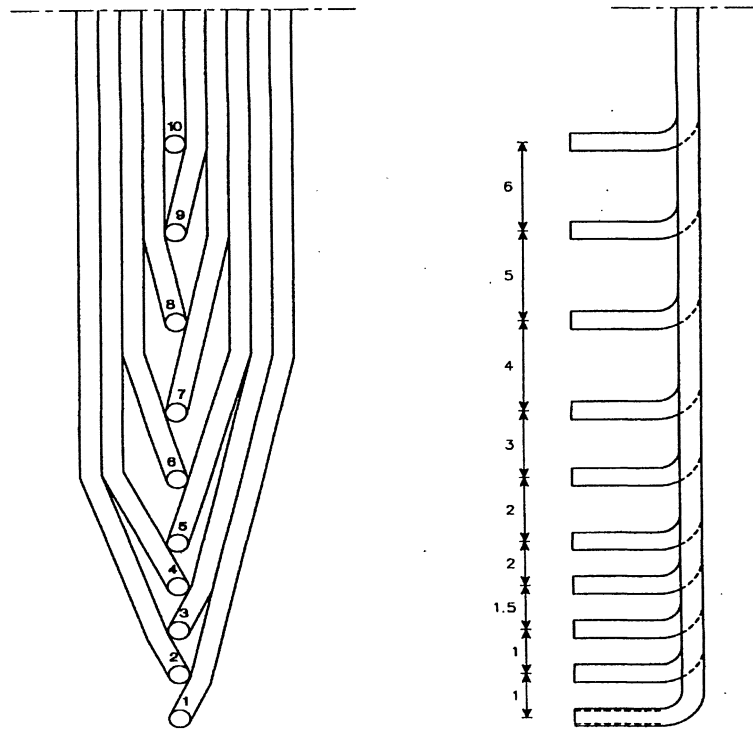


Figure 2.6 General outline of Transverse Suction System (TSS)

Ten peristaltic pumps drive the suction system; each connected to one of the intake nozzles. The water samples containing the suspended sediment, is collected in 10 buckets and the volume of the water is measured. The dry weight of the collected sand in the buckets is determined using calibrated tubes. The calibration of the tubes counts for errors due to suction normal to the flow and the conversion from wet sand volume to dry weight. Knowing the dry weight of the sand, it is possible to calculate the suspended sediment concentration at each elevation.

The collected sand samples have also been used to determine the grain-size distribution of the suspended sediment, using a settling tube: the Visual Accumulation Tube (VAT), see section 2.4.5 for a detailed description.

Pump Bed Load Trap sampler (PBLT)

The PBLT consists of two tube-type intake nozzles placed in opposite direction on a metal footplate (length of about 0.1 m, width of about 0.05 m). Each nozzle (internal diameter of 8 mm) is connected to a plastic hose for pumping of water and sediment. The nozzles are opened and closed alternatively by circular metal valves (with rubber cover) through the action of oscillatory fluid drag on a metal pivoting plate connected by thin steel rods to the valves. The valve of the nozzle facing the forward (onshore) fluid motion will be opened during the forward stroke of the wave and closed during the backward stroke. The intake nozzle facing the forward motion will be termed the ‘onshore’ nozzle and that facing the backward motion will be termed the ‘offshore’ nozzle.

The scour around the instrument was found to be minimum during previous tests with orbital velocities up to 1.7 m/s (Reference?????). The maximum scour depth behind the offshore nozzle was about 5 mm. The scour length was about 50 mm.

Tests were done previously to study the effect of the intake velocity on the bed surface in still water. The maximum intake velocity was about 2.5 m/s, which did not produce any scour of the bed in front of the nozzle; the foot plate was just long enough (edge was about 10 mm beyond intake opening) to prevent scour. Thus, the bed load sampler can be operated at maximum intake velocity. Ideally, sampling should be done at an intake velocity equal to the ambient velocity. This requires continuous adjustment of the intake velocity, which is too problematic. Operation of the sampler at a fixed maximum intake velocity will create a small sampling error, which can be accounted for by a calibration factor.

Some results of the PBLT during previous tests are given in Table 2.4. The onshore concentration represents the time-averaged concentration over the onshore phase of the wave cycle in the lowest 8 mm of the depth (which is a height of 8 mm direct above the sand surface). Similarly, the offshore concentration is that for the offshore phase of the wave cycle. The measured mean sand concentrations varied in the range between 1 and 100 kg/m³.

Table 2.4 Test results of PBLT during previous tests in wave tunnel

Condition	U _{rms} [m/s]	Sand concentration onshore (kg/m ³)	Sand concentration offshore (kg/m ³)
B-7	0.5	25 (+/-5)	3 (+/- 1)
B-8	0.7	45 (+/- 5)	7 (+/- 1)
B-9	0.9	75 (+/- 25)	25 (+/- 5)

The onshore and offshore bed load transport rates can be computed by:

$$q_{b,on} = \alpha DC_{on} U_{max,on} \tag{2.1}$$

$$q_{b,off} = \alpha DC_{off} U_{max,off} \tag{2.2}$$

Where: α = calibration factor
 D = internal diameter of intake nozzle (=0.008 m)
 C = time -averaged concentration [kg/m³]
 U_{max} = peak velocity at small distance above the bed (say 0.1 m) [m/s].

The net bed load transport is:

$$q_{b,net} = \alpha D (C_{on} U_{max,on} - C_{off} U_{max,off}) \quad (2.3)$$

It is assumed that the thickness of the bed load layer is about 0.008 m.

The calibration factor accounts for:

- Scour effects;
- Incorrect thickness of bed load layer;
- Incorrect velocities and concentrations.

The computed α -value was found to be in the range of 0.24 ∓ 0.08 based on previous tests (Ribberink and Al-Salem, 1992). The variation of the calibration factor is related to all possible sources of sampling errors.

The dry weight of the collected sand samples is determined using calibrated tubes. Knowing the dry weight and the extracted volume it is possible to calculate the onshore and offshore bed load concentrations.

The collected sand samples have also been used to determine the grain-size distribution of the bed load transport, using the Visual Accumulation Tube (VAT).

Conductivity Concentration Meter (CCM)

An electro-resistance measuring technique (CCM), developed by WL | DELFT HYDRAULICS was used for measuring the time-dependent sediment concentrations in the sheet-flow layer and inside the sand bed. The CCM measures large concentrations (5 – 50 % volumes, 100 – 1600 g/l) with a four-point electro-resistance method.

The CCM measuring principle is based on the conductivity change of a sand-water mixture due to the variation of the quantity of (non-conductive) sand particles present in the measuring volume. A constant electrical current is generated between two outer electrodes and the voltage between the inner electrodes is measured. The measured voltage is proportional to the electro-resistance of the sand-water mixture in a small measuring volume directly above the electrodes. The height and the length of the volume is 1 and 2 mm respectively, (Koelewijn, 1994).

The absolute change in current strength in the case of a sand-water mixture in comparison with clear water is determined by the change in conductivity. The water conductivity can vary considerably, therefore a relative conductivity Gr is used, defined as:

$$Gr = (1 - (V_0 / V_m)) * 100 \% \quad (2.4)$$

$$C \text{ (volume \%)} = K * Gr \text{ (\%)} \quad (2.5)$$

Where: V_0 = output voltage of the probe for clear water
 V_m = output voltage of the probe for the sand-water mixture
 K = calibration factor.

CCM probe tests in various sand-water mixtures with different sand grain sizes show a constant linear calibration, with a possible measurement error of ($\pm 10\%$), See Koelewijn (1994) and Van der Wal (1996).

The CCM probe is brought into the middle of the test section from below; through the tunnel bottom and the sand bed in order to minimise the flow disturbance at $x = + 2.0$ m. Figure 2.7 shows the configuration of the CCM in the tunnel and the CCM probe.

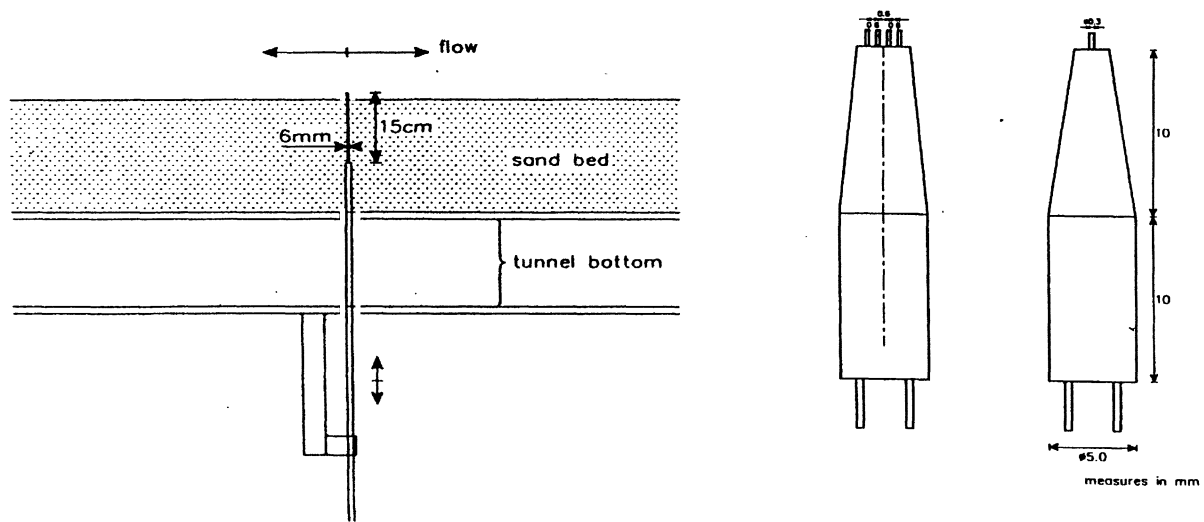


Figure 2.7 CCM configuration in the tunnel and CCM probe outline (measured in mm)

Suction Tube

In order to analyse the change of composition of the upper layer of the sand bed a Suction Tube was used to take samples of the sand bed at different positions along the tunnel.

The Suction Tube consists of a perplex cylinder with a diameter of 25 mm and a height of about 100 mm which was pushed into the sand bed up to 50 mm.

For each test, bed samples were taken at 3 to 5 positions along the tunnel. These samples were divided into three sub samples with a thickness of about 3 mm each. Only the upper 9 mm was divided in layers. The remaining part of the bed sample was not further analysed.

Dividing the samples in layers was done in order to determine the grain-size distribution as a function of depth below the sand surface. The grain-size distribution of each sample and the percentage of the coarse and fine fraction, present in each sample, were determined by using the Visual Accumulation Tube (VAT).

At some tests bed samples were taken at more positions and at some other tests the samples were divided in more subsamples with an increasing thickness of the layers with depth (depth up to 50 mm), see Tables B.1 to B.3.

Video camera

A normal video camera (50 frame / sec) was used for the measurement of the bed level variations during the wave-cycle and the sheet-flow layer thickness. The camera was focused horizontally on an area of 50 * 50 mm² at the sand surface level (location $x = + 2.5$ m). A transparent grid was placed in the recording area (50 * 50 mm) above the sand bed.

2.4 Analysis methods

2.4.1 Computation of net sand transport rates (mass conservation technique)

A mass-conservation technique was used to estimate the net sediment transport rates. The volume of sand collected in the sand traps must be equal to the change of volume in the horizontal test section. Given the sand mass in the traps on both ends of the test section and the volume changes derived from bed level soundings, the porosity of the bed material can be obtained for the test considered.

This computed porosity can be used to determine the net sand transport rates in the tunnel. The computed porosity values are generally larger than the natural porosity value of the sand mixture, which is about 0.3 to 0.35 (based on special tests, see Section 2.2). Inaccuracies of the bed level sounding system and slight compaction of the top layer of the bed during the test are likely to cause this difference. The compaction of the sand bed during the test may have been as large as 10%, based on the results of the special porosity tests.

To account for these errors as much as possible, the net transport rates have been computed by using a porosity value of 0.4. This latter value has been found to be most reliable based on many previous test results.

Based on the sand trap masses (determined by weighing under water), the bed levels measured before and after each test and the assumed porosity of 0.4, the sediment continuity equation was integrated starting from the left as well from the right side of the tunnel with help of a computer program.

This results in two estimates of the net transport rates. The average of these two estimates is taken as the net sand transport rate for the test in question. The program uses as boundary conditions the sand masses collected in the sand trap. For a more detailed description of this technique and the formula's, see Appendix F.

Based on the variation of the net sand transport rates over the different test runs and the use of the imposed porosity value (0.4), the computed net sand transport rates may on average have a maximum error of about 30%. The error related to porosity effects due to compaction is a systematic error. It results in underestimation of the net transport rate, because the volume changes derived from the soundings are too large yielding a relatively large computed porosity.

2.4.2 Computation of net sand transport rates per fraction

The net transport rates per fraction was calculated in a similar way as the total bed load transport rates, using the PBLT results (see section 2.3). The following data have been used to determine the transport rate per fraction:

- The measured time-averaged onshore and offshore bed load concentrations, using the PBLT;
- The percentages of coarse and fine fractions in the onshore and offshore directions (determined by the VAT analysis);
- The measured onshore and offshore peak flow velocities;
- The measured net transport rates (using mass conservation technique)

First the calibration factor α is determined using:

$$q_{net,total} = \alpha D (C_{on} U_{crest} - C_{off} U_{trough}) \quad (2.6)$$

Where:

α	=	Calibration factor
D	=	internal diameter of intake nozzle [=0.008 m]
C	=	time-averaged concentration, onshore and offshore [kg/m ³]
U	=	peak velocity at a small distance above the bed, onshore and offshore [m/s].

The time-averaged concentrations are obtained from the Pump Bed Load Trap sampler and the peak velocities (U_{crest} and U_{trough}) from the Laser Doppler Velocity meter.

Second, the transport rates per fraction in the onshore and offshore directions can be computed, using the following equations :

$$q_{fine,on} = \alpha D C_{fine,on} U_{max,on} \quad (2.7)$$

$$q_{fine,off} = \alpha D C_{fine,off} U_{max,off} \quad (2.8)$$

$$q_{coarse,on} = \alpha D C_{coarse,on} U_{max,on} \quad (2.9)$$

$$q_{coarse,off} = \alpha D C_{coarse,off} U_{max,off} \quad (2.10)$$

The net transport rate per fraction is then equal to:

$$q_{net,fine} = q_{fine,on} - q_{fine,off} \quad (2.11)$$

$$q_{net,coarse} = q_{coarse,on} - q_{coarse,off} \quad (2.12)$$

2.4.3 Computation of orbital velocities outside wave boundary layer

- The time-dependent orbital flow velocities outside the wave boundary layer were measured using a forward scatter Laser Doppler Flow Meter (LDA), using 40 Hz as a sampling frequency.
- The LDA was positioned at $x = + 2.0$ m at the same position as that of the CCM.
- Flow velocities were measured usually at 0.2 m above the bed. Below this level, it turned out to be impossible to measure velocities, because the suspended fine material was so large during the experiments.
- The LDA was kept at the same height during each test ($z = 0.2$ m), keeping in mind that the bed level changes up and down during the test. The averaged bed levels during each test have been used to determine the actual LDA height above the bed.
- The measured two velocity components V_A and V_B (with slope 45°, see Figure 2.8) are transferred to horizontal (in flow direction) and vertical (perpendicular to the flow) directions.

The ensemble-averaged flow velocities are based on choosing a certain number of waves for each test. The first minute at the beginning of each test has been ignored to avoid the initial effects at the beginning of the test.

- The down crossing piston velocity has been used as reference to determine the start and the end of each wave.
- The ensemble-averaged velocities in x direction have been used to calculate different parameters, the mean flow velocity $\langle U \rangle$, maximum forward velocity U_c , the maximum backward velocity U_t , the root mean square U_{rms} and the third order velocity moment $\langle U^3 \rangle$.

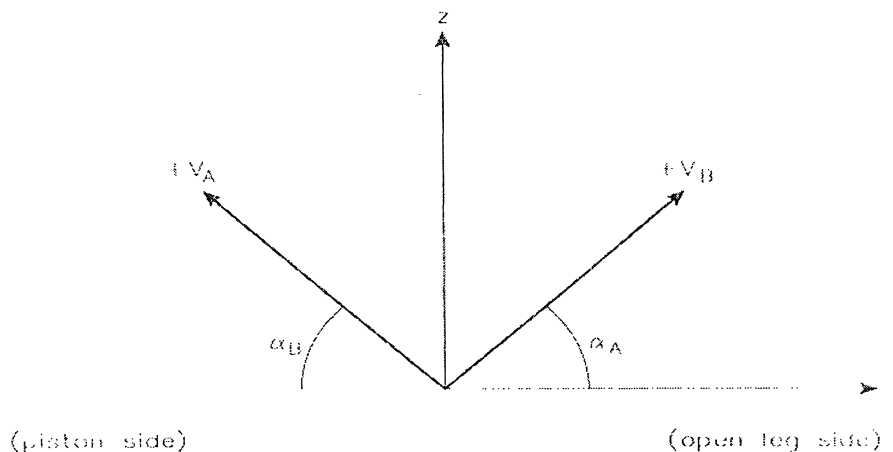


Figure 2.8 Configuration of measured velocity components by LDA in the tunnel

2.4.4 Computation of sand concentration in sheet-flow layer (CCM results)

- The sediment concentrations in the sand bed and inside the sheet-flow layer ($z < 8$ mm; with respect to the initial bed level) were measured using a Conductivity Concentration Meter (CCM).
- The CCM was positioned at $x = + 2.0$ m (the same position of the LDA). The CCM was mounted on a positioning system that measured the vertical position within a precision of 0.1 mm, below the wave tunnel.
- The CCM was kept at fixed position, during each test, in order to measure sediment concentrations around the initial sand bed. However, due to changes in the level of the sand bed during a test, this resulted in some different measuring points (levels).
- The bed level was measured visually by reading a ruler with mm scale every 30 s at the moments of upward zero crossing through the glass window, in order to determine the actual CCM elevations above the sand bed.
- The CCM clear water reading was measured before and after each test, in order to calculate the relative conductivity Gr and the sediment concentrations (see CCM description in section 2.3.2, Chapter 2).

- The time-series were carefully inspected and time intervals with relatively stable signal and bed levels were used for each test.
- In order to avoid the initial effects, the first two minutes of each tunnel run have been ignored in the computations.
- The ensemble-averaged sediment concentration was calculated for the different intervals, using the downward crossing of the piston velocity as a reference to determine the start and the end of each wave.
- The ensemble-averaged sediment concentrations have been used to calculate the mean concentration ($\langle C \rangle$ (g/l)) and the standard deviation (σ (g/l)) for each time interval.

2.4.5 Computation of particle size composition from settling tube tests (VAT)

- A Visual Accumulation Tube (VAT) or settling tube was used to analyse the grain-size distribution of each sample and to determine the percentages fine and coarse fractions.
- The settling tube was filled with water and small sand samples (about half a teaspoon) was released at the opening of the tube.
- A stopwatch was switched on as soon as the valve at the top of the tube was opened.
- At the bottom of the tube the sediment falls into a glass tube after passing a funnel-type section; a reading scale is present along the glass tube; the sand surface can be followed as a function of time. When the sand surface passes a certain level at the scale of the tube, the fall time is measured (every 5 mm until 100 to 150 mm)
- From these fall times and sand surface levels the fall velocity distribution of the sample can be determined and these velocities can be converted to grain diameters.
- This grain-size distribution was calculated from the fall velocity distribution using Van Rijn's formula ('Van Rijn corrected'):

$$w_s = 0.87 * \frac{\Delta g D^2}{18\nu} \quad 1 < D < 100 \mu\text{m} \quad (2.13)$$

$$w_s = 0.87 * \frac{10\nu}{D} \left[\sqrt{1 + \frac{0.01\Delta g D^3}{\nu^2}} - 1 \right] \quad 100 < D < 1000 \mu\text{m} \quad (2.14)$$

$$w_s = 0.87 * 1.1 \sqrt{\Delta g D} \quad D \geq 1000 \mu\text{m} \quad (2.15)$$

Where:

w_s	=	settling velocity
Δ	=	$(\rho_s - \rho_w) / \rho_w$
g	=	gravity acceleration
D	=	grain diameter
ν	=	kinematic viscosity
ρ_s	=	density of sediment
ρ_w	=	density of water

From the sieve analysis it was known that the base mixture of bed material hardly contains grains with size of 0.5 mm. Thus all grains smaller than 0.5 mm belong to the fine fraction and all grains larger than 0.5 mm belong to the coarse fraction. The fall time of 0.5 mm sand is about 37 seconds. Therefore, the percentage of the coarse fraction of a sand sample is given by relative sand surface level after about 37 seconds.

A more easy way to determine the percentage fine and coarse fraction is by visual observation of the sand in the glass tube at the bottom. The coarse fraction has a much higher fall velocity than the fine fraction and will reach the bottom of the tube first. The fine and coarse fraction are completely separated and now it is very easy to read the surface level of the coarse fraction and the fine fraction and by using the total level one can determine the individual percentages.

2.5 Steering signals, data acquisition and storage

The steering signal of the piston was imposed by a signal generated on a PC. During each test the following time-dependent parameters were stored on computer files using a PC data acquisition system: the steering signal, the measured piston position, piston velocity, piston pressure and the two components V_A and V_B of the velocity measured by LDA.

The measured analogue signals were digitized by means of an analogue to digital (A/D) converter and stored on PC (two files for each test, a binary file with extension .dat and an ASCII file with extension .seq). All the measured signals were also recorded on paper, for each test. Table 2.5 includes all information about the measured parameters, the codes, the units, the calibration factors and the computer channels on which the different parameters are recorded (these data are also included in the ". Seq" -files).

The bed levels, measured by the bed profiling system were recorded on a separate PC and stored in ASCII files. The measured CCM signals were recorded on a separate PC with the measured piston velocity. The local bed levels, measured every 30 s during each test of the time-dependent measurements and the bed levels measured before and after each test at the location of the instruments were recorded on measuring forms (for TSS and PBLT). The near bed video recording was recorded on a normal VHS videocassette.

Table 2.5 Measured signals, channel codes and calibration factors

Computer recording channel	Measured parameter	Units	Code (in *.seq file)	Calibration factors	
				C_1 ([units])/Volt)	C_0 ([units])
1	Steering signal	m	SSN01	0.075	0
2	Displacement	m	DPM01	0.0847	0
3	Piston velocity	m/s	VCM01	1.87	0
4	Piston pressure	KN/m ²	PRM01	100.0	0
5	Component V_A of flow velocity, measured by LDA	m/s	VCM11	0.145	-0.00186
6	Component V_B of flow velocity, measured by LDA	m/s	VCM12	0.144	-0.00173
7	Concentration, measured by CCM	Volts	CCM01	1	0

Note: A separate computer have been used to record the CCM signals with the piston velocity

3 EXPERIMENTAL RESULTS

3.1 Orbital velocities outside wave boundary layer

The flow velocity measurements above the wave boundary layer were performed using the LDA, during all tests at $x = + 2.05$ m. Tables 3.1 to 3.4 show the computed horizontal flow velocities measured in the middle of the tunnel cross section, outside the wave boundary layer for the different flow conditions and sand types. These four Tables include the following information:

z	=	averaged height above the bed (mm)
Start	=	starting time for the velocity computations in seconds
End	=	end time of the velocity computations in seconds
No of waves	=	number of waves used for computing the ensemble-averaged
$\langle U \rangle$	=	mean value of the flow velocities (m/s)
U_c	=	maximum forward flow velocity (onshore) (m/s)
U_t	=	maximum backward flow velocity (offshore) (m/s)
U_{rms}	=	Root mean square of the measured flow velocities (m/s)
$\langle U^3 \rangle$	=	the third order velocity moment (m^3/s^3)

- It was possible to measure flow velocity at 100 mm above the bed only for one test (P7A1). The suspended fine materials were too high during the other tests, which disturbed the laser-beam.
- It was not possible to measure any laser signals during test P9A5 and P9A6, because the suspended fine material was so large during these two tests.
- The measured flow velocities of each individual test show minor variations around the mean value of each flow condition.

Table 3.1 Flow velocities for all tests of condition P6A (measured by LDA)

Test	Laser analysis				U_{laser} (m/s)				$\langle U^3 \rangle$ (m^3/s^3)	Remarks
	z (mm)	Start (s)	End (s)	No. of waves	$\langle U \rangle$	U_c	U_t	U_{rms}		
P6A1	204	98.20	891.21	122	0.031	1.08	0.55	0.585	0.150	Laser 2 ch
P6A2	198	66.9	398.4	51	0.029	1.09	0.56	0.594	0.156	Laser 2 ch
P6A3	204	85.67	657.67	88	0.031	1.07	0.56	0.585	0.141	Laser 2 ch
P6A4	203	67.13	463.63	61	0.014	1.09	0.59	0.595	0.142	Laser 1 ch
P6A5	201	34.53	106.03	11	0.026	1.11	0.57	0.597	0.160	Laser 2 ch
P6A6	198	60.63	411.63	54	0.029	1.11	0.57	0.594	0.159	Laser 2 ch
Mean					0.026	1.092	0.57	0.592	0.151	

Table 3.2 Flow velocities for all tests of condition P7A (measured by LDA)

Test	Laser analysis				U_{laser} (m/s)				$\langle U^3 \rangle$ (m^3/s^3)	Remarks
	z (mm)	Start (s)	End (s)	No of waves	$\langle U \rangle$	U_c	U_t	U_{rms}		
P7A1	103	241.7 4	898.24	101	0.03	1.21	0.64	0.676	0.214	Laser 2 ch
P7A2	202	162.3 3	727.88	87	0.031	1.23	0.63	0.689	0.227	Laser 2 ch
P7A3	204	67.18	886.18	126	0.034	1.21	0.63	0.671	0.212	Laser 2 ch
P7A4	199	64.55	942.07	135	0.026	1.21	0.65	0.677	0.208	Laser 2 ch
P7A5	203	115.9 4	463.63	81	0.029	1.26	0.66	0.691	0.237	Laser 2 ch
P7A6	201	60.46	547.96	75	0.004	1.23	0.67	0.680	0.193	Laser 1 ch
P7A7	203	62.95	589.45	81	0.020	1.26	0.66	0.691	0.225	Laser 1 ch
Mean					0.025	1.23	0.65	0.682	0.217	

Table 3.3 Flow velocities for all tests of condition P9A (measured by LDA)

Test	Laser analysis				U_{laser} (m/s)				$\langle U^3 \rangle$ (m^3/s^3)	Remarks
	z (mm)	Start (s)	End (s)	No. of waves	$\langle U \rangle$	U_c	U_t	U_{rms}		
P9A1	198	134.4 6	420.47	44	0.031	1.57	0.84	0.891	0.457	Laser 1 ch
P9A2	201	98.84	514.86	64	0.032	1.59	0.84	0.893	0.481	Laser 2 ch
P9A3	200	85.72	755.25	103	0.025	1.58	0.85	0.897	0.459	Laser 2 ch
P9A4	197	115.8 3	759.33	99	0.031	1.61	0.85	0.904	0.496	Laser 2 ch
P9A5	-	-	-	-	-	-	-	-	-	No laser
P9A6	-	-	-	-	-	-	-	-	-	No laser
mean					0.029	1.587	0.85	0.896	0.473	

Table 3.4 Flow velocities for different conditions, sand type B (measured by LDA)

Test	Laser analysis				U_{laser} (m/s)				$\langle U^3 \rangle$ (m^3/s^3)	Remarks
	z (mm)	Start (s)	End (s)	No. of waves	$\langle U \rangle$	U_c	U_t	U_{rms}		
P6B1	200	16.6	81.6	10	0.018	1.12	0.58	0.590	0.151	Laser 2 ch
P6B2	200	18.81	64.31	7	0.027	1.13	0.58	0.592	0.161	Laser 2 ch
P7B1	200	18.76	64.26	7	0.031	1.33	0.66	0.710	0.271	Laser 2 ch
P9B1	200	24.40	89.40	10	0.036	1.62	0.83	0.898	0.507	Laser 2 ch

Figure 3.1 shows the ensemble-averaged horizontal flow velocities outside the wave boundary layer for the different flow conditions ($U_{rms} = 0.6, 0.7$ and 0.9 m/s) at 200 mm above the sand bed.

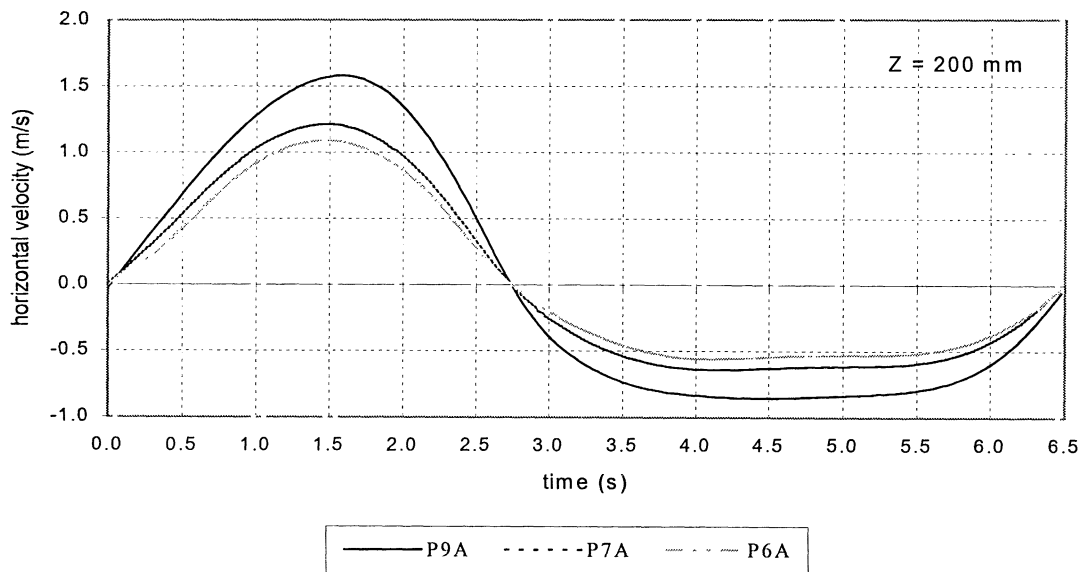


Figure 3.1 Ensemble-averaged flow velocities outside the wave boundary layer, measured by LDA for different wave conditions

3.2 Net sand transport rates

3.2.1 Introduction

For the computation of the net sand transport rates four tests were available for conditions P6A, P7A and P9A. For condition P6B two tests were available and for conditions P7B, P9B and PSB only one test.

The bed level along the test section was measured twice before and twice after the experiment with the bed level profiling system. The second measurement was a check on the first one. The under water weight of the sand collected in the sand traps was also measured.

The net sand transport rate was computed integrating the mass balance equation (using mass conservation technique) twice for each test, starting either from the left (piston side) or the right sand trap (open-leg side). The net sand transport for a specific test was the average value of both computations, after averaging the net sand transport rates over a certain length of the test section for both calculations. See Appendix A for the used length interval.

The net transport rates per fraction were computed using the bed load concentrations and composition measured by the PBLT and using the net sand transport rates from the mass balance equation (mass conservation technique). See section 2.4.2.

Detailed information on the net transport rates can be found in Appendix A for each test. In addition, figures on the net transport rates and the bed levels before and after a test can be found in Appendix A.

Detailed information on the net transport rates per fraction can be found in Appendix C.

In Figure 3.2 (section 3.2.1) the net sand transport rates are summarised for conditions P6A, P7A and P9A. Crosses represent the values of each individual test.

Figure 3.4 (section 3.2.2) shows the net sand transport per fraction for conditions P6A, P7A and P9A.

3.2.2 Net sand transport rates for both fractions

For condition P6A six tests were performed. The net transport rates were measured during four tests. The following can be concluded for condition P6A:

- The net sand transport rates for condition P6A are positive, they are directed 'onshore'.
- The net sand transport rates for each individual test have a small deviation around the mean value.
- The net sand transport rates in the test section are not uniform along the test section. The instruments inside the tunnel create some disturbances (scour effects) of the bed. For test P6A4 this disturbance is relatively large: at $x = +3$ m an erosion hole was formed of about 8 centimeters. This phenomenon explains the deviation of the net sand transport rate at the right

part of the test section for test P6A4, compared with the three other tests. See also Appendix A: figure A.1.

- There is a relatively large difference between the net sand transport rates calculated from the left side of the tunnel and the calculations from the right side of the tunnel. The difference is about a factor 1.3 to 2. This phenomenon is related to the computed porosity from the mass balance equation. The computed porosity values (about 0.6) are much higher than the average porosity from previous experimental series (about 0.4). This large computed porosity is probably caused by some compaction of the bed and possible inaccuracies of the bed level profiling system. Before each test the upper layer of the sand bed was replaced with new sand (mixture).
- The amount of sand collected in the forward sand trap (open-leg side) is about 10 times higher than in the backward sand trap (piston side). This is caused by the asymmetry of the wave motion. The sand transport rate obeys a power law: $q_s \sim u^3$. The forward wave motion has a higher maximum velocity than the backward wave motion.

For condition P7A seven tests were performed. During five tests the net sand transport rates were measured. Due to some problems with the bed level soundings the net sand transport rate for test P7A1 could not be determined. The following can be concluded for condition P7A:

- The net sand transport rates for condition P7A are positive, they are directed 'onshore'.
- The net sand transport rates for each individual test have a small deviation around the mean value.
- The net sand transport rates calculated from the left side of the wave tunnel are somewhat higher than the net transport rates calculated from the right side. Only for test P7A2 there is a relative large difference between the two computations (about 35%).
- The net sand transport rates are approximately uniform along the test section. See also Appendix A: Figure A.2.
- The computed porosity values (about 0.5) are slightly higher than the average porosity values from previous experiments (about 0.4).
- The amount of sand collected in the forward sand trap is about 3 to 4 times higher than in the backward sand trap. Compared with condition P6A the amount of sand in the backward trap has increased strongly.
- The net sand transport rates of condition P7A are approximately 30% higher than that of condition P6A.

For condition P9A six tests were performed. During four tests the net transport rates were measured. The following can be concluded for condition P9A:

- The net sand transport rates for condition P9A are positive, they are directed 'onshore'.
- The net sand transport rates for each test show some differences. The net sand transport rates of test P9A1 are lower than those of tests P9A2, P9A3 and P9A4.

- For test P9A2 the net sand transport rates calculated from the left side of the wave tunnel are somewhat higher than the net transport rates calculated from the right side except for tests P9A1, P9A3 and P9A4 the opposite occurs, the difference between the two computations is not big.
- The computed porosity values (about 0.3) are lower than the average porosity values from previous experiments (about 0.4). This is in contrast to condition P6A and P7A.
- The net sand transport rates are approximately uniform along the test section. See also Appendix A: Figure A.3.
- The amount of sand collected in the forward sand trap is about 2.5 times higher than that in the backward sand trap (test P9A4 is an exception). This difference is smaller than the difference at conditions P6A and P7A.

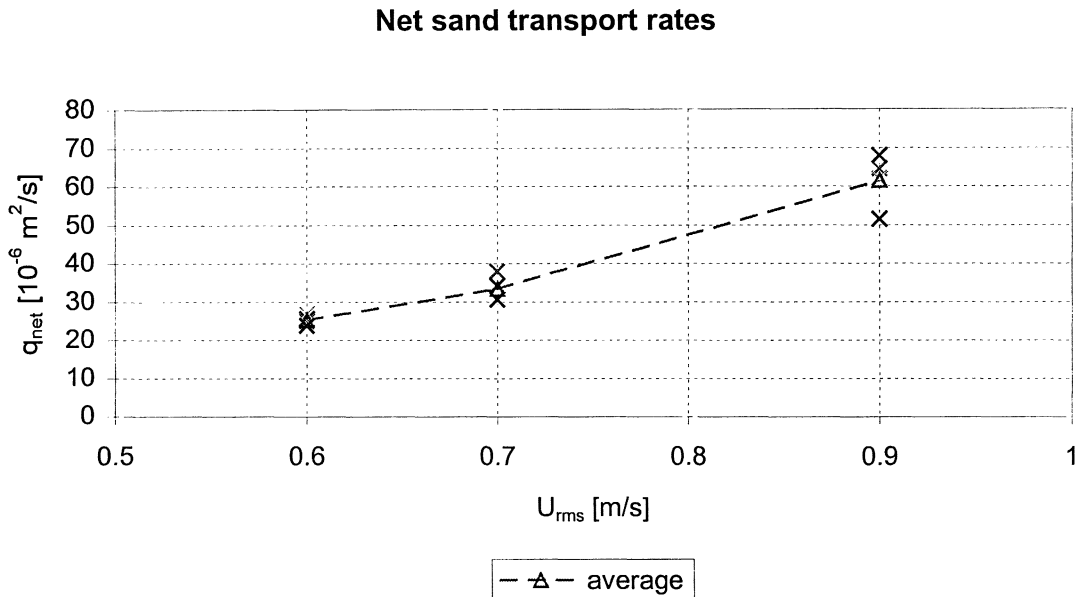


Figure 3.2 Net sand transport rates as a function of U_{rms} (sand type A)

For sand type B (100% coarse sand) five tests were performed with four different wave conditions. The aim of these experiments was to investigate the net sand transports rates in case of very coarse sand for different wave conditions. The following can be concluded:

- No flat bed situation developed for the different flow conditions, large dunes were created, and on top of the dunes a sheet-flow layer developed. See also Appendix A: Figures A.22 to A.25.
- The net sand transport rate is directed offshore. As U_{rms} increases from 0.6 m/s to 0.7 m/s the net sand transport increases in the offshore direction. But as the U_{rms} increases from 0.7 m/s to 0.9 m/s the net sand transport decreases in the offshore direction (unsteady effects appear). See Figure 3.3.

- In case of a sine wave plus a net current the net sand transport rate is directed onshore.
- The net sand transport rates are not uniform along the test section. See also Appendix A: Figures A.4 to A.9. For condition PSB1 the net sand transport rates are positive again.

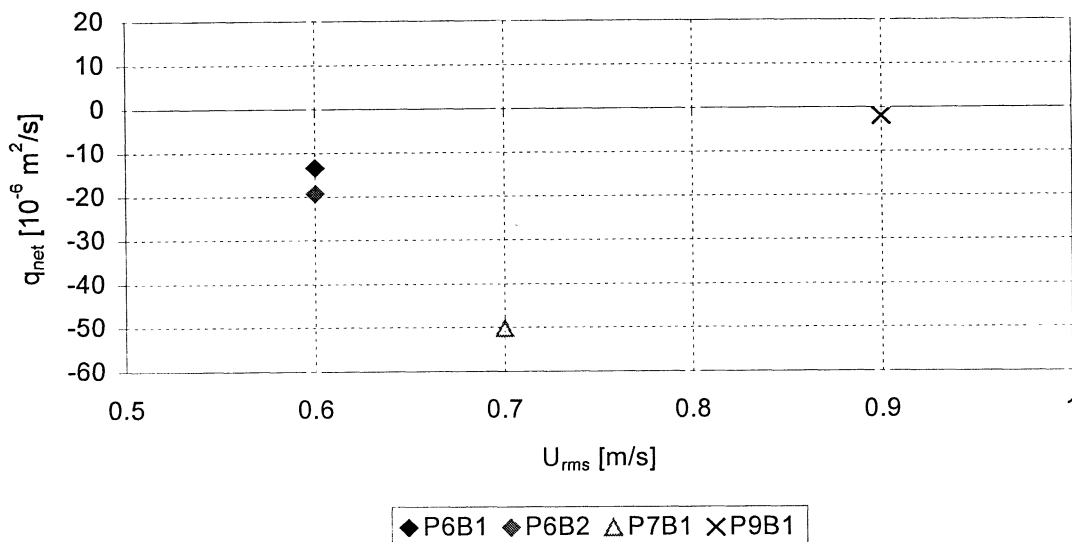


Figure 3.3 Net sand transport rates as a function of U_{rms} (sand type B)

In Table 3.5 the total net sand transport rates are summarised for condition P6A, P7A and P9A. See also Figure 3.2.

Table 3.5 Total net sand transport rates (series P), sand type A.

Condition	U_{rms} [m/s]	Duration of test [s]	q_{net}		Average of test
			[kg/s/m]	$10^{-6} m^2/s$	
P6A	0.592	728	0.067	25.3	P6A1, P6A2, P6A4, P6A4
P7A	0.682	913	0.089	33.4	P7A2, P7A3, P7A4, P7A5
P9A	0.896	690	0.163	61.5	P9A1, P9A2, P9A3, P9A4

In Table 3.6 the total net sand transport rates are summarised for condition P6B, P7B, P9B, and PSB1. See also Figure 3.3.

Table 3.6 Total net sand transport rates (series P), sand type B.

Condition	U_{osc} [m/s]	$U_{current}$ [m/s]	Duration of test [s]	q_{net}		Average of test
				[kg/s/m]	[10^{-6} m ² /s]	
P6B	0.6 ¹	0.0	1340	-0.0433	-16.3	P6B1, P6B2
P7B	0.7 ¹	0.0	518	-0.133	-50.2	P7B1
P9B	0.9 ¹	0.0	456	-0.0053	-2.0	P9B1
PSB	1.5 ²	0.25	900	0.143	+54.0	PSB1

Notes:

- 1: 2nd order Stokes waves, root mean square velocity
 2: sine wave, U_{max}

The following can be concluded from the analysis of the net sand transport rates:

- In case of a sand bed consisting of sand type A (mixture of 30% coarse sand, $d_{50}= 0.97$ mm, and 70% fine sand, $d_{50} = 0.21$ mm) a flat bed and sheet-flow situation developed during the present experiments.. The net sand transport rate is directed onshore.
- An increase of the flow velocity (U_{rms}) leads to an increase of total net sand transport.
- The increase of the net sand transport rate seems to become larger when the flow velocity becomes larger.
- In case of a sand bed consisting of sand type B (100% coarse sand, $d_{50}= 0.97$ mm) no flat bed situation developed for the conditions P6B, P7B and P9B. Large dunes were created and on top of the dunes a sheet-flow layer developed. The net sand transport rate is directed offshore.
- For sand type B there is no relation between the flow velocity (U_{rms}) and the net sand transport rate. Unsteady effects are present. An increase of the flow velocity does not lead to an increase of the net sand transport rate.

3.2.2 Net sand transport rates per fraction

In Table 3.6 and Figure 3.4 the net sand transport rates per fraction are summarised for conditions P6A, P7A and P9A. See also Appendix C: Tables C.4 to C.9.

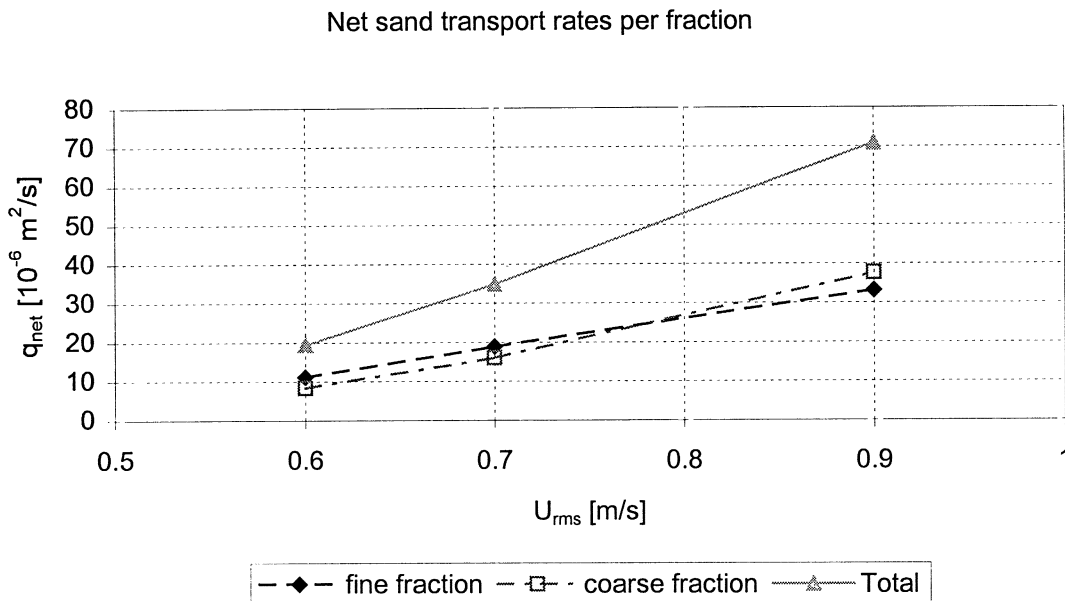


Figure 3.4 Net sand transport rates per fraction as a function of U_{rms}

Table 3.6: Net sand transport per fraction (series P)

Condition	U_{rms} [m/s]	$q_{net, fine}$		$q_{net, coarse}$		Average of test
		[kg/s/m]	[$10^{-6} m^2/s$]	[kg/s/m]	[$10^{-6} m^2/s$]	
P6A	0.592	0.0294	11.1	0.0221	8.3	P6A1, P6A2
P7A	0.682	0.0502	18.9	0.0423	16.0	P7A2, P7A3
P9A	0.896	0.0880	33.2	0.100	37.7	P9A1, P9A2

The following can be concluded from the analysis of the net sand transport rates per fraction:

- The net sand transport rate of the fine fraction for condition P6A and P7A is just a little larger than the net sand transport rate of the coarse fraction, while the percentage coarse fraction in the mixture is only 30%. Relatively much of the coarse fraction is transported under sheet-flow conditions. Selective transport occurs.
- An increase of the flow velocity (U_{rms}) leads to an increase of net sand transport rate for both the fine and the coarse fraction (almost a linear relation). At condition P9A the net sand transport of the coarse fraction has even become larger than the net sand transport of the fine fraction.

3.3 Composition of sand

3.3.1 Composition of bed material before and after tests

As mentioned before the sand bed consisted of a mixture of 70% fine sand ($d_{50}=0.21$ mm) and 30% coarse sand ($d_{50}=0.97$ mm). A settling tube analysis (VAT) of this mixture resulted in the following characteristic diameters:

- $d_{10} = 0.16$ mm;
- $d_{50} = 0.23$ mm;
- $d_{90} = 0.87$ mm.

Also a sieve analysis was performed. The sieve analysis of this mixture resulted in the following characteristic diameters (see also Figure 2.1):

- $d_{10} = 0.16$ mm;
- $d_{50} = 0.24$ mm;
- $d_{90} = 0.99$ mm.

A comparison between both results shows a deviation for the d_{90} of the mixture. This deviation can also be seen from the analysis of the samples taken from the sand bed after a test. This deviation is considered not to be important in the present study, because the main interest is the percentage of coarse and fine sand fraction.

Before each test the upper layer (about 5 cm) of the sand bed was replaced. After each test (condition P6A, P7A and P9A), bed samples were taken at different locations using the Suction Tube.

For two tests of condition P6A and P9A and three tests of condition P7A bed samples were taken at 3 locations inside the tunnel (at $x = - 2.5$ m, $x = + 1.0$ m and $x = + 3.5$ m). A distinction was made in three separate slices or layers of 3 mm (3 slices of 3 mm). At tests P6A3, P7A4 and P9A3 the composition of the sand bed after a test was examined more thoroughly. Samples were taken at 5 different locations (at $x = - 2.5$ m, $x = + 1.0$ m, $x = + 3.5$ m, $x = + 4.5$ m and $x = + 5.5$ m). Here a distinction was made in separate slices or layers of 3 to 10 mm (3 slices of 3 mm, 4 slices of 5 mm and 2 slices of 10 mm) over a depth of 50 mm. For tests P6A4, P7A5 and P9A4 more bed samples were taken: every 0.5 m up to every 0.25 m. For these three tests a distinction was made in two layers of about 20 mm.

Before each test a well-mixed sand bed (horizontally and vertically) was brought into the tunnel. Analyses of bed samples taken during the test phase, preliminarily to this experimental series, showed that the coarse sand and the fine sand mix very well using a mechanical mixer. It must be emphasised that the upper layer of the sand bed is replaced before every test, this in contrast to most previous experimental series. Thus each test started with the same bed composition for the whole test section.

The individual bed samples were analysed in the Visual Accumulation Tube (VAT) or settling tube of WL | DELFT HYDRAULICS to get information of the grain-size distribution and the percentage coarse fraction and fine fraction.

Detailed information of the grain-size distribution of samples from the sand bed and the percentages coarse and fine fraction of the different layers and locations can be found in Appendix B. Also figures on the change of bed composition with depth can be found in this appendix.

Figure 3.5 shows the distribution of the percentage coarse fraction with depth for conditions P6A, P7A and P9A. These distributions have been obtained by taking the average of all locations where the sand bed stayed uniform (concerning all tests of one condition). These locations are considered to be representative. Note that for the layers from 10 to 50 mm only one test per condition is available (average from five different locations).

The following can be concluded from the bed samples analysis:

- The bed composition (percentage coarse fraction and fine fraction) after the tests is not uniform with depth anymore. Selective transport has occurred. The upper layers of the bed change of composition. The top 3 mm of the bed has roughly the same composition as that before the test (conditions P6A and P7A) or is a little coarser (condition P9A). Beneath the top layer there is a layer that mainly contains fine sand (10-20% coarse sand). This layer is about 10 to 20 mm thick. At larger depths the composition of the bed seems not to have changed much. The big deviation of condition P7A at a depth between 15 and 24 mm below the bed surface is probably caused by a location in the sand bed where the mixture was poorly mixed. Analysis (VAT) showed that a bed sample of test P7A4, at location $x = +3.5$ m, was very coarse at a depth between 15 and 24 mm below the bed surface.
- For condition P6A the “active layer” is about 10 to 20 mm thick. For condition P7A the “active layer” is about 10 to 25 mm thick and for condition P9A this layer is 20 to 30 mm thick.
- On average the bed has become less coarse during a test. This occurs at each of the three wave conditions. This is in accordance with the composition of the sand collected in the sand traps (contains more than 30% coarse sand fraction, see also section 3.3.3). As the flow velocity (U_{rms}) increases the upper layers of the bed seem to become more and more fine. See also Appendix B: Figures B.12, B.19, B.25 and B.26.
- The bed composition results from different tests (same flow condition) show a lot of scatter at the same locations along the tunnel. Condition P7A is an exception to this. All tests of this condition show a decrease of the percentage coarse fraction near the center of the tunnel (at +1.0 m) and an increase at the open-leg side of the tunnel (+3.5 m).
- The instruments inside the tunnel during a test produce vortices, which create scour effects. These scour effects lead to a local change of the bed composition, especially in the right part (open-leg side) of the test section (erosion or sedimentation). Generally these scour effects developed after about 10 minutes of testing. If they became too large the test was stopped. The process of local erosion and sedimentation makes the bed sample analysis more difficult.

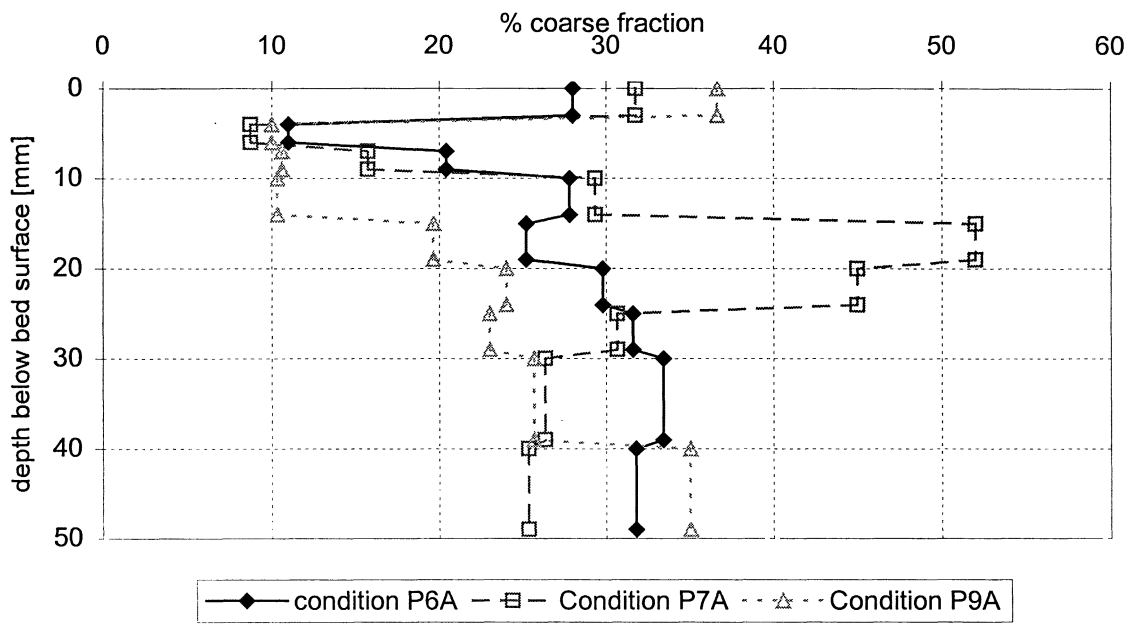


Figure 3.5 Distribution of the percentage of coarse fraction with depth for different flow conditions (average values per condition)

3.3.2 Composition of bed load transport (PBLT)

For the measurement of the bed load concentrations and composition four tests were available for conditions P6A and P9A and five tests for condition P7A. During a test 30 liters of water and sand were extracted from the tunnel at each nozzle of the PBLT. The dry weight of the collected sand was determined using calibrated tubes.

The actual measurement (extraction of water/sediment mixture) started 2 minutes after the start of a test when the sheet-flow was fully developed. The extraction was stopped as soon as the amount of 30 liters for one of the nozzles was reached. During a test it was made sure that the metal footplate of the PBLT was kept on the sand bed.

The sand samples collected by the PBLT (onshore and offshore bed load transport) were analysed in the Visual Accumulation Tube (VAT) in order to determine the grain-size distribution and the percentages coarse and fine fraction.

Detailed information of the composition of the bed load transport, onshore and offshore, can be found in Appendix C. This appendix also includes figures of the grain-size distribution of the bed load transport.

The results from the PBLT measurements (bed load composition) are summarised in Table 3.7 and Figure 3.6. Crosses (onshore transport) and triangles (offshore transport) represent the values of the individual tests.

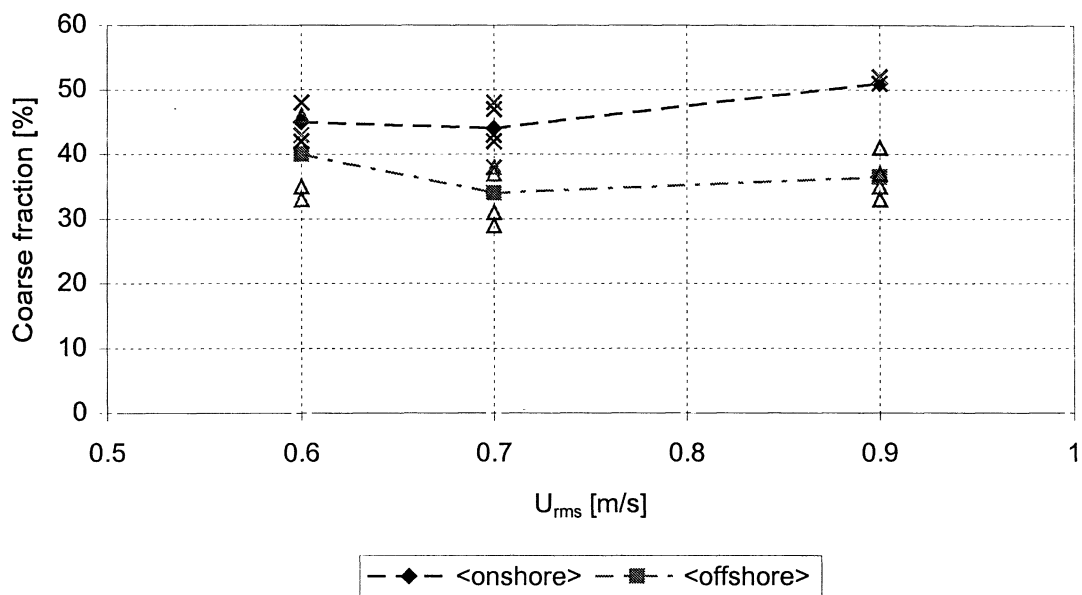


Figure 3.6 Bed load composition, measured by PBLT, as a function of U_{rms}

Table 3.7 Composition bed load transport (PBLT)

Condition	U_{rms} [m/s]	Onshore (forward)		Offshore (backward)		Average of tests
		% fine	% coarse	% fine	% coarse	
P6A	0.592	55 (+/- 3)	45 (+/- 3)	60 (+/- 7)	40 (+/- 7)	P6A1, P6A2, P6A5, P6A6
P7A	0.682	56 (+/- 6)	44 (+/- 6)	66 (+/- 5)	34 (+/- 5)	P7A1, P7A2, P7A3, P7A6, P7A7
P9A	0.896	49 (+/- 1)	51 (+/- 1)	63.5 (+/- 4)	36.5 (+/- 4)	P9A1, P9A2, P9A5, P9A6

The following can be concluded from the VAT analysis of the PBLT samples:

- The bed load transported in the onshore direction is coarser than the bed load transported in the offshore direction.
- For both directions the percentage of coarse fraction is larger than one would expect, as the percentage of coarse fraction in the sand bed is only 30%. Selective transport is occurring.
- As the flow velocity (U_{rms}) increases, the percentage coarse fraction in the onshore direction at first slightly decreases and later, from $U_{rms}=0.7$ m/s to $U_{rms}=0.9$ m/s it increases. The percentage coarse fraction in the offshore direction shows a sharp decrease from $U_{rms}=0.6$ m/s to $U_{rms}=0.7$ m/s and a small recovery from $U_{rms}=0.7$ m/s to $U_{rms}=0.9$ m/s. The difference between the onshore and offshore direction increases for increasing flow velocities.

3.3.3 Composition of sand from sand traps

For the calculation of the net sand transport rates it was necessary to measure the weight of the sand inside the two sand traps after each test. One sand trap is located beneath the piston tube, the other one at the open leg tube of the wave tunnel. For tests P6A1 to P6A4, P7A1 to P7A5 and P9A1 to P9A4 samples from the sand inside the two sand traps were analysed in the Visual Accumulation Tube (VAT) in order to determine the grain-size distribution and the percentages coarse and fine fraction.

Detailed information of the composition of the sand from the sand traps can be found in Appendix B. The amount of sand collected in each trap can be found in Appendix A (submerged weight).

The results from the VAT analysis of the samples taken from the two sand traps are summarised in Table 3.8 and Figure 3.7. Crosses represent the values of each individual test.

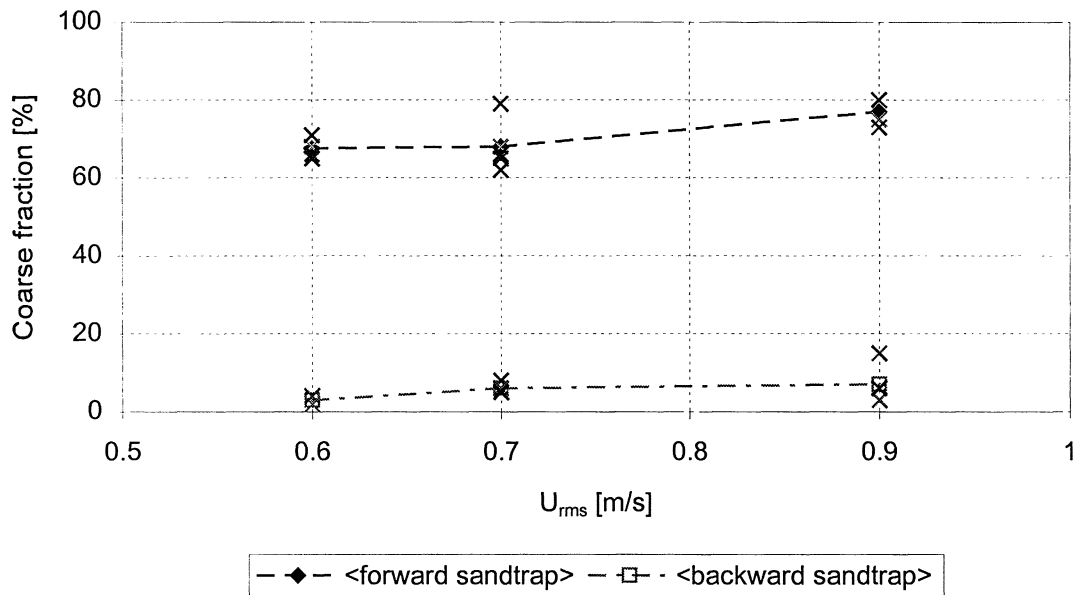


Figure 3.7 Composition sand from sand traps as a function of U_{rms}

Table 3.8 Composition of sand from sand traps

Condition	U_{rms} [m/s]	Forward sand trap (onshore)		Backward sand trap (offshore)		Average of tests
		% fine	% coarse	% fine	% coarse	
P6A	0.592	32.5	67.5	97	3	P6A1, P6A2, P6A3, P6A4
P7A	0.682	32	68	94	6	P7A1, P7A2, P7A3, P7A4, P7A5
P9A	0.896	23	77	93	7	P9A1, P9A2, P9A4, P9A4

The following can be concluded from the VAT analysis of the samples from the sand traps:

- The forward sand trap (open-leg side) contains very little fine fraction, about 30% compared to the percentage of fine fraction in the sand bed (70%).
- The backward sand trap (piston side) contains hardly any coarse fraction (<10%).
- The difference between the two sand traps is related to the asymmetry of the wave motion. The maximum onshore velocity is larger than the maximum offshore velocity. At low oscillating velocities only the fine grains are transported while at higher oscillating velocities also the coarse grains begin to move. This implies that at the offshore wave motion the transported sand will be finer than at the onshore wave motion. This was also seen from the analysis of the composition of the bed load transport (PBLT).
- As the flow velocity (U_{rms}) increases the percentage coarse fraction inside the forward sand trap also increases.
- As the flow velocity (U_{rms}) increases the percentage coarse fraction inside the backward sand trap only slightly increases.
- The sand found in the backward sand trap is in general more fine (smaller d_{50}) than the fine sand from the sand bed (sand type A).
- Selective transport is occurring in the test section.
- The composition of the sand from the sand traps is different than that from the bed load transport (PBLT). The forward sand trap contains a much larger percentage of *coarse* fraction than the onshore bed load transport and the backward sand trap contains a much larger percentage of *fine* fraction than the offshore bed load transport. It is suspected that the PBLT does not cover the complete bed load layer, that the bed load transport is actually coarser. This could be a partly explanation for the difference described above. Another contributory cause could be the change of composition of the upper layer of the sand bed along the test section, especially at the boundaries. The right part of the test section seemed to have become a little coarser and the left part a little finer (selective storage).

3.3.4 Composition of suspended sand (TSS)

A transverse suction system was used to measure the time-averaged suspended concentrations for conditions P6A, P7A and P9A. For each condition two tests were performed (P6A3, P6A4, P7A4, P7A5, P9A3 and P9A4). The horizontal position of the Transverse Suction System (TSS) was at $x = +0.35$ m. The lowest tube of the TSS was positioned about 5 mm above the bed before the start of a test, resulting in a range of elevations from about 260 mm above the bed to about 5 mm above the bed. See Figure 2.6 for the distances between the nozzles. After a test the distance between the lowest tube and the sand bed was recorded in order to determine the average position of each nozzle above the bed.

The peristaltic pumps were switched on one minute after the start of a test. The actual measurement (extraction of water/sediment mixture) started two minutes after the start of a test, when the concentration profile was fully developed.

For each nozzle an equal amount of water was extracted from the tunnel during a single test. In general this amount varied between 5 to 7 liters per nozzle.

The extraction was stopped as soon as erosion holes began to develop. After each test the upper layer of the sand bed was replaced.

The sand samples collected by the TSS were analysed in the Visual Accumulation Tube (VAT) to determine the grain-size distribution and the percentage coarse and fine fraction.

Detailed information of the composition of the suspended sediment samples can be found in Appendix D. Figures of the vertical distribution of the d_{50} of the suspended sediment samples can also be found here.

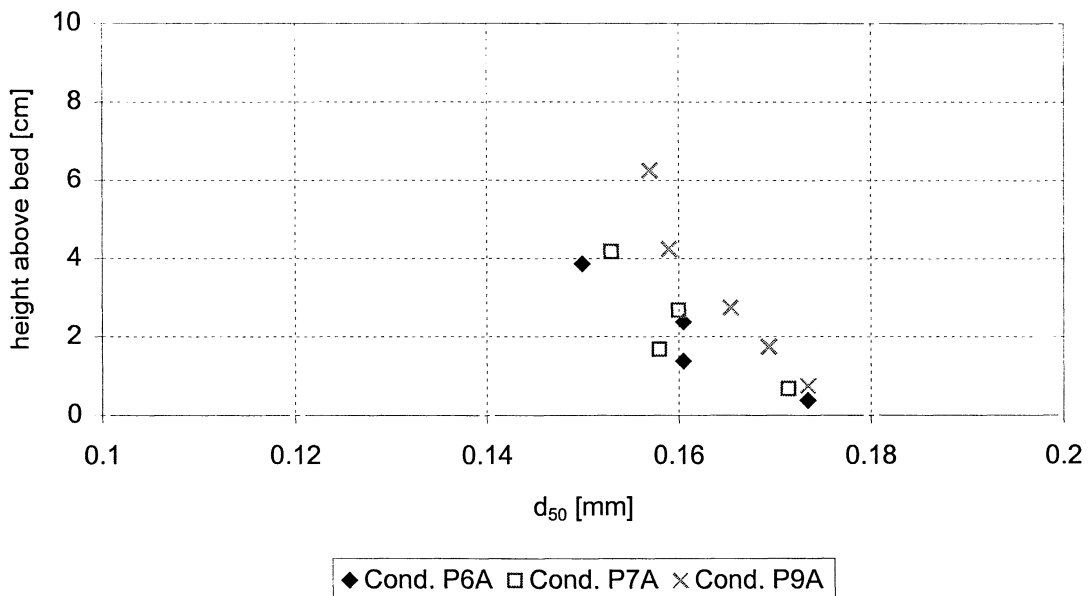


Figure 3.8 Vertical distribution of d_{50} of suspended sediment (TSS), 3 flow conditions

The results from the VAT analysis of the suspended sediment samples are summarised in Figure 3.8. The values of two tests of one condition have been averaged. Note that only the lower 4 or 5 tubes extracted enough suspended sediment to determine the grain-size distribution. The amount of sand from the upper tubes was too small to determine the grain-size distribution. Therefore the sand from the upper tubes was put together and the obtained grain-size distribution was assigned to the lowest tube concerned. See also Appendix D for more detailed information.

The following can be concluded from the VAT analysis of the samples from transverse suction:

- The suspended sediment contains no coarse fraction, only fine fraction.
- The grain-size of the suspended sediment becomes finer as the distance above the bed increases. There seems to be a linear relation between the elevation and the d_{50} of the suspended sediment.
- Only the smaller particles of the fine sand from the sand bed go in suspension (compare the d_{50} of fine bed material sand with the d_{50} of the suspended sediment samples).
- As the flow velocity (U_{rms}) increases, the suspended sediment at a certain elevation becomes coarser (larger d_{50}). See Figure 3.8.

Although the original bed has a d_{50} of 0.232 mm (VAT analysis) the largest median diameter in the lowest measuring point (elevation < 1 cm) of the suspension layer is about 0.18 mm (test P9A4). This indicates that only the finest fraction of the finebed material sand is set into suspension for all flow conditions.

3.4 Sand concentrations in sheet-flow layer, CCM results

The sediment concentrations inside the sheet-flow layer were measured with CCM at different elevations very close and inside the sand bed. The bed level measurements (every 30 s) show big changes during one test, between 5 and 12 mm. The number of CCM tests for each flow condition can be summarised as follows:

- Five tests were performed for condition P6A, with measurements in the range from 3 mm below to 5 mm above the bed.
- For condition P7A, six tests were performed with a range of depths from 1 below to 5 above the bed.
- For condition P9A, six tests were performed with a range of depths from 3 below to 5 above the bed.
- The number of waves for the ensemble-averaged concentrations varies between 9 and 60 waves, based on the bed levels changing during each test. All information about the chosen intervals of each elevation can be found in appendix E.

Time-averaged concentration profiles

Figure 3.9 shows the time-averaged sediment concentration profiles inside the sheet-flow layer, for the three flow conditions (P9A, P7A and P6A) on a log-linear scale, between 5 mm above the bed and 3 mm below the bed. The measured sediment concentration profiles show that:

- The sediment concentrations inside the bed ($z < 0.0$ mm) are constant for the three flow conditions (1300 – 1500 g/l)
- The sediment concentrations decrease rapidly reaching 100 g/l at approximately 4/5 mm above the mean bottom level, for the three flow conditions.
- Increasing U_{rms} leads to small increase in the sheet-flow layer thickness. The sheet-flow layer thickness is defined as the distance between the top of the non-moving sand bed, which has an averaged concentration about 1400 g/l and the level where the concentration is about 200 g/l. This thickness was found to be approximately 5.5 mm in case PA9 and 4.0 mm in the two cases P6A and P7A.
- The time-averaged sediment concentration profiles for the different flow conditions, including the possible errors in sediment concentration measurements and the possible inaccuracies in the determined levels can be found in appendix E.

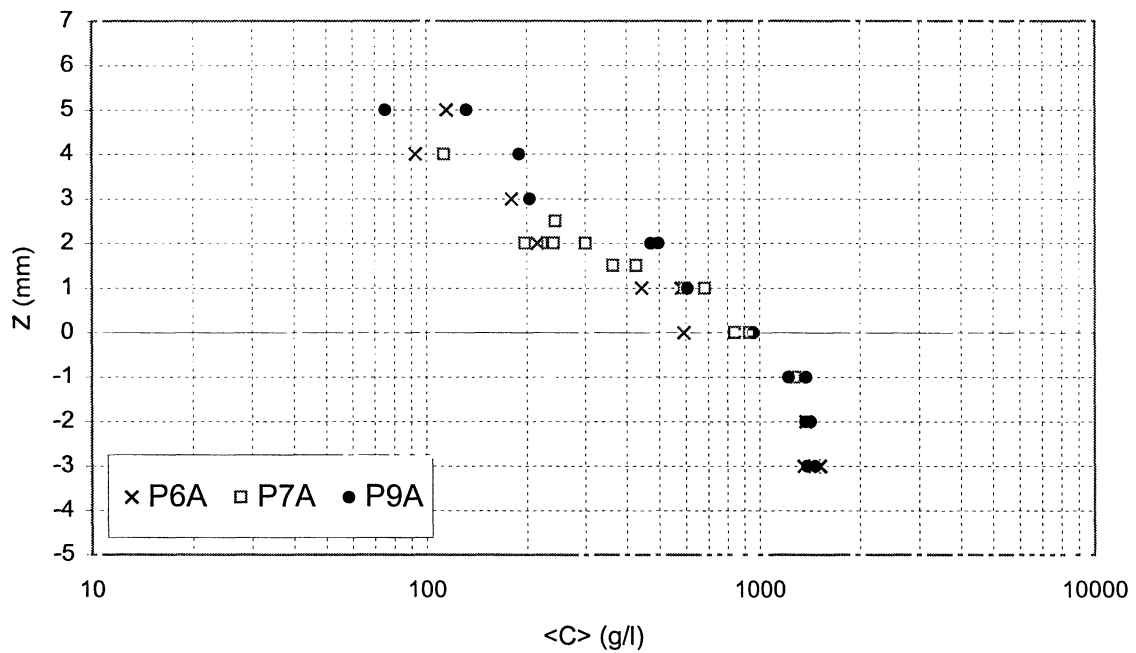


Figure 3.9 time-averaged concentration profile inside the sheet-flow layer, measured by CCM, on log-linear scale, different flow conditions

Time-dependent concentrations

The ensemble-averaged concentration values over a certain number of waves are used to represent the time-dependent sediment concentrations inside the sheet-flow layer. The behavior of the time-dependent sediment concentrations during the wave-cycle was analyzed, using the ensemble-averaged flow velocity at 200 mm above the bed. It should be noted that the time-dependent velocity is level dependent, i.e. the magnitudes of the maximum positive (onshore), negative velocities (offshore) and the moment of flow reversal are changing with elevation above the bed.

Figures 3.10 to 3.12 show the measured ensemble-averaged concentrations inside the sheet-flow layer for the different flow conditions (P9A, P7A and P6A), in the lower panels of each Figure. Each curve is representing a different elevation around the initial bed level. The upper panel of each Figure shows the measured ensemble-averaged flow velocities at 200 mm above the bed. The measured time-dependent sediment concentrations show that:

- A clear distinction can be found between two different layers: the pick-up layer ($z < + 1.0$ mm) and the upper sheet-flow layer ($z > + 1.0$ mm). These two layers show exactly the opposite behavior; i.e. the pick-up layer shows a maximum sediment concentration reduction at the moments of maximum positive and negative free stream velocity. At the same moments the upper sheet-flow layer shows a maximum increase in sediment concentrations. See for example the two levels $- 1.0$ mm and $+ 3.0$ mm in Figure 3.10.
- A sharp transition was found between the pick-up and the upper sheet-flow layers around $+ 1.0$ mm, with almost constant sediment concentration during the wave-cycle (600 g/l). This sharp transition was found to occur at approximately the same level ($\approx +1.0$ mm), for the three flow conditions.
- The pick-up layers ($z < + 1.0$ mm), show a large reduction of the sediment concentrations during the maximum positive (onshore) free stream velocities for all three test conditions, reflecting the pick-up of sand particles into higher elevations. These maximum reductions in concentrations are clearer in conditions P9A and P7A than condition P6A (note that the maximum positive velocity has a larger magnitude for larger U_{rms}).
- These sediment concentration reductions in the pick-up layers were found to be smaller during the negative part (offshore) of the free stream velocity than the positive part (onshore). This difference between offshore and onshore concentrations is increasing with increasing U_{rms} (note that the maximum positive velocity has a larger magnitude than the maximum negative velocity). See Figures 3.10 to 3.12.
- In the upper sheet-flow layers ($z > + 1.0$ mm) higher sediment concentrations occur during the phases of maximum positive velocities for the three flow conditions. This increase in concentrations is much smaller during the negative part of the free stream velocities.
- There is no clear difference in phases between the moments of maximum sediment concentrations at different elevations in the upper sheet-flow layer. There is also no clear phase difference between the pick-up and upper sheet-flow layer (moments of maximum reduction in the pick-up layer and maximum concentration increase in the upper sheet-flow layer). In fact, the very thin sheet-flow layers cause this.

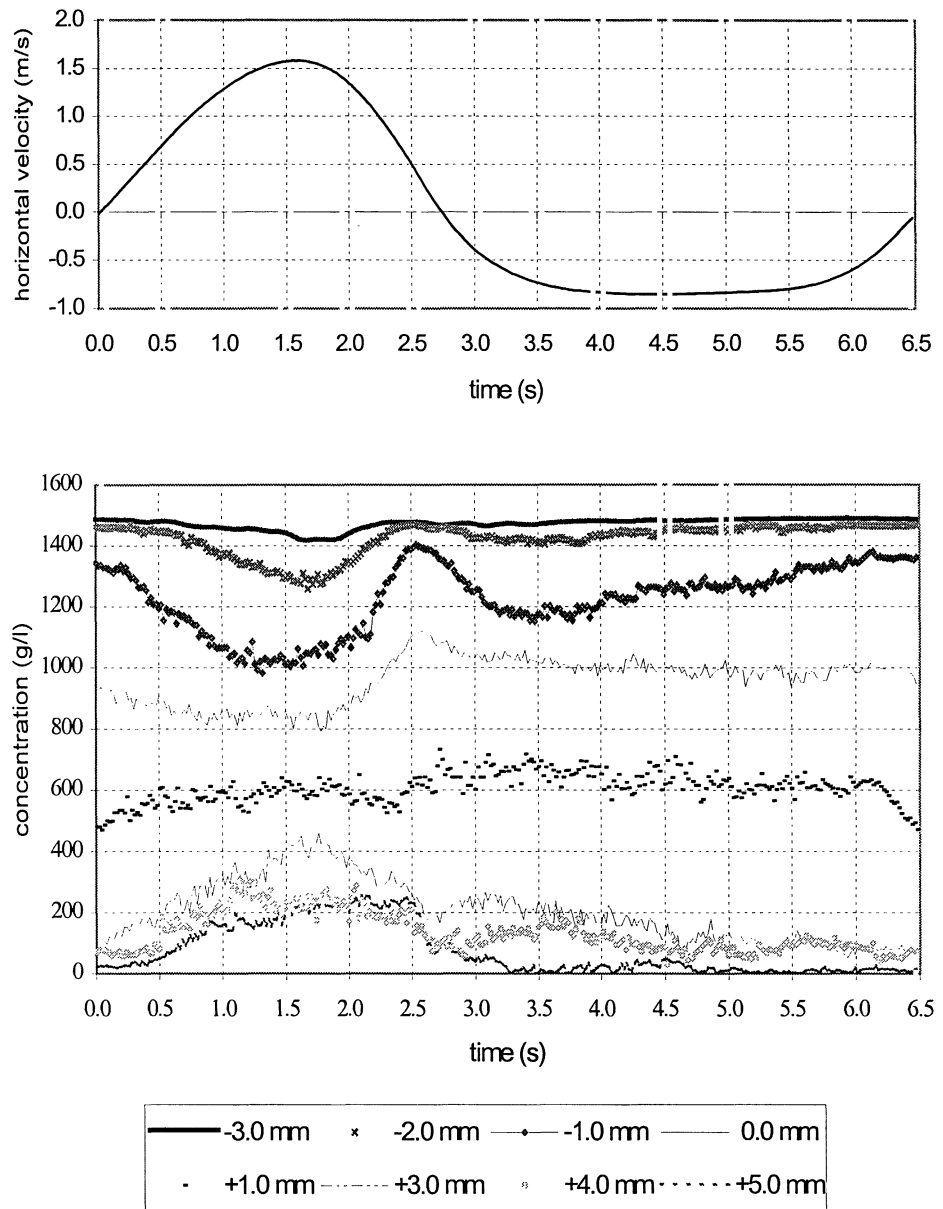


Figure 3.10 Ensemble-averaged concentrations inside the sheet-flow layer, measured by CCM at different elevations above the bed, together with the free-stream velocity, condition P9A

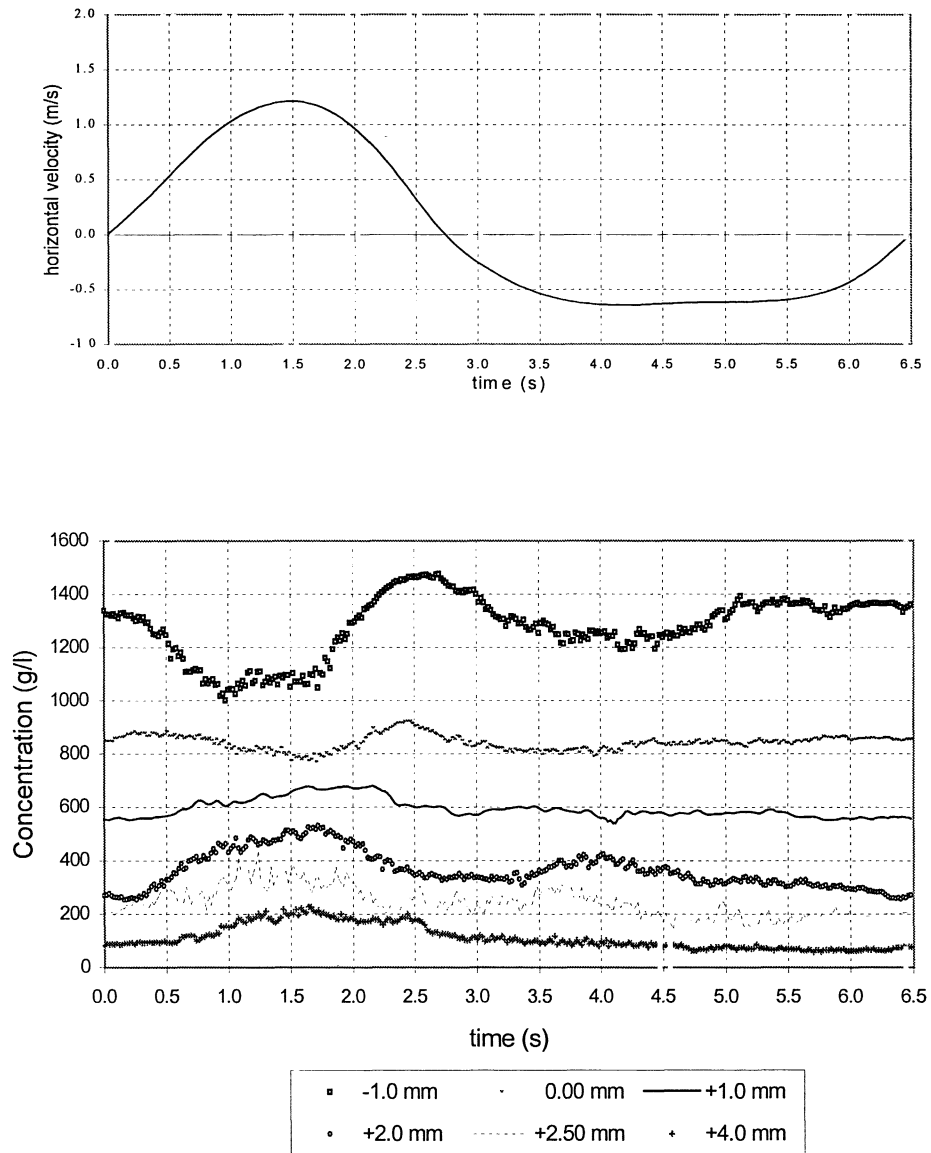


Figure 3.11 Ensemble-averaged concentrations inside the sheet-flow layer, measured by CCM at different elevations above the bed, together with the free-stream velocity, condition P7A

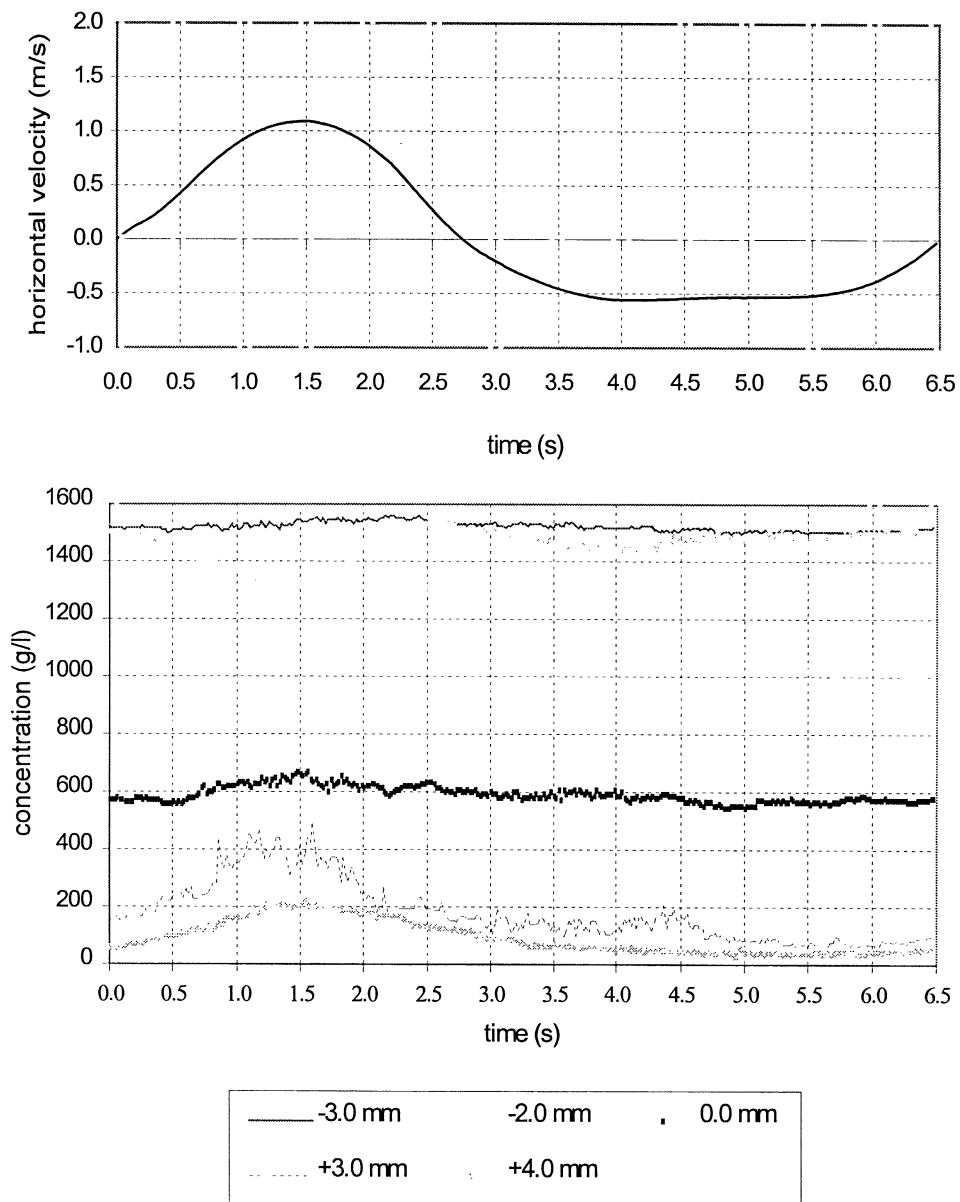


Figure 3.12 Ensemble-averaged concentrations inside the sheet-flow layer, measured by CCM at different elevations above the bed, together with the free-stream velocity, condition P6A'

3.5 Bed load and suspended concentrations

3.5.1 Bed load concentrations

The time-averaged bed load concentrations were measured using the Pump Bed Load Trap sampler (PBLT). For condition P6A and P9A four tests were performed with the PBLT and five tests for condition P7A. The dry weight of the sand extracted by the PBLT was determined using calibrated tubes. The time-averaged bed load concentrations onshore and offshore were determined by calculating the ratio of the dry weight of the extracted sand and the total volume of the extraction.

Detailed information of the time-averaged bed load concentrations, onshore and offshore, can be found in Appendix C.

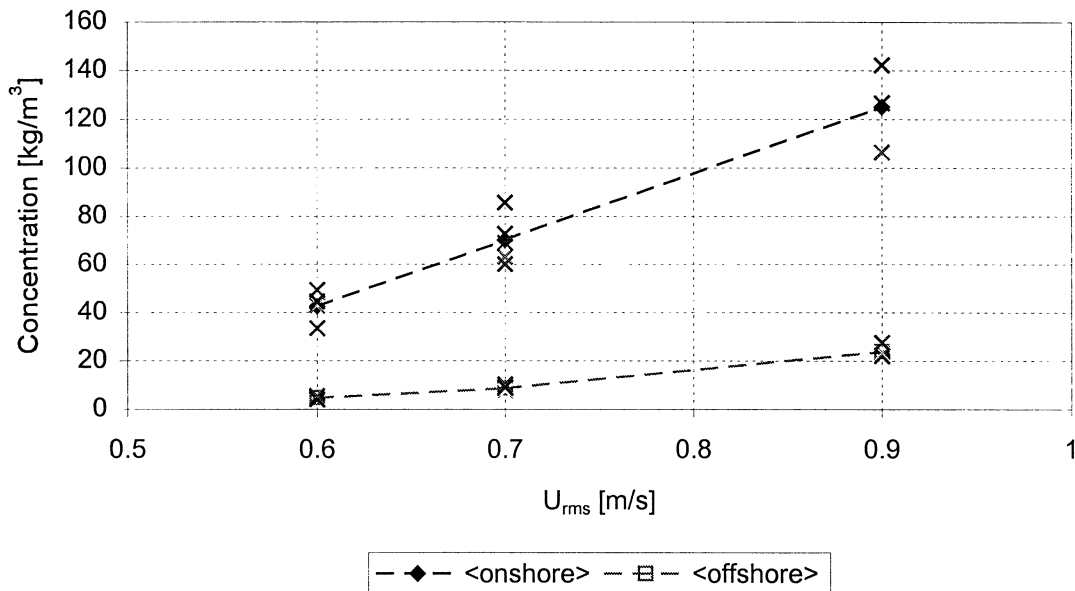


Figure 3.13 Bed load concentrations, measured by PBLT, as a function of U_{rms}

The results from the PBLT measurements are summarised in Table 3.9 and Figure 3.13. Crosses represent the values of the individual tests.

Table 3.9 Bed load concentrations (PBLT)

Condition	U_{rms} [m/s]	Sand concentration onshore (kg/m ³)	Sand concentration offshore (kg/m ³)	Average of tests
P6A	0.592	42.65 (+/- 9)	4.8 (+/- 0.8)	P6A1, P6A2, P6A5, P6A6
P7A	0.682	70.1 (+/- 15)	8.7 (+/- 1.7)	P7A1, P7A2, P7A3, P7A6, P7A7
P9A	0.896	125.1 (+/- 19)	23.8 (+/- 3.8)	P9A1, P9A2, P9A5, P9A6

The following can be concluded from the analysis of the time-averaged bed load concentrations:

- The time-averaged onshore bed load concentration is 5 to 10 times higher than the time-averaged offshore bed load concentration. This is related to the difference between the onshore and offshore velocities.
- The ratio between the onshore and offshore bed load concentration decreases as the flow velocity (U_{rms}) increases.
- When the flow velocity increases both the onshore and the offshore concentration increase rapidly. It seems that a linear relation exists between the flow velocity (U_{rms}) and the onshore and offshore concentration. See Figure 3.13.

3.5.2 Suspended sediment concentrations (TSS)

The Transverse Suction System was used to measure the time-averaged suspended sediment concentrations for condition P6A, P7A and P9A. For each condition two tests were performed (P6A3, P6A4, P7A4, P7A5, P9A3 and P9A4).

The dry weight of the sand extracted by the TSS was determined using calibrated tubes. The time-averaged suspended sediment concentrations were determined by calculating the ratio of the dry weight of the extracted sand and the total volume of the extraction.

Detailed information of the time-averaged suspended sediment concentrations can be found in Appendix D.

The measured suspended sediment concentrations for condition P6A, P7A and P9A are summarised in Figure 3.14. The values of both tests of one condition have been averaged.

For test P6A4 the suspended sediment concentrations at higher elevations were remarkably large compared with test P6A3 and the tests from the other two conditions. These large concentrations are probably caused by an erosion hole that was formed at the end of test P6A4, stirring up a lot of sand. This erosion hole was located about 2.5 m from the TSS, towards the open-leg side of the wave tunnel. These high concentrations for test P6A4 lead to a rather deviating concentration profile for condition P6A, as the values of 2 tests (P6A3 and P6A4) are averaged. For condition P7A and P9A the results of the two tests of each condition were similar.

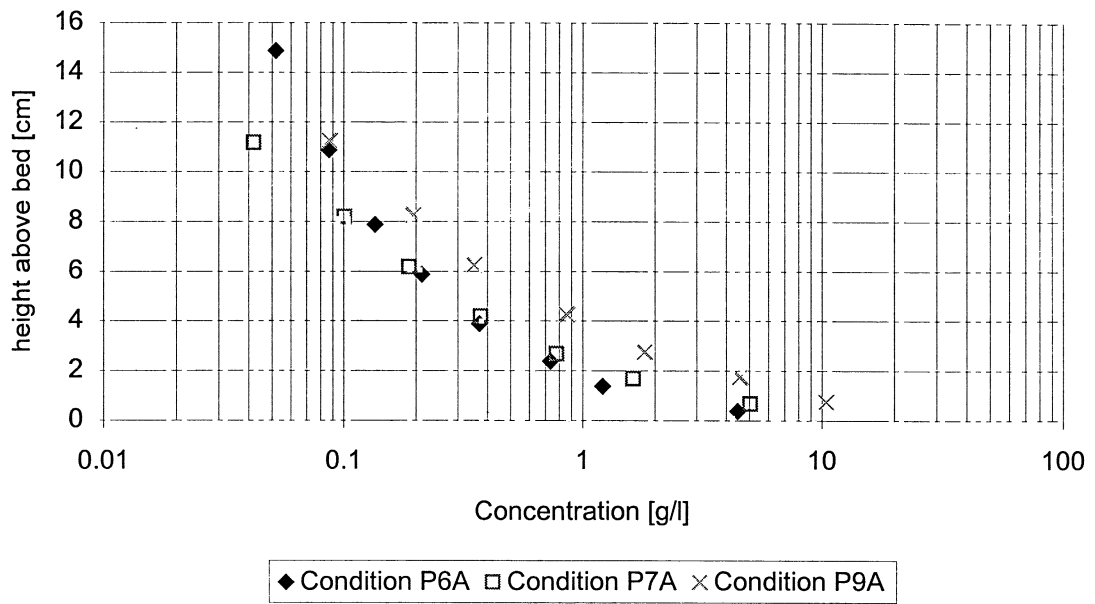


Figure 3.14 Time-averaged suspended concentrations (TSS), 3 flow conditions, on a log-linear scale

The following can be concluded from the analysis of the time-averaged suspended sediment concentrations:

- The time-averaged suspended sediment concentration decreases rapidly as the height above the bed increases. There seems to be a power law relation between the suspended sediment concentration and the distance above the bed.
- An increase of the flow velocity (U_{rms}) generally leads to higher concentrations of suspended sediment (at the same elevation).

3.6 Bed level variations based on video recording

For sand mixture A one video recording of about 300 s was made for the three flow conditions P6A, P7A and P9A with a wave period 6.5 s, in order to determine the bed level variation during the wave cycle (δ_2). The initial bed level before each test was recorded in order to determine the overall bed lowering during a test (δ_1), caused by sand which remains in suspension during the test. Figure 3.15 show the exact definitions of δ_1 and δ_2 .

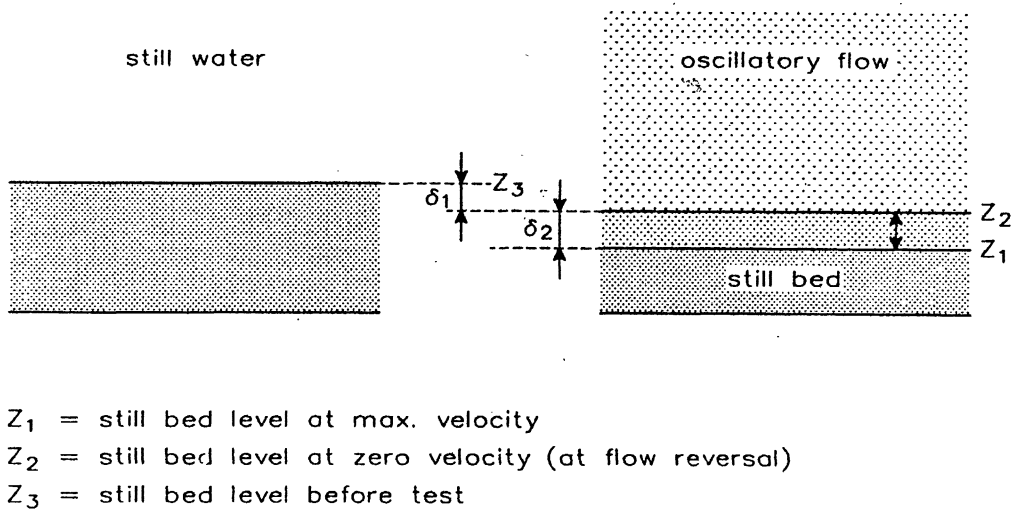


Figure 3.15 Definition sketch of overall bed lowering and bed level variation during wave cycle

The values of δ_1 and δ_2 , as determined from the video recordings, are given in Table 3.10 for each flow condition. It is clear that the variation of bed level during a wave cycle, as well as the overall lowering of the sand bed is found to increase for increasing oscillatory velocities, as could be expected.

Table 3.10 Bed level variations during the wave cycle, for different flow conditions

Condition	Overall bed lowering δ_1 (mm)	Bed level variation during wave cycle δ_2 (mm)		Remarks
		Onshore	offshore	
P6A	0	1.0	0.25 - 0.5	Rolling and saltation of sand particles is clear during offshore motion
P7A	0	1.5 - 2.0	0.25 - 0.5	
P9A	0 - 0.5	2 - 2.75	0.5 - 1.0	

4. EVALUATION OF EXPERIMENTAL RESULTS

In the past 10 years a long series of experiments has been conducted in the Large Oscillating Water Tunnel of WL | DELFT HYDRAULICS. The main objective of these series was to study the near bed sediment transport mechanisms under prototype flow and sediment conditions. For most series of experiments uniform sand has been used. In nature the bed material is in general not uniform. The bed material is transported selectively depending on its size and density. Therefore also experiments with a non-uniform sand bed were executed. This was the case for series K (Cloin, 1998) and the present experiments (series P, 2nd order Stokes waves). The hydraulic conditions have been chosen in close connection with previous experimental series in the wave tunnel for reasons of comparison. In total 24 tests were performed.

4.1 Summary of present results (graded sand)

The results of the present experiments are summarised per topic below:

Net sand transport rates

Net transport rates for all fractions

- In case of a sand bed consisting of sand type A (mixture of 30% coarse sand, $d_{50} = 0.97$ mm, and 70% fine sand, $d_{50} = 0.21$ mm) a flat bed and sheet-flow situation developed during the present experiments. The net sand transport rate is directed onshore for conditions P6A, P7A and P9A. There is a direct relation between the flow velocity (U_{rms}) and the net sand transport rate. The net sand transport rates are increasing for increasing flow velocities. This increase in transport rate is larger when the flow velocities are larger.
- In case of a sand bed consisting of sand type B (100% coarse sand, $d_{50} = 0.97$ mm) no flat bed situation developed for the three conditions P6B, P7B and P9B. Large dunes were created and on top of the dunes a sheet-flow layer developed. The net sand transport rate is directed offshore. There is no direct relation between the flow velocity and the net sand transport rate. The transport rate does not increase for every increase of the flow velocity. This is called unsteadiness: the response time of the sediment is so large that phase-lags between the sand transport and the near bed velocities occur.

Net transport rates per fraction (sand type A)

- An increase of the flow velocity (U_{rms}) leads to an increase of net sand transport for both the fine and the coarse fraction. This relation is almost linear.
- The net transport rate of the coarse fraction is almost equal to the net transport rate of the fine fraction (about 50% coarse fraction). This is in contrast to the proportion of both fractions in the sand bed at the start of a test (about 30% coarse fraction). At lower flow velocities ($U_{rms} = 0.6$ or 0.7 m/s) the net transport rate of the coarse fraction is just a little smaller than of the fine fraction. But at $U_{rms} = 0.9$ m/s the opposite happens. Apparently relatively much of the coarse fraction is transported under sheet-flow conditions. Selective transport processes are clearly present.

Composition

Bed material

- The composition of the sand bed after a test is not uniform with depth anymore. The upper 3 mm of the bed after a test has roughly the same composition as before (P6A) or is a little coarser (P7A and P9A). Beneath the upper layer there is a layer that mainly consists of fine sand (only 10-20% coarse fraction). This layer is about 10-20 mm thick.
- At larger depths below the sand surface the composition of the bed seems not to have changed much (percentage of coarse fraction is between 25 and 35).
- As the flow velocity (U_{rms}) increases, the upper layers of the bed seem to become finer.
- The measuring instruments in the tunnel produce vortices, creating erosion holes and sedimentation at the end of a test. These processes lead to a local change of bed composition, complicating the bed sample analysis. These disturbances are mainly present in the right part of the test section (open-leg side).
- The bed composition after the test did not always show the same trends at the same horizontal locations for all the tests of one condition. So some scatter was observed in the bed composition data.

Bed load transport

- The bed load transported in the onshore direction is coarser than the bed load transported in the offshore direction.
- For both directions the percentage coarse fraction is larger than one would expect, as the sand bed consists of 30% coarse fraction. The percentage of coarse fraction measured in the onshore bed load transport is considerably higher (> 44%). Even the offshore bed load transport contains more than 30% coarse fraction. This is a strong indication for selective transport processes. This can be seen at all three conditions.

Sand traps

- The forward sand trap (open-leg side) contains a lot of coarse fraction, about 70% (mixture: 30% coarse fraction). The backward sand trap (piston side) contains hardly any coarse fraction (<10%). This difference between the two sand traps is related to the asymmetry of the wave motion. The maximum onshore velocity is larger than the maximum offshore velocity.
- As the flow velocity (U_{rms}) increases the percentage coarse fraction inside the forward sand trap increases too. The percentage coarse fraction inside the backward sand trap only slightly increases.
- The sand found in the backward sand trap is in general more fine (smaller d_{50}) than the fine fraction from the sand bed (sand type A).

- The composition of the sand from the sand traps is different from that of the bed load transport (PBLT). The forward sand trap contains a much larger percentage of *coarse* fraction than the onshore bed load transport and the backward sand trap contains a much larger percentage of *fine* fraction than the offshore bed load transport. The change of composition of the sand bed probably plays an important role.

Suspended sediment

- The suspended sediment contains no coarse fraction, only fine fraction for conditions P6A, P7A and P9A. Apparently the coarse fraction is only transported as bed load.
- The suspended sediment becomes finer (smaller d_{50}) as the distance above the sand bed increases (vertical sorting of grain-size). Only the smaller particles of the fine fraction present in the sand bed go in suspension.
- A larger flow velocity (U_{rms}) leads to an increase of the mean particle diameter at a certain elevation.

Concentrations

Bed load transport

- The time-averaged onshore bed load concentration is a factor 5 to 10 higher than the time-averaged offshore bed load concentration. This ratio decreases as the flow velocity (U_{rms}) increases and is related to the amount of sand found in the two sand traps after a test.
- When the flow velocity increases both the onshore and the offshore bed load concentration increase rapidly. It seems a linear relation exists between the flow velocity and the onshore and offshore bed load concentration.

Suspended sediment

- The time-averaged suspended sediment concentrations decrease rapidly as the height above the bed increases. There seems to be a power law relation between the concentration suspended sediment and the distance above the bed.
- An increase of the flow velocity (U_{rms}) leads to higher concentrations of suspended sediment (at the same elevation above the bed).

It has become clear that gradation effects occur. This can be seen from the analysis of samples from the two sand traps, the samples from the bed load transport (PBLT) and the samples from the sand bed after a test. Gradation effects also become clear from the determination of the net sand transport rates per fraction. The coarse fraction is more easily transported by the flow than the fine fraction.

The main results of the present experiments are summarised in table 4.1 and 4.2. The net sand transport rates are averaged over all tests for each condition. In table 4.2 the standard deviation and the relative errors are presented.

Table 4.1: Summary of present experiments (2nd order Stokes waves, T = 6.5 s, R = 0.65)

Cond.	$\langle u \rangle$ [m/s]	U_c [m/s]	U_t [m/s]	U_{rms} [m/s]	% fine	% coarse	Mixture [mm]			$\langle q_{s,net} \rangle$ [10 ⁻⁶ m ² /s]	$\langle q_{s,net} \rangle$ [kg/s/m]
							d_{10}	d_{50}	d_{90}		
P6A	0.027	1.09	0.57	0.592	70 ($d_{50}=0.21$)	30 ($d_{50}=0.97$)	0.16	0.24	0.99	25.3	0.0671
P7A	0.025	1.23	0.65	0.682	70 ($d_{50}=0.21$)	30 ($d_{50}=0.97$)	0.16	0.24	0.99	33.4	0.0885
P9A	0.030	1.59	0.85	0.896	70 ($d_{50}=0.21$)	30 ($d_{50}=0.97$)	0.16	0.24	0.99	61.5	0.163

Table 4.2: Standard deviation and relative error of present experiments

Condition	U_{rms} [m/s]	$\langle q_{net,av.} \rangle$ [10 ⁻⁶ m ² /s]	σ [10 ⁻⁶ m ² /s]	r [%]	r/ \sqrt{N} [%]	Average of tests
P6A	0.592	25.3	1.12	4.4	2.5	P6A1, P6A2, P6A3, P6A4
P7A	0.682	33.4	3.04	9.1	4.6	P7A2, P7A3, P7A4, P7A5
P9A	0.896	61.5	6.15	10.0	5.0	P9A1, P9A2, P9A3, P9A4

4.2 Summary of previous experimental results (uniform and graded sand)

In the past many experiments have been carried out with oscillatory flow only. In table 4.3 some of the results of previous experiments with 2nd order Stokes waves (T = 6.5 s) and uniform sand are summarised. Only tests with the same wave period, the same flow conditions and a similar degree of asymmetry are mentioned here. Note that also for series K the sand bed consisted of graded sand.

Table 4.3: Summary of previous experiments with 2nd order stokes waves (T = 6.5 s, R = 0.63-0.67)

Cond.	$\langle u \rangle$ [m/s]	U_c [m/s]	U_t [m/s]	U_{rms} [m/s]	% fine	% coarse	Mixture [mm]			$\langle q_{s,net} \rangle$ [10 ⁻⁶ m ² /s]	$\langle q_{s,net} \rangle$ [kg/s/m]
							d_{10}	d_{50}	d_{90}		
B8	0.038	1.31	0.70	0.70	100 ($d_{50}=0.21$)	0	0.15	0.21	0.32	38.9	0.103
B9	0.030	1.72	0.86	0.92	100 ($d_{50}=0.21$)	0	0.15	0.21	0.32	69.8	0.185
C1	0.015	1.11	0.58	0.55	100 ($d_{50}=0.21$)	0	0.15	0.21	0.32	18.7	0.0496
C2	0.055	1.09	0.62	0.55	100 ($d_{50}=0.21$)	0	0.15	0.21	0.32	25.5	0.0676
C11	0.029	?	?	0.83	100 ($d_{50}=0.21$)	0	0.15	0.21	0.32	51.5	0.136
K1	0.035	1.54	0.78	0.84	50 ($d_{50}=0.13$)	50 ($d_{50}=0.32$)	0.097	0.194	0.406	35.2	0.0933
K2	0.023	1.10	0.55	0.59	50 ($d_{50}=0.13$)	50 ($d_{50}=0.32$)	0.097	0.194	0.406	17.4	0.0461

C Data report

Sediment concentrations due to currents and irregular waves; measurement report

by

C. Jacobs, S. Dekker

TU Delft

WL Delft Hydraulics

Sediment Concentrations due to Currents and Irregular Waves Measurements Report

October 1999

Christiaan Jacobs / Sander Dekker



TU Delft

Delft University of Technology
Faculty of Civil Engineering and Geosciences
Hydraulic and Offshore Engineering section

Sediment Concentration due to Currents and Irregular Waves

Measurements Report

**Master of Science Thesis
CTwb5060**

**S. Dekker
C.E.J. Jacobs**

**Committee Prof.ir. K. d'Angremond
Prof.dr.ir. L.C. van Rijn
dr.ir. J. van de Graaff
dr.ir. H.L. Fontijn
ir. P.G.J. Sistermans**

Contents

Measurements Report

Chapter 1 Introduction

1. General
2. Structure of this report

Chapter 2 Experimental set up

1. The 'Grote Speurwerk'-flume
2. Measured parameters and instruments
3. Bed material

Chapter 3 Description of tables

1. Introduction
2. Table 'Basic Measurement Data'
3. Table 'Overview Ripple Parameters'
4. Table 'Overview Sediment Parameters'

Chapter 4 Description of datafiles

1. Introduction
2. General
3. Daisylab files
4. Excel files
5. Sediment characteristics
6. Macros

Chapter 5 Description of graphs

1. Introduction
2. Graph 'Overview Concentrations'
3. Graph 'Comparison Concentrations'
4. Graph 'Concentration per fraction'

Chapter 6 Report

1. Introduction
2. Preparations
3. Uniform series
4. Well-graded series
5. Checklist
6. Procedure list
7. Problems/Solutions

Appendices

- | | |
|--------------|------------------------------------|
| Appendix I | Basic Measurement Data |
| Appendix II | Graph 'Overview Concentrations' |
| Appendix III | Graph 'Comparison Concentrations' |
| Appendix IV | Ripple parameters |
| Appendix V | Sediment parameters |
| Appendix VI | Graph 'Concentration per fraction' |

Chapter 1 Introduction

By Christiaan Jacobs

1. General

Sediment transport in a coastal zone can be calculated with different methods. One of them multiplies the time-averaged sediment concentration profile by the time-averaged velocity profile. For this type of calculation, an accurate description of the concentration profile is essential.

To achieve a more accurate description of this concentration profile, experiments have been conducted in the 'Lange Speurwerk Goot', a flume in the Laboratory of Fluid Mechanics at Delft Technical University. Special attention has been paid to the influence of the grading of the bed-material on the concentration profile.

This report summarises and describes the measured parameters. It mainly consists of tables and figures. Analysis of these data will be described in the 'Analysis Report'.

2. Structure of this report

Roughly, this report can be divided in two parts. The first part consist mainly of texts, whereas the second part contains the tables and figures.

In Chapter 2, the experimental set up is described. In Chapter 3, the description of the table 'Basic Measurement Data' can be found. These tables are placed in Appendix I.

Chapter 4 contains information on the datafiles made during the measurements and how these can be used. Chapter 5 describes the graphs that have been made from the datafiles. And finally in Chapter 6 an overview is given of the procedures and encountered problems during the measuring period.

Chapter 2 Experimental set up

By Sander Dekker

1. The 'Grote Speurwerk'-flume

1.1. Description of the physical model

All experiments were conducted in the 'Grote Speurwerk'-flume, a flume of the Laboratory of Fluid Mechanics of the Faculty of Civil Engineering of the Delft University of Technology. Figure 1 shows a sketch of the flume.

The total length of the flume is 45 m, the width 0.8 m and the flume has a depth of 1.0 m. This makes it possible to perform experiments with a 30 m bed length.

The flume consists of various sections (see figure 1 at the end of this chapter):

- A : wave-generator section
- B/E : in- and out-flow section
- C : test section
- D : section with wave damping slope structure

1.2. Current generation

The current enters the flume through the inflow section B. Current in the wave direction, the direction which is investigated only during this experiments, is generated by opening gate valve 1 (see figure 1), while gate valve 2 is closed. By manipulating gate valve 1 for inflow and the weir and measuring the fluid velocity at $z = 0.38 * h$ (\approx depth averaged velocity), the desired discharge can be obtained. The weir is also used to achieve the desired water depth of 0.50 m above mean bed level at the test section, by adjusting the height of this weir.

1.3. Wave generation

The irregular movements of the wave paddle generate the irregular waves. The desired wave spectrum is created by a computer file. The spectrum is single topped, with a peak frequency of 0.4 Hz and a JONSWAP-shape. The wave height is also variable in the computer-file and can be adapted for more accuracy by an amplifier.

1.4. Wave damping structure

To reduce the wave reflection as much as possible, the effect of the wave damper was examined in earlier flume-studies (Van der Kaay and Nieuwjaar (1987) and Van Kampen and Nap (1988)). Based on the results of these studies, the wave damper was placed in the flume. The reflection coefficient, defined as the ratio of the reflected wave height H_r and the incident wave height H_i , was found to be less than 0.1 in these studies. In this study a reflection coefficient between 0.1 and 1.5 was found.

1.5. Sand bed

For both test series (the series with uniform sand and the series with graded sand) a horizontal sand bed has been created with a thickness of 0.1 m. At the beginning of the bed, in front of the wave paddle, and at the end of the bed, in front of the wave damper, a bed slope of 1:20 was created. The test section is approximately x m from the beginning of the sand bed.

2. Measured parameters and instruments

2.1. Discharge and water level

To get an estimation of the desired current velocity U , the velocity was measured with an EMS at a height of $0.38 \cdot h$ at the test section, as an indication of the mean velocity. At the same time the water level was determined by using a reading scale at the test section. So, the desired velocity and water level could be reached at the same time by manipulating the weir height and/or gate valve 1 for the incoming discharge.

The water level was related to the zero-level (the bottom of the flume).

2.2. Wave parameters

In each experiment, the wave spectrum was determined at five locations in the flume. One wave height meter (WHM) was located on the carriage, two between the carriage and the wave paddle (at $x = 11$ m and $x = 18.5$ m) and two between the carriage and the wave damping structure (at $x = 25.5$ m and $x = 27$ m).

The output of the WHM placed on the carriage was used to represent the wave conditions at the test section, while the other four WHM's were used to check the uniformity of the wave conditions in the flume.

The data of the WHM's were stored in the computer. These files have been analysed using an MATLAB-program, developed by DELFT HYDRAULICS. The output of the program was the significant wave height (H_s) and the peak period (T_p). With the program it was possible to create an energy density spectrum. The wave height distribution can be described by a Rayleigh distribution, because the spectrum is single topped (Holthuijsen (1997)).

2.3. Bed level

To determine the mean bed level and the maximum ripple height of the test section, a Profile Follower (PROFO) was used. This instrument was mounted on the moving carriage. The PROFO-signal was stored in the computer and averaged by an Excel-program, by which the maximum ripple height could also be determined. The bottom level of the flume near the test section was chosen as reference level ('zero-level'). The bed level was determined before and after each experiment and the maximum ripple height was used to determine the final height of the measuring instruments above the bed (app. 1 cm above the highest ripple).

2.4. Fluid velocity

The fluid velocities were measured using an Electro Magnetic Velocity meter (EMS) and an Acoustical Sediment Transport Meter (ASTM).

The EMS generates an electro magnetic field; the degree of disturbance of this field is a measure for the fluid velocity at the position of the measuring volume of the probe, which is 3 mm below the probe. The time-averaged fluid velocity was determined by the computer measure-program. This program averages the electronic input signal over a chosen time period, which was 300 seconds. Earlier studies showed (i.e. Grasmeijer and Sies (1995)) that a period of 300 seconds appeared to give reproducible results.

For sediment transport measurements DELFT HYDRAULICS developed an ASTM. The instantaneous concentrations and velocities are determined simultaneously by measuring scattered ultrasonic energy. A probe containing piezo-electric crystals transmits this energy. A transducer receives the scattered signal from the transmitter. Sediment particles in the measuring volume reflect the ultrasonic energy. The transducer detects the reflected energy. By determining the Doppler-shift between received and the transmitted signal, the velocity of the sediment particles can be measured. The intensity of the received signal is related to the number of sediment particles in the measuring volume and can be used to as a measure for the sediment concentration. For large sediment concentrations (i.e. close to the bottom), the received signal is too weak for accurate measurements. The scattered signal can be corrected with the help of a second transducer. This transducer directly receives a part of the transmitted signal. The relation between the output signal of the ASTM and the velocity and concentration is approximately linear (Grasmeijer and Sies (1995)).

Both the EMS and the ASTM were attached to the moving carriage and their measurements were done simultaneously during each experiment. At 10 different heights above the bed, corresponding with the positions of the intake tubes of the concentration sampler, the instantaneous velocities and concentrations were measured during 5 minutes. The mean velocities and concentrations during this period could also be determined by the used computer measuring-program. The measuring height of both the EMS and the ASTM was adjusted using a reading scale attached to the EMS and ASTM.

2.5. Sediment concentration

The sediment concentration measurements were carried out using an array of 10 brass intake tubes of 3 mm internal diameter. This Transverse Suction System (TSS) was attached to the moving carriage; the openings of the intake tubes were placed perpendicular to the current direction. Each tube was connected to a pump, bringing the sediment and water mixture with a 1.5 m/s intake velocity in an 8 l bucket. The intake tubes were used to determine the time-averaged concentration distribution over the water depth.

In an earlier study (Van Kampen and Nap (1988)) a test was carried out to study the influence of the measuring equipment on the measured concentrations. A comparison was made between the array of 10 intake tubes and a single intake tube. The conclusion was that the differences in concentration between the array of 10 intake tubes and the single tube are within the standard deviation of the concentration.

The sediment concentrations were measured by the following procedure, which is almost the same as in the earlier studies. First, with the use of the PROFLO, the bed level was determined. The instruments were then adjusted approx. 1 cm above the highest ripple top. For adjusting, a reading scale was used, which was related to the reference level (the flume bottom). Before starting the test, the carriage was moved along the measuring section to check whether the instruments were moving freely over the ripples.

The test was now ready to start, the carriage moving to perform bed averaging, and the pumps running for 13 minutes. In this time the ten buckets were filled. After filling, the water in the buckets was poured off and the remaining sediment was washed out in a volume meter. The volume meter consists of 10 small calibrated glass cylinders with decreasing diameters. By reading the height of the sediment in the cylinder, the wet sediment volume was measured. Using a calibration table for each cylinder, the dry mass was determined for every bucket. In the calibration table a correction factor, the so-called trapping factor, was used to determine the concentration properly. This trapping factor is necessary to eliminate errors in the measured concentration, because of the fact that the sediment particles can not completely follow the curved water particle trajectories to the intake tubes placed perpendicular to the current direction (Bosman et al. (1987)).

During each test, one concentration measurement was carried out. Only during the last series ($U = 0.4$ m/s and with the graded bottom-material), two series of concentration measurements were carried out during one measurement. Based on the concentration measurements, a mean, minimum and maximum of the concentrations was determined. All sediment samples were collected in a sample bottle for analysis of the fall velocity- and the particle diameter-distribution of the suspended sediment for each test. The Visual Accumulation Tube of DELFT HYDRAULICS determined these parameters. Van der Kaay and Nieuwjaar (1987) gave a detailed description of the VAT.

In all experiments instantaneous sediment concentrations were measured by means of the ASTM (see Section 2.4). A calibration factor for the ASTM output signal (voltage) was computed using the concentrations from the pump measurements. This was done for the series with uniform sand and the series with well-graded sand separately. This gave the most accurate results.

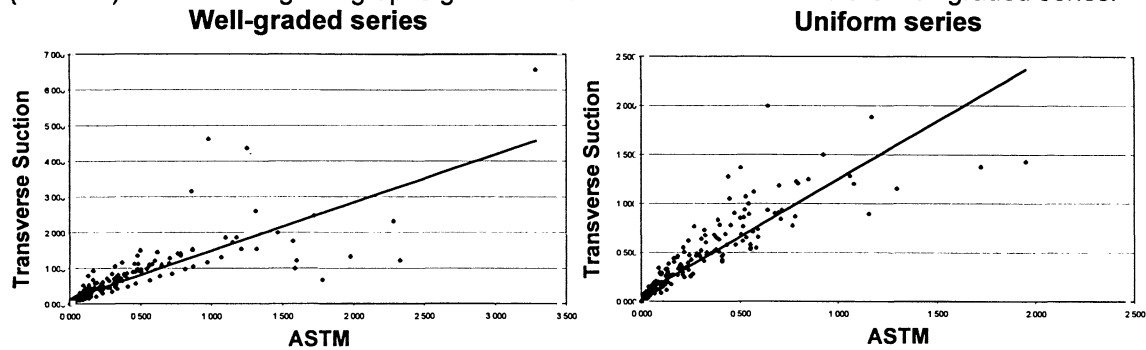
The formula for calibrating the ASTM signal is given below:

$$(2.1) \quad c(t) = A \cdot V + B$$

where:

$c(t)$: bed-averaged concentration (kg/m³)
 V : output signal ASTM (Volt)

The factors A and B have been calculated with help of the Linear Regression function of Excel (LINEST). The following two graphs give the result for the uniform and the well-graded series.



For the series with uniform sand, the factors are calculated at:

$$\begin{aligned} A &= 1.177 \\ B &= 0.071 \\ R^2 &= 0.804 \end{aligned}$$

For the series with well-graded sand, the factors are calculated at:

$$\begin{aligned} A &= 1.345 \\ B &= 0.142 \\ R^2 &= 0.675 \end{aligned}$$

The value of R^2 indicates how well the fit of this line is (if $R^2=1$, then all the values in the series lay on the same line). With the re-calculation of the values for the ASTM-averages, the B-factors have been neglected.

3. Bed material

During the experiments two types of sediment were used. The first type was used for the third series with uniform sediment (S85). The second type, for the second series with graded sediment, was a mixture of three types (Trip Popken, S85 and H32). Table 2.1 shows the characteristics of the used sediment types.

Uniform		Name sand	D10	D50	D90	D90/D10
		S85	117	165	230	2
Graded	Part	Name sand	D10	D50	D90	D90/D10
Fine	3	Trip Popken	63	97	128	2
Middle	1	S85	117	165	230	2
Coarse	3	H32	225	332	450	2
Mixture			80	170	385	4.8

Table 1 Characteristics of the used sediment

A sand layer of 0.10 m thickness was brought into the flume. After every experiment the sand was stirred a little to restore the original grading and, if necessary, filled up with new sand. Also were several bottle samples taken after each experiment, including in the test section, to check the grading and to get samples to investigate the hiding. The characteristics of the bed material were determined in the VAT, the Visual Accumulation Tube.

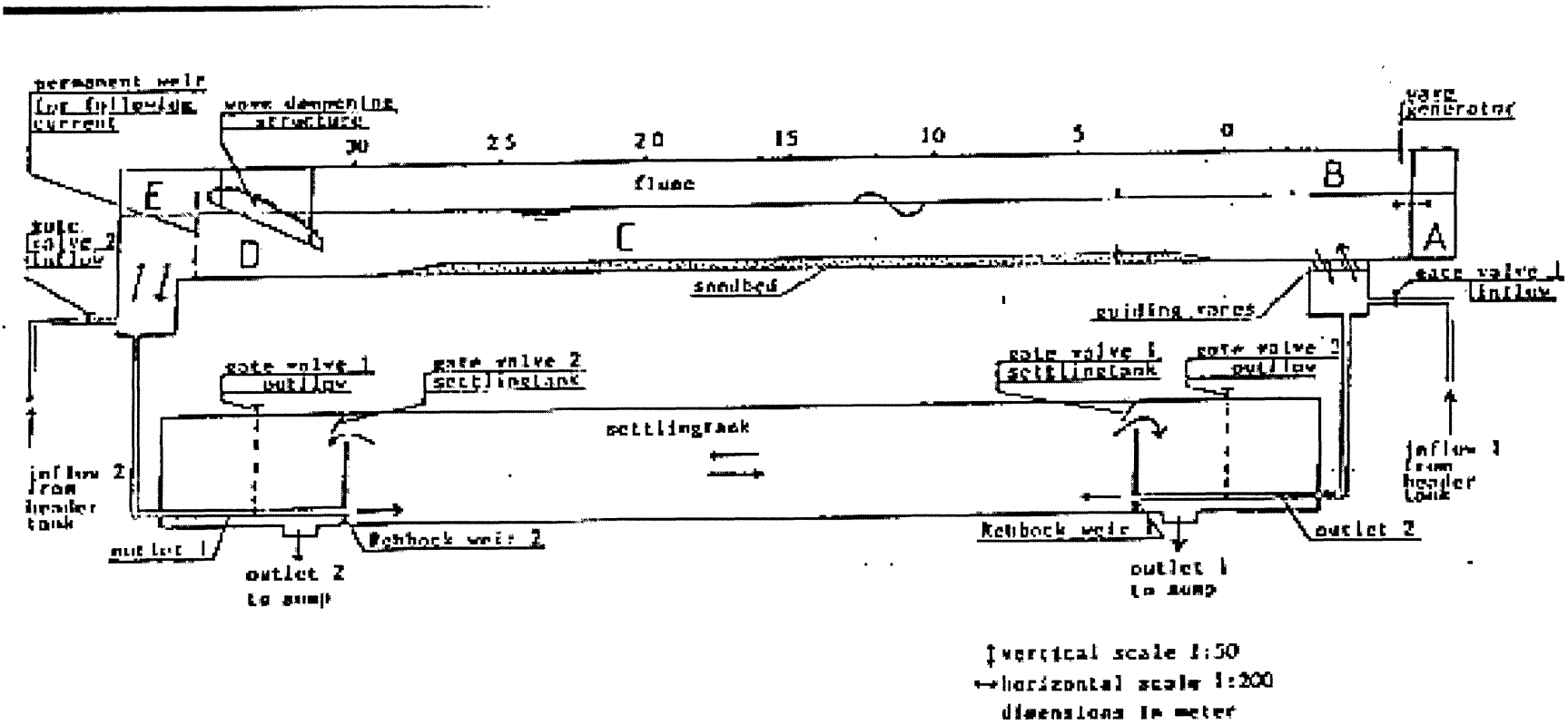


Figure 1 Overview flume

Chapter 3 Description of tables

By Christiaan Jacobs

1. Introduction

In this chapter, the tables that can be found in Appendix I will be described. These tables, titled 'Basic Measurement Data' contain basically all the relevant data that has been collected during measuring. Most of it has been directly registered; some figures have been calculated from sampled data.

2. Table 'Basic Measurement Data'

2.1. General Information

Basic Measuring Data			Christiaan Jacobs & Sander Dekker	
Averages			Testnumber: m212u8	Test Date: 22-07-99
Current Vel. (Vc)	0.22	m/s	Starting Time: 14:00:00	
Sign. Waveh. (Hs)	10.58	cm	Water Temperature: 26.0 °C	
Peak Period (Tp)	2.46	s	Water level (cm) on loc. 1: 60.1	
Mean bed level	8.35	cm	Water level (cm) on loc. 2: 59.9	
Maximum bed level	10.4	cm	Water level (cm) on loc. 3: 59.8	
Waterdepth	51.55	cm		
			Sediment Characteristics	
			<i>determined for measuring section</i>	
Ripples	-height	1.23 cm	before test	1.10 cm
	-length	8.63 cm		9.66 cm
	-velocity	4.10E-3 cm/s		cm/s
	-shape	current-dominated		wave-dominated
			D10= 128 10 ⁻⁶ m	
			D50= 164 10 ⁻⁶ m	
			D90= 215 10 ⁻⁶ m	

Figure 1 General Information

The first half of the table contains some general information on the measurement. First of all, testnumber and -date. The testnumber consist of two letters and four numbers. The first letter is an 'm', meaning the wave- and current directions are the same. The following number gives information on the (desired) current velocity. It gives the value in decimetres per second. The next two numbers give the desired significant waveheight, in centimetres. The last letter gives information on the grading of the bed-material: an 'u' stands for uniform graded sand, the 'g' for well-graded sand.

The starting time is the time at which the first activity for this test was initiated. The water temperature was measured before each test.

The water levels have been measured at three different locations. Location 1 is at the beginning of the flume, just after the water enters it. Location 2 is at the measuring section. Location 3 is a few meters in front of the wave damping structure.

The current velocity (Vc) has been calculated by averaging over the depth the averaged velocities measured with the EMS. The significant waveheight (Hs) and the peak period (Tp) are averages of the significant waveheight and peak period calculated for each sample. (See Samples)

The Mean bed level has been calculated from measurements with the Profile Follower (PROFO). See Chapter 2 (2.3. Bed level) for more information.

The waterdepth has been calculated by subtracting the mean bed level from the waterlevel at location 2 (the measuring section).

The ripple-height and -length have been calculated from the same PROFO-registrations as the mean bed level. The ripple-velocity has been calculated from drawings of the ripples. On overhead-sheets placed on the sidewindows of the flume near the measuring section the ripples were drawn every 5 to 10 minutes during the first half of the tests. The drawings of some tests appeared to be unclear: it was unclear which ripple migrated to which ripple, or there were too little ripples to calculate an accurate average velocity.

The ripple-shape has been determined from the ratio λ_1/λ_2 . If this ratio is less than 1.3, the ripples are wave-dominated. If this ratio exceeds 1.5, the ripples are current-dominated. The lengths λ_1 and λ_2 have been calculated from the PROFO-registrations.

2.2. Samples

Transverse suction								From computer					
sample #	height z'	start	end	dur.	tube	level	D50	Conc. (g/l)	AZTM conc.	AZTM vel.	EMS vel.	Sigh. Wavesh.	Peak Period
1	2.7	14:08:00	14:21:30	13:30	V	28	150	0.3400	0.3197	0.094	0.113	10.74	2.34
2	3.7	14:08:05	14:23:40	15:35	VI	27	148	0.2437	0.1466	0.119	0.126	10.52	2.34
3	4.7	14:08:10	14:22:20	14:10	VII	27	148	0.1836	0.1029	0.137	0.137	10.59	2.50
4	6.2	14:08:15	14:21:50	13:35	VIII	28	148	0.1325	0.0796	0.147	0.159	10.58	2.36
5	8.7	14:08:20	14:22:40	14:20	IX	24	143	0.0722	0.0456	0.176	0.180	10.39	2.34
6	11.7	14:08:25	14:25:30	17:05	X	15	143	0.0289	0.0285	0.191	0.204	10.68	2.59
7	15.2	14:08:30	14:23:05	14:35	X	3	143	0.0058	0.0169	0.219	0.234	10.64	2.61
8	18.7	14:08:35	14:23:50	15:15	X	2	143	0.0038	0.0089	0.231	0.243	10.39	2.65
9	22.7	14:08:40	14:22:50	14:10	-	-	-	0.0000	0.0056	0.243	0.241	10.64	2.50
10	27.7	14:08:45	14:23:55	15:10	-	-	-	0.0000	0.0034	0.252	0.234	10.60	2.36

Figure 2 Samples

The middle part of the table is an overview of the data collected per height. The measurement by means of transverse suction was started at the beginning of the test. The measurement with the computer had to be carried out sequential. The height z' is the height of the instruments and the brass tube of the transverse suction related to the mean bed level.

The concentration (Conc. (g/l)) has been calculated from the level reached in the volume meter. For each tube of the volume meter, there is a relation between the level and the D50 of the sediment. This D50 (meaning 50% of the sediment has a diameter smaller than the value) has been determined with the Visual Accumulation Tube (VAT).

The concentration measured with the AZTM (Acoustical Sand Transport Meter) has been averaged from 5 minutes of measuring. More on the calibration factor of the AZTM can be found in Chapter 2.

The velocities were measured with both the AZTM and the EMS (Electro Magnetic Velocity Meter), and afterwards averaged.

From registrations with WHM3 (the Wave Height Meter mounted on the moving carriage), a wavespectrum was determined with help of a Matlab-file. From this wavespectrum, the significant waveheight and the peak period are displayed in the table.

2.3. Velocity

Velocity Profile without waves			
level #	height z'	AZTM vel.	EMS vel.
1	2.7	0.018	0.139
2	3.7	0.029	0.167
3	4.7	0.053	0.175
4	6.2	0.051	0.186
5	8.7	0.059	0.206
6	11.7	0.057	0.216
7	15.2	0.048	0.249
8	18.7	0.033	0.256
9	22.7	0.053	0.256
10	27.7	0.108	0.240
11	34.7	0.127	0.246
12	44.7	0.112	0.237
average		0.081	0.229

Bed samples taken: yes

filename velocity sm212a
measurements:

Notes
Dirty water, caused by cleaning one of the other flumes in the laboratory

Figure 3 Velocity

The last part of the table contains the data of the velocity measurement without waves, if available. For tests with both waves and current, the velocity profile was determined after all the tests were done. The result of this measurements (velocities, averaged over 5 minutes) are displayed in this part of the table.

If a bed-sample was taken during the test, a note is made here.

In the 'Notes'-area all the notes that were written down during the measurements are copied. Here you can find particularities of the measurements, like in this example the dirty water, caused by cleaning one of the other flumes.

3. Table 'Overview Ripple Parameters'

In appendix IV, an overview is given of the calculated ripple parameters. These have been calculated from PROFO-registrations. The following values can be found:

Ripple-height

This is the average of vertical distances from ripple-top to the first following ripple-trunch.

Ripple-length

This is the average of horizontal distances from ripple-top to ripple-top.

Lambda 1

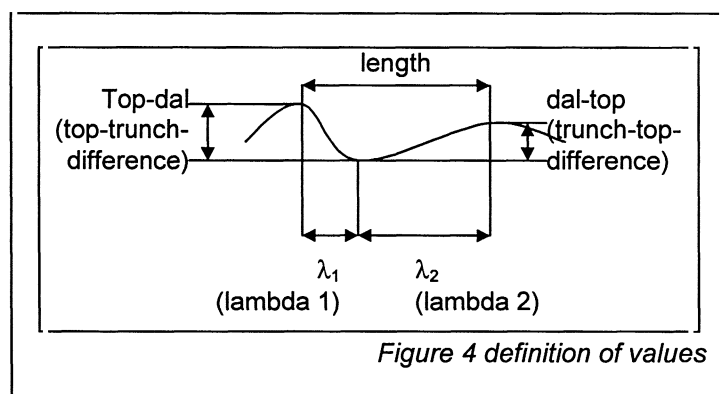
This is the average of horizontal distances from ripple-top to the first following ripple-trunch.

Lambda 2

This is the average of horizontal distances from ripple-trunch to the first following ripple-top.

Wave- or current-dominated

From the ratio λ_1/λ_2 , it can be determined whether the ripples are mainly formed by the current or by waves. If this ratio is less than 1.3, the ripples are wave-dominated. If this ratio exceeds 1.5, the ripples are current-dominated.



4. Table 'Overview Sediment Parameters'

In appendix V, an overview is given off the characteristics of the samples from the Transverse Suction System. These are values determined with help of the VAT.

During the testseries, we had some difficulties with this VAT. The characteristics calculated by the program VAT.EXE were not corresponding to the characteristics as we determined with the sieve-method. Therefore some adjustments were made to the program VAT.EXE, based on the results of the first series with uniform sand. The values shown in the table for the uniform sand are directly coming from the 'old' version of VAT.EXE, and therefor a calibration has to be applied:

$$D_{\text{actual}} = 1.2495 \cdot D_{\text{VAT.EXE}} - 15.717$$

For the series with well-graded sand, this calibration had been built in into VAT.EXE. But also now, poor correspondence was seen between values determined by VAT.EXE and those from the sieve-method. Again, a calibration factor has been calculated:

$$D_{\text{actual}} = 1.1258 \cdot D_{\text{VAT.EXE}} - 22.1397$$

To calculate the right values, the following formulas have to be applied to the values mentioned in the table:

For uniform sand:

$$D_{\text{corrected}} = 1.1258 \cdot D_{\text{table}} - 22.1397$$

For well-graded sand

$$D_{\text{corrected}} = 1.1258 \cdot ((D_{\text{table}} + 15.717)/1.2495) - 22.1397$$

For later calculations, the corrected values will be used.

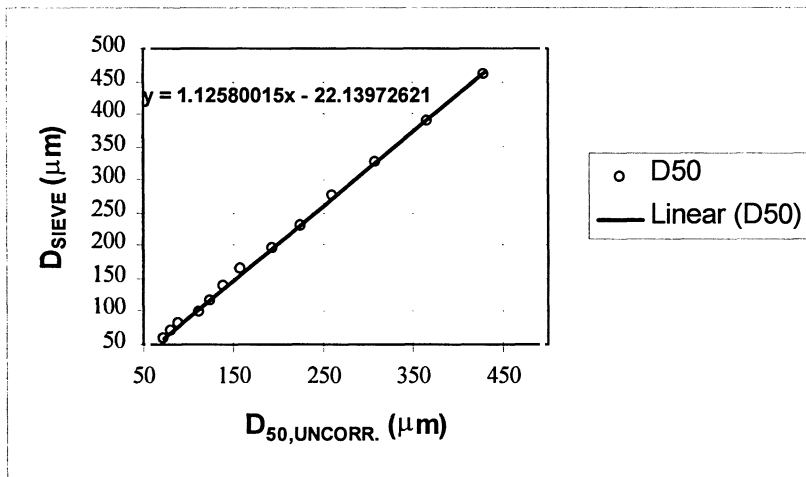


Figure 5 D_{50} form from sieve compared to D_{50} from VAT.EXE

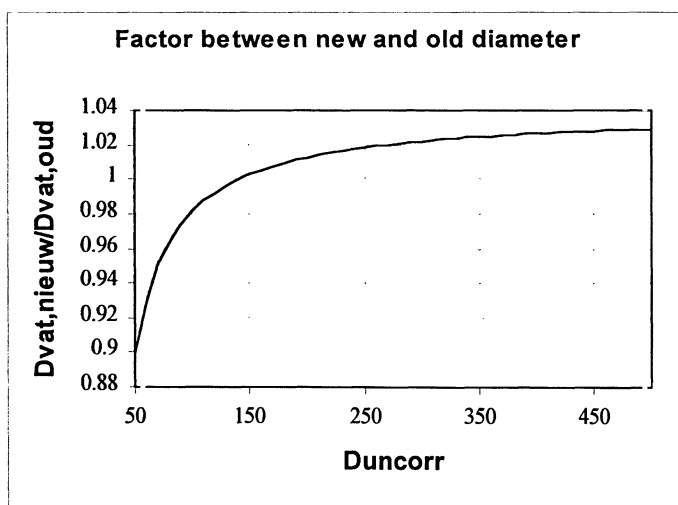


Figure 6 Effect on uncorrected value

Chapter 4 Description of datafiles

By Christiaan Jacobs

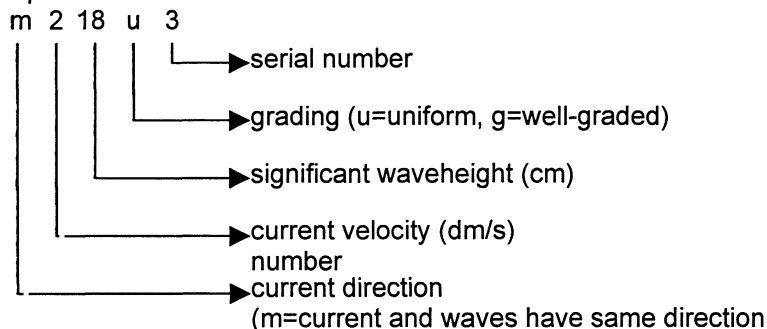
1. Introduction

In this chapter, the files used to collect data and to process the gathered data are described. During measurements, data were collected by use of a program named Daisylab. After finishing the testseries, the data were processed using Microsoft Excel. These files are also described in this chapter. Thirdly, datafiles (both ASCII and Excel) connected to the sediment characteristics are described.

2. General

2.1. Name-giving

To name the files, the coding of the tests has been used. In the following figure this code is explained:



Files produced by Daisylab can be recognised by their extension .ASC. During measurements, Daisylab was used to produce four different kinds of files:

- gm218u.asc This file was produced during the first half-hour of measuring. It contains wave-data only.
- pm218u1.asc This file was produced while measuring with the PROFO before test m218u1
- m218u1xx.asc This file was produced during the actual measurement. The 'xx' stands for a serial number in the range from 01 to 10. This number corresponds with the tube serial number of the Transverse Suction System
- sm218uxx.asc This file was produced while measuring the current velocity without waves. The 'xx' stands for a serial number in the range from 01 to 12. This number corresponds with the tube serial number of the Transverse Suction System. The height of number 11 is 7 cm above intake-tube 10, the height of number 12 is 17 cm above intake-tube 10, or 42 cm above the lowest intake-tube, number 1.

2.2. Formats

Daisylab produces files in ASCII-format. Within the program it is possible to decide if the decimal-sign should be a comma (,) or a point (.). Except for the velocity files (s*.asc), the point is used as decimal-sign. This is especially important when the files are used in a spreadsheet-program like Microsoft Excel. If a comma is used in the data-file and a point is normal within the program, the numbers will be read as strings. Replacing all the commas by points can solve the problem.

The list-separation mark used by Daisylab can also be chosen. We decided to use the semicolon (;).

3. Daisylab files

3.1. *gm218u1.asc*

Before starting a measurement, characteristic ripples had to be formed first. To achieve this, half an hour of waves (and currents) were produced. During this period, the computer measured the changing waterlevels (by means of the Wave Height Meters). This measurement took 20 minutes, and is recorded in the files starting with a 'g'. The g-files consist of 6 columns:

Column 1	zeros only. This column was meant for time-registration.
Column 2	registration of WHM 1
Column 3	registration of WHM 2
Column 4	registration of WHM 3 (on the moving carriage)
Column 5	registration of WHM 4
Column 6	registration of WHM 5

The sample rate of this file is 6.8267Hz. This rate has been chosen to measure 8192 ($=2^{13}$) points in 1200 seconds. This power of 2 eases the calculation of the wave spectrum.

3.2. *pm218u1.asc*

This file contains the PROFO-registration, made before test number 1 in the 20 cm/s current and 18 centimetre waves series. The files consists of 5 columns:

Column 1	time-registration
Column 2	PROFO-registration
Column 3	velocity measured with EMS in x-direction
Column 4	velocity measured with EMS in y-direction
Column 5	steering signal for the moving carriage

The sample rate of this file is 5Hz.

Normally, the moving carriage had a speed of approximately 2cm/s. In these cases, the value of the steering signal will be around +0.15 (Volts) while moving in negative x-direction and around -0.16 (Volts) while moving in positive x-direction. There are a few files with a lower steering signal, in these few cases the speed of the carriage was approximately 1 cm/s. The position of the carriage can best be calculated by multiplying the time with ± 2 cm/s (+ in case of a negative steering signal, - with a positive signal).

All measurements were started on top of a calibration block, with known heights. The highest part of the block was 27.14 cm above the bottom of the flume, the lower part on 17.14 cm above the bottom of the flume. The highest measured value corresponds to 27.14 cm. The difference between this value and 27.14 cm has to be subtracted from the measurements to attain the correct height of the bed relative to the bottom of the flume.

After this 'calibration' the carriage was moved to the beginning of the measuring section, most of the time at a high speed. (Hence the higher value of the steering signal.) The start of this section can be recognised by a change in direction of the carriage.

The PROFO measured in three lines with different y-positions. The beginning and ending of each line can be recognised by a change in direction of the carriage. The first line (in positive x-direction) is approximately 20 cm from the left flume-wall (seen in positive x-direction), the second in the middle of the flume, the third 20 cm from the right flume-wall. Some measurements were done on more lines, somewhere in between these lines.

3.3. *m218u1xx.asc*

The actual measurements are collected in the 'm-files'. For every height, 5 minutes of data were collected. These files consist of 14 columns:

Column 1	zeros only. This column was meant for time-registration
Column 2	registration of WHM 1
Column 3	registration of WHM 2
Column 4	registration of WHM 3 (on the moving carriage)
Column 5	registration of WHM 4
Column 6	registration of WHM 5
Column 7	registration of EMS1 in x-direction
Column 8	registration of EMS1 in y-direction
Column 9	registration of EMS2 in x-direction
Column 10	registration of EMS2 in y-direction
Column 11	registration of the AZTM, velocity in x-direction
Column 12	registration of the AZTM, velocity in y-direction
Column 13	registration of the AZTM, concentration
Column 14	steering signal of the carriage

The sample rate of this file is 6.8267Hz. This rate has been chosen to measure 2048 ($=2^{11}$) points in 300 seconds. This power of 2 eases the calculation of the wave spectrum.

After facing problems with measuring with two EMS-probes, we decided on July 17th to stop using EMS1. The output-files have not been changed, hence the two columns with zeros in most of the files.

While the signals of the WHM-probes and the EMS-probes were calibrated before starting the measurements, the AZTM was not. Only after all the measurements were finished this had been done. The values of the velocity-measurements don't have to be calibrated (the value is the measured velocity in meters per second). For the concentration measurement, the calibration-factor appeared to be: <factor AZTM>

3.4. *sm218uxx.asc*

For every day of measuring with a current velocity not equal to zero, a velocity measurement was carried out without waves. Most of the time, this was done at the end of the day; sometimes it was more convenient for planning to do this in between the other measurements.

The 's-files' consist of 9 columns:

Column 1	zeros only. This column was meant for time-registration
Column 2	registration of EMS2 in x-direction
Column 3	registration of EMS2 in y-direction
Column 4	registration of EMS1 in x-direction (not in use)
Column 5	registration of EMS1 in y-direction (not in use)
Column 6	registration of the AZTM, velocity in x-direction
Column 7	registration of the AZTM, velocity in y-direction
Column 8	registration of the AZTM, concentration
Column 9	steering signal carriage

The sample rate of this file is 6.8267Hz, the duration of the measurement was 2½ minutes per height.

4. Excel files

4.1. Introduction

Since the output-files, produced by Daisylab are not directly accessible by Excel, all files had to be transformed into readable files. At the same time, some basic calculations have been performed.

After this transformation, the data of most interest were collected into bigger overview files. In these files, also graphs have been produced.

All these files will be shortly described in this part.

4.2. pm218u1.xls

After transformation of the ASCII-file with the name pm218u1.asc, this file was made. This type of file contains the data of the PROFO-registration, calibrated and made relative to the bottom of the flume. Also, a graph is made of the steering signal of the carriage (sheet named 'Steering') and a graph is made of the registration (sheet named 'measuring').

In column 'F', a logical function outputs 'change' every time the value of the steering signal of the carriage changes from positive to negative and vice versa. This can help finding the changes in direction of the movement of the carriage.

4.3. Provo pm218u1.xls

This file is made with references to the file 'pm218u1.xls'. On sheet 1, the numeric data of each PROFO registration-line are copied. On sheet 2, for each line a graph is drawn. On the sheet called 'Overzicht' (Dutch for 'overview') some basic ripple-parameters have been calculated (with help of the sheets called 'raai 1', 'raai 2' and 'raai 3'). Average values of lambda 1, lambda 2, top-trunch difference and trunch-top difference and the average length can be found. In the following graph the different values are explained.

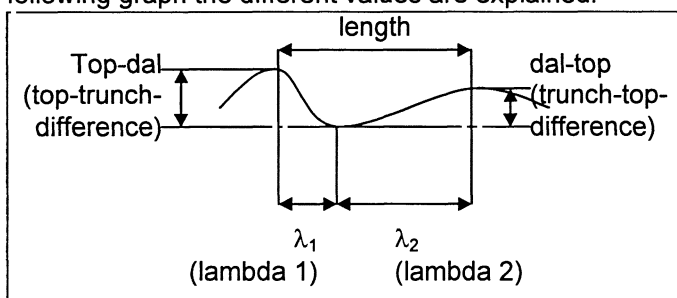


Figure 1 definition of values

4.4. Provo overzicht.xls

This file contains an overview of all the values that could be calculated from PROFO-registrations. On the sheet called 'data overview (G)', an overview is given of the PROFO registrations in the well-graded testseries. The following values can be found:

- Test # This is the name of the test (including a 'p' for PROFO-registration)
- Ribbelhoogte The calculated average ripple height
- Ribbellengte The calculated average ripple length
- Lambda 1 The average distance from top to trunch
- Lambda 2 The average distance from trunch to top
- Soort The shape of a ripple can be dominated by waves or by the current. This can be determined by the ratio λ_1/λ_2 . When $\lambda_1/\lambda_2 > 1.5$, the ripples are current dominated, when $\lambda_1/\lambda_2 < 1.3$, the ripples are wave-dominated. In this column, the dominant mechanism is given.

On the sheet called 'data overview (U)', the same values for the uniform graded series can be found. The last sheet ('start_end_points') has been used for calculation.

4.5. m218u1xx.xls

The content of this file is exactly the same as the file 'm218u1xx.asc'. The difference is that this file has a layout for Excel, a header row is added with the name of the kind of that can be found in the column, a row is added with the average value of the data and a row with the standard deviation. Some of the average values have been used in other Excel-files.

4.6. sm218uxx.xls

The same is valid for the file named 'sm218uxx.xls'. The content of this file is the same as 'sm218uxx.asc'. Also here, a header row and to rows with calculated values have been added.

4.7. m218u1 meetblad.xls

This file summarises some of the values measured during the test m218u1. It gives information on desired and measured current-velocities, wave-parameters and depth, some basic information on the bed-levels, a calculation of the concentration measured with the Transverse Suction System and an overview of average values of the electronic measurements. Nota Bene: The average value for the concentration measurement with the Acoustical Sand Transport Meter has been calibrated, so these values are in kilograms per cubic metre instead of Volts. The data displayed on the sheet called 'Meetblad' has been used to draw two graphs. On the sheet 'Velocities', the velocity profile measured with the EMS can be compared to that of the ASTM. On the sheet 'Concentrations', the calculated values of the concentration measurement with the TSS can be compared to the average voltages measured with the ASTM.

4.8. m218u overzicht.xls

In this file, some values of the different tests within one testserie have been collected for comparison. This makes it easy to spot strange differences and is a first check to see if the tests are trustworthy. To keep the overview relatively simple, only the average data from the TSS and the average EMS-velocities have been collected here. Also here two graphs were drawn, one to compare the velocities and one to compare the concentrations.

4.9. comparison m218.xls

This file has roughly the same structure as the 'overzicht'-file. Only here, a comparison is made between the results of the tests from the series with uniform graded sand, and the tests from the series with well-graded sand.

5. Sediment characteristics

5.1. Introduction

To determine some characteristics of the sediment samples (taken with both the Transverse Suction System and direct bottom-samples), the Visual Accumulation Tube developed by Delft Hydraulics was used. Time-registration was done by a computer, which also calculated the characteristic values. In connection to this registration and calculation three type of file were produced, some other were made afterwards to collect all the data. All these files are described in this part.

5.2. Pcf-files

To register the times at which certain levels were reached, a program named 'sw.exe' was used. The output of this program was stored in files with the extension '.pcf'. For suspension samples, the name of the files consists of the test-number and the serial-number of the intake-tube. If not enough sand was available to make a single test, samples from the same height were put together. If even this was not enough, several heights were put together. In the case of test series m218u this led to the following table:

#	Test 1 (m218u1)	Test 2 (m218u2)	Test 3 (m218u3)
1	m218u1b1.pcf	m218u2b1.pcf	m218u3 b1.pcf
2	m218u1b2.pcf	m218u2b2.pcf	m218u3 b2.pcf
3	m218u1b3.pcf	m218u2b3.pcf	m218u3 b3.pcf
4	m218u1b4.pcf	m218u2b4.pcf	m218u3 b4.pcf
5		m218uxb5.pcf	
6		m218uxb6.pcf	
7			
8			
9		m218uxbx.pcf	
10			

5.3. Out-files

The output-files of 'sw.exe' were the input files of a program named 'vat.exe'. This program calculates from the time-registrations via the fall-velocities the particle-diameters. The output of this file is stored in files with the extension '.out'. The names of these files are the same as the '.pcf'-files (save the extensions).

In the output file, the original time-registrations are given, then for each deposit-height the fall-velocity and the grain size and finally the cumulative percentages.

5.4. Xls-files

To make it more easily to calculate with the sediment-characteristics, the values were transferred to Microsoft Excel files. In these files, only the cumulative percentages can be found. The D10, D50 and D90 values (meaning respectively 10%, 50% and 90% of the grains are smaller than the given value) have been highlighted. Also, a graph has been drawn to illustrate all the values calculated.

5.5. Sediment characteristics m218u.xls

In these files, an overview is given of the determined values for the characteristics of the suspension samples. These have already been used in the calculation of the concentration measured with the TSS.

We had some troubles with the calibration of the 'vat.exe'-program. It seemed to give inaccurate values, compared to characteristic values determined with sieves. Therefore, the values had to be corrected. During the tests with uniform sand, this has been done afterwards in these files. The values given on the sheet named 'invoer' came from the old 'vat.exe'-program, the values on the sheet 'uitvoer' are the corrected values. After the tests with uniform sand, a corrected version of the 'vat.exe'-program has been used, so here no correction factor was needed.

6. Macros

6.1. Introduction

To convert the different types of text-files to usable Microsoft Excel-files, use has been made of some macros. The most useful macros are stored in the file 'macros.xls'. A short description of these macros, and on which files they can be used is given in this part.

6.2. Datamacro

This macro can be used to convert the 'm218u1xx.asc'-files to 'm218u1xx.xls'-files. It inserts the header rows and averages.

6.3. Macro 'SedChars'

This macro converts the '.txt'-files (which have been made by a Pascal program that selects the cumulative values only from the '.out'-files from 'vat.exe') to Microsoft Excel files ('.xls'). It creates a graph from the values, and highlights the D10, D50 and D90.

6.4. ProvoMacro

This macro calibrates the files with the PROFO-registration. It calculates a calibration-factor, and after calibrating creates graphs of the steering signal and the registration itself.

6.5. *SnelheidsMacro*

With help of this macro, the files with the registration of the velocity profile without waves can be transformed into Microsoft Excel files. The macro itself calls a subroutine that opens the different DaisyLab-files, calls a subroutine named 'Snelheidsomwerkproc', and closes the transformed file, saving it as Excel file. The subroutine 'Snelheidsomwerkproc' inserts the header row and averages.

Chapter 5 Description of graphs

By Christiaan Jacobs

1. Introduction

In the appendices, a collection of graphical presentations of the collected data can be found. For each of the types of graph, a short explanation is given in this chapter. In this stage of the project, no intention is made to draw conclusions from these data.

2. Graph 'Overview Concentrations'

For each condition, a series of test was executed. Every condition was repeated three times. In this way, you can find an average value for each condition.

For each series of test, a graph called 'Overview Concentrations' has been made. In this graph, the concentrations are drawn against the height above the average bed level. The values for these concentrations have been taken from the registrations with the Transverse Suction System. For small concentrations, it is difficult to determine the exact value. For sand with a D50 of 150 μm , the minimum measurable concentration is 0.002 g/l (corresponding to 1 mm sand in volume-meter X). This explains the small number of data in the regions higher above the bottom in case of smaller waves and smaller current velocities.

A quick look at the graphs for the series with uniform sand shows the small differences between the successive tests. It indicates little variations. This however doesn't count for the tests with well-graded sand. Especially in case of current and waves, the concentrations tend to diminish in time (the first test of the day shows higher concentrations compared to the latest). This might have been caused by the washing out of the smaller sand-particles by the water motions.

3. Graph 'Comparison concentrations'

While the graphs in Appendix II were meant for comparison of test with exactly the same conditions, the graph 'Comparison concentrations' shows the results for tests with both uniform graded and well-graded sand. In these graphs, it is possible to see the effect of this difference in grading. Also these values have been determined by use of the TSS.

The most obvious result of this comparison seems to be the higher concentrations in case of well-graded sand. This is probably caused by smaller sand-particles, which are more easily brought into suspension.

4. Graph 'Concentration per fraction'

One of the main goals of this project is to find the influence of the grading of the bedmaterial on the concentration verticals. To show part of this influence, these graphs have been made. They show the concentration per fraction. After the characteristics of the bedmaterial have been determined, a value for the D25, D50 and D75 have been calculated (indicating that respectively 25% of the material is smaller than the value calculated, 50% is smaller and 75% is smaller). With this value and the determined characteristics of the Transverse Suction samples, the share of each fraction can be calculated. Only four fractions have been used to keep the graph clear. For some tests, especially in the uniform series, no bed samples have been taken. In these cases, no information is available on the bedmaterial. Therefore, the desired, standard bedmaterial was used.

The following table gives the values, used if no other information was available.

	D10	D25	D50	D75	D90
Uniform sand	111	137	163	191	233
Well-graded sand	81	100	173	314	390

From the graphs, it is clear that mostly the finer parts come into suspension. These are lighter and more easily brought into suspension. More detailed investigation follows in a later report.

Chapter 6 Report

By Christiaan Jacobs

1. Introduction

In this chapter, an overview in texts will be given of the measurements. This includes an overview of all the procedures during testing, and some information on the problems we have encountered during testing. It will be in chronological order, so starting with the preparation period, then the part with the tests with uniform sand and finally the part with the test with well-graded sand. After this, the check- and procedure lists are given. In the last part, the problems and their solutions (if any) are summarised in a table.

2. Preparations

The 'Grote Speurwerk'-flume in the Laboratory for Fluid Mechanics was first available in the beginning of May. On May 10th we started with trying to set-up the valves for the desired discharge. This led to the first problem: the valve at the beginning of the flume was stuck, the electric device to open it was broken. This has been replaced by a manual valve-opener. The desired discharge was first reached on May 31st.

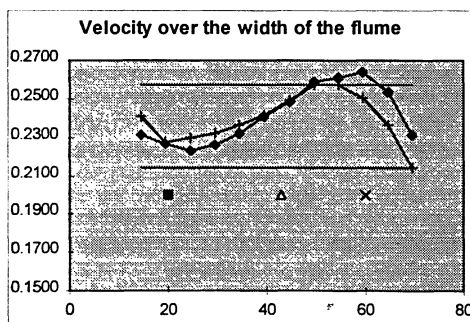
The next step was to try to produce the desired wave spectra with the help of the wave-board. This seemed quite simple at first, but proved to be more complicated. The wave-board has a possibility to compensate for reflected waves. It is this compensation that gives problems, resulting in a too large displacement of the board, which leads to shutting off of the system. We decided not to use the reflection compensation. This, together with some adjustments made to the wave-board, solved the problem. It was now possible to produce the wave spectra we desired.

On June 7th, a first, uniform sand bed was placed. The idea was to try our measurement procedures first, before the actual tests. The next weeks were used to test these procedures and the files we made for the collection of data. Also, preparations were made to produce graphs and tables from the data, to make it easy for a first check during testing.

One of the biggest problems in this testing period was the performance of the Electro Magnetic Velocity Meters (EMS). When measuring with two meters, these interfere with each other. But also with only one meter, some interference is measured. On July 9th this was solved with help of Wim Taal, of Delft Hydraulics. He suggested connecting the engine that moves the carriage to the rail that is part of the flume. This as grounding for the engine. In this way, the EMS produced a quite steady signal.

3. Uniform series

Actual measurements started on July 12th. The first three days were used to run the tests without current. On July 15th, we tried to produce the desired current velocities. The average values of the EMS and the average velocity values of the Acoustical Sand Transport Meter differed a lot. To find an explanation for this difference, we measured average velocities for 12 points on different y-positions in the flume. This gave a profile, as displayed in the graph.



The origin of the problem was the inflow device, placed at the beginning of the flume. This was not symmetric. After changing this device and placing nets to produce a more uniform flow, the problem was solved.

Analysis of the data measured with the Wave Height Meters (WHM) showed lower values for the significant waveheight for tests with a current. In stead of the desired $H_s=18\text{cm}$, the average value was $H_s\approx 15\text{cm}$, and in stead of $H_s=15\text{cm}$, $H_s\approx 12\text{cm}$. This meant that we could use the results of the tests with desired $H_s=18\text{cm}$ for comparison with test with $H_s=15\text{cm}$ without currents and the tests with desired $H_s=15\text{cm}$ for comparison with test with $H_s=12\text{cm}$ without currents. Only for the comparison with the test without currents and $H_s=18\text{cm}$, a new test had to be run. In the table at the end of this chapter, an overview is given of the testnames. In this table, also the average values for the significant waveheight H_s and the average current velocities are given.

On July 27th, the last test in the uniform series was measured.

4. Well-graded series

In the week of August 2nd, the sand bed was removed and exchanged with the bed of well-graded sand. Also, the first analysis of the uniform series was made.

For the well-graded series, we decided to change the procedure. Since a lot more sample had to be tested in the Visual Accumulation Tube (VAT), after each day of measuring, a day of testing and analysis followed. This day could also be used to prepare the sand bed. This preparation consisted of determining the characteristics of the sand and, if necessary, changing (part) of the sand. The top of the sand bed was always mixed with the lower layers and made more or less horizontal.

During the tests with current and waves, the concentrations diminished. The cause of this was probably the washing out of the finer sand particles. To achieve a more accurate measurement with the high current velocities, four measurements with the Transverse Suction System (TSS) were conducted during the first two electronic measurements. By doing this, the time between to TSS-measurements became less, so the finer particles were washed out less.

No big problems were encountered during this last period, making it possible to end the measuring program on September 1st.

5. Checklist

Before starting a measurement, a checklist was followed to ensure a good test. For illustration purposes, this checklist is printed here.

<u>Daily checklist before starting the tests.</u>	
•	Turn on equipment:
	<input type="checkbox"/> Electrical power
	<input type="checkbox"/> MeasuringPC2
	<input type="checkbox"/> MeasuringPC8
	<input type="checkbox"/> WHM1
	<input type="checkbox"/> WHM2
	<input type="checkbox"/> WHM3
	<input type="checkbox"/> WHM4
	<input type="checkbox"/> WHM5
	<input type="checkbox"/> EMS
	<input type="checkbox"/> AZTM
	<input type="checkbox"/> Generator wave-board
	<input type="checkbox"/> Steering carriage ('REMOTE' and 'AUTOMATIC')
	<input type="checkbox"/> Pumps (only necessary for tests with currents)
•	Checks
	<input type="checkbox"/> connections
	<input type="checkbox"/> PROFO (connected and grounded)
	<input type="checkbox"/> EMS calibrated to zero
	<input type="checkbox"/> Connection TSS with pumps
	<input type="checkbox"/> Removing obstacles in flume
•	And
	<input type="checkbox"/> Start on new measuring scheme, date etc.
	<input type="checkbox"/> Change filename in DEFSETUP.DSB to appropriate testnumber (e.g. m015g1)
	<input type="checkbox"/> Change filename in PROVO.DSB to appropriate testnumber (e.g. m015g1)
	<input type="checkbox"/> Change filename in GOLVEN.DSB to appropriate testnumber (e.g. m015g1)

- start steering wave-board
- start moving carriage
- start measuring with GOLVEN.DSB
- afterwards measure ripples (with PROVO.DSB)
- change height of TSS and ASTM/EMS (NB: note height!!!)
- start measuring with DEFSETUP.DSB and TSS (NB: does carriage move?!?)

6. Procedure list

Also during the tests, a checklist was followed, to ensure taking all the steps necessary for good results. This list is printed here, for illustration.

Procedure

1. Preparation of bed (desired thickness, slopes on each end of the bed).
2. Bottomsample to determine state of bedmaterial.
3. Calibration of EMS at still water.
4. Calibration of waveheight meters.
5. Generation of desired currents by adjusting the valves.
6. Generation of desired waterdepth by adjusting overflow wire.
7. Switching ON wavegenerator.
8. Waiting period of ± 30 minutes for generation of characteristic ripple pattern and checking of significant waveheight and waterdepth.
9. Determination of watertemperature.
10. Switching OFF wavegenerator.
11. Registration of ripple pattern by means of the PROFO and determination of the mean bed level.
12. Adjusting height of concentration sampler, just above the highest rippletop as determined in step 11.
13. Switching ON wavegenerator.
14. Starting program for data processing of waveheight meters, EMS and ASTM.
15. Starting transverse suction system. (until buckets are filled with 10l of water) (registration of time needed to do so)
16. Measuring concentrations and velocities with ASTM and velocities with EMS at 10 heights above the mean bed level (5 minutes per height above bed). These measurements take place in the same area as the transverse suction.
17. Determination of sedimentconcentrations from transverse suction by means of volume meter
18. Determination of sediment characteristics with the Velocity Accumulation Tube.
19. Repeating step 10 through 18 twice (which totals to 3 series of measurements).
20. Switching OFF wavegenerator.
21. Determine velocity profile by measuring current velocities at 10 different heights above the bed. The EMS in the measuring section is used here.
22. Switching OFF pump system.
23. Determining waterdepth (still water).
24. Calibration of EMS at still water (to determine drift, see step 3).
25. Take bottom samples to determine rate of "afpleistering" and to determine state of bed material.
26. If useful and/or necessary empty sand deposit to determine sandtransport.

7. Problems/Solutions

In the following table, an overview is given of the most imported problems we have encountered, and their solutions.

Problem	Solution
Interference between to EMS-devices	Most simple: removing one device. Another possibility is to connect to EMS-devices if it is really necessary to measure with two (or more) devices. More information can be found in literature.
Interference electric engine and EMS-device	Proper grounding of the engine.
Non-symmetric current	Make sure the inflow has a symmetric shape. If so, some improvement is achieved by placing nets on top of the inflow